AD-A097 201 ENVIRONMENTAL RESEARCH INST OF MICHIGAN ANN ARBOR RA--ETC F/G 14/5
THICK PHASE HOLOGRAMS.(U)
JAN 81 K A WINICK F49620-78-C-0061
UNCLASSIFIED ERIM-134200-10-F AFOSR-TR-81-0196 NL

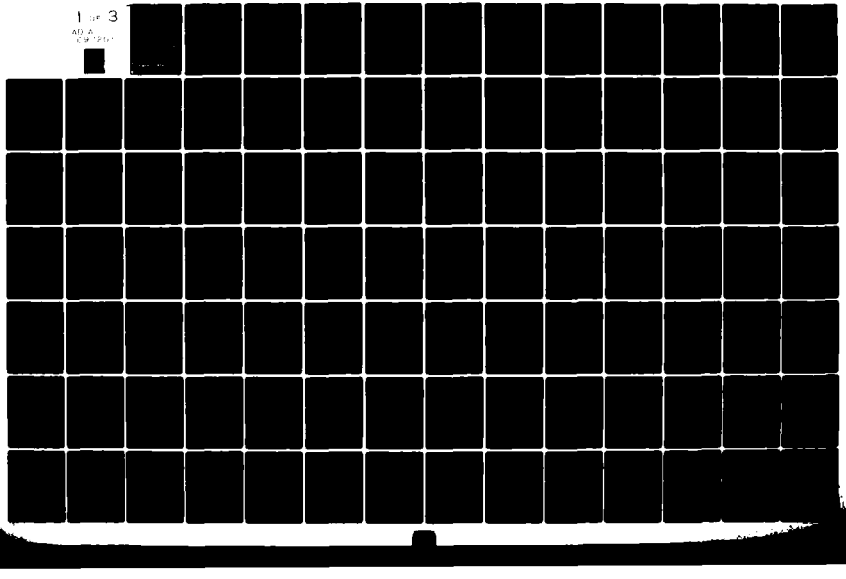

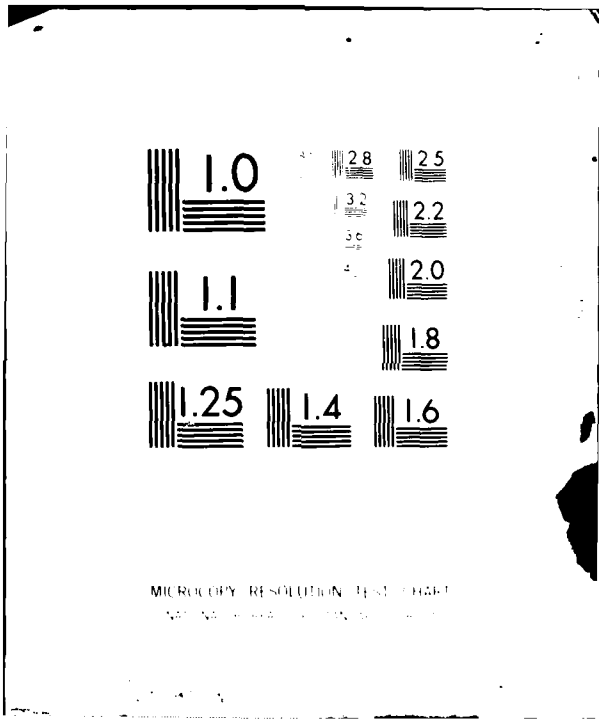
1.0
2.8
2.5
3.2
2.2
2.0
1.1
1.8
1.25
1.4
1.6
MICROCOPY RESOLUTION

LEVEL II (12) SC

Final Scientific Report

THICK PHASE HOLOGRAMS

1 May 1978-30 September 1980

K. A. WINICK
Radar and Optics Division

JANUARY 1981

Directorate of Electronics and Solid State Science
AFOSR/NE, Building 410
Bolling Air Force Base, Washington, DC 20332

ENVIRONMENTAL
RESEARCH INSTITUTE OF MICHIGAN
FORMERLY WILLOW RUN LABORATORIES, THE UNIVERSITY OF MICHIGAN
BOX 618•ANN ARBOR•MICHIGAN 48107

UNCLASSIFIED

SECURITY CLASSIFICATION OF THIS PAGE (When Data Entered)

REPORT DOCUMENTATION PAGE	READ INSTRUCTIONS BEFORE COMPLETING FORM
1. REPORT NUMBER: AFOSR-TR-81-0196	2. GOVT ACCESSION NO: AD-A097 201
3. RECIPIENT'S CATALOG NUMBER	
4. TITLE (and Subtitle): THICK PHASE HOLOGRAMS	5. TYPE OF REPORT & PERIOD COVERED: Final, 1 May 78-30 Sep 80
6. PERFORMING ORG. REPORT NUMBER: ERIM-134200-10-F	
7. AUTHOR(s): K. A. Winick	8. CONTRACT OR GRANT NUMBER(s): F49620-78-C-0061
9. PERFORMING ORGANIZATION NAME AND ADDRESS: Environmental Research Institute of Michigan, Radar and Optics Division, P.O. Box 8618, Ann Arbor, Michigan 48107	10. PROGRAM ELEMENT, PROJECT, TASK AREA & WORK UNIT NUMBERS: 61102F 2305/B2
11. CONTROLLING OFFICE NAME AND ADDRESS: Directorate of Electronics and Solid State Science AFOSR/NE, Building 410, Bolling AFB, Washington, DC 20332	12. REPORT DATE: January 1981
	13. NUMBER OF PAGES: 219
14. MONITORING AGENCY NAME AND ADDRESS (if different from Controlling Office)	15. SECURITY CLASS (of this report): UNCLASSIFIED
	15a. DECLASSIFICATION/DOWNGRADING SCHEDULE

16. DISTRIBUTION STATEMENT (of this Report)

Approved for public release: distribution unlimited.

17. DISTRIBUTION STATEMENT (of the abstract entered in Block 20, if different from Report)

18. SUPPLEMENTARY NOTES

19. KEY WORDS (Continue on reverse side if necessary and identify by block number)

Holography	Reflection gratings
Holographic optics	Interference filters
Thick phase holograms	Dichromated gelatin

20. ABSTRACT (Continue on reverse side if necessary and identify by block number)

This report describes a two year research program to investigate thick phase holographic gratings. The first year effort primarily involved a study of hologram formation in dichromated gelatin. The results of that study can be found in the interim scientific report. The second year effort was a theoretical study of optical propagation through horizontally stratified, thick, phase reflection gratings. (over)

DD FORM 1 JAN 73 1473 EDITION OF 1 NOV 65 IS OBSOLETE

UNCLASSIFIED

SECURITY CLASSIFICATION OF THIS PAGE (When Data Entered)

4 0 8 7 1 2

20. Continued.

In this report, a general theory is developed for determining the complex reflection and transmission coefficients of such gratings as a function of incident angle, wavelength and polarization. The theory does not require that the Bragg condition be either approximately or exactly satisfied, nor does it place any restrictions on the degree to which the undiffracted wave is depleted.

Theorems are stated and proved about polarization effects and about the relationship between the spectral and angular characteristics of such gratings. Compact, closed-form expressions for the complex reflection and transmission coefficients are derived. Strong similarities are shown to exist between these gratings and conventional multilayer dielectric stacks. For a particular sinusoidal grating, our results are compared with those derived using coupled wave theory.

The inverse scattering problem is considered. Given the spectral and angular characteristics of a horizontally stratified, quasi-sinusoidal, phase grating, first and second order approximate techniques are developed for determining the corresponding refractive index profile. Examples of the procedures are given.

It is also shown that horizontally stratified phase gratings can be used as position-invariant, frequency domain filters in coherent optical systems. Their basic filtering properties are presented.

Finally, an interferometric technique is developed for fabricating horizontally stratified, quasi-sinusoidal, phase gratings. The technique uses a spatially incoherent source which has a tailored intensity profile.

PREFACE

This final report was prepared by the Electro-Optics Department, Radar and Optics Division of the Environmental Research Institute of Michigan. The work was sponsored by the Air Force Office of Scientific Research under Contract No. F49620-78-C- 0061.

This report covers work performed between 1 May 1978 and 30 September 1980. The contract monitor is Dr. John A. Neff, Directorate of Electronics and Solid State Sciences, AFOSR/NE Building 410, Bolling Air Force Base, Washington, D.C., 20332. Principal Investigator for this work is K. Winick. Major contributors to the effort are Kim Winick, B. Jin Chang and W.S. Colburn.

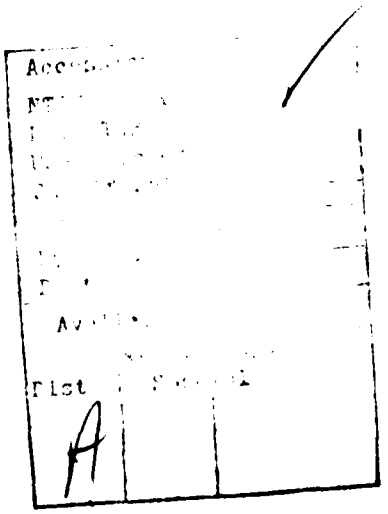

AIR FORCE OFFICE OF SCIENTIFIC RESEARCH (AFSC)
NOTICE OF TRANSMITTAL TO DTIC
This technical report has been reviewed and is approved for public release IAW AFR 190-12 (7b).
Distribution is unlimited.
A. D. Blose
Technical Information Officer

CONTENTS

LIST OF FIGURES

LIST OF FIGURES
(Continued)

LIST OF FIGURES
(Contined)

1
INTRODUCTION

Holographic optics is continuing to find important applications ranging from laser scanning systems to combiners for aircraft head-up displays. A holographic optical element is produced by recording an optical interference pattern in a photosensitive material. When the photosensitive material is processed following exposure, the recorded interference pattern is transformed into a spatial variation of refractive index and/or a conductivity within the material [1]. The refractive index and conductivity will vary significantly over distances on the order of an optical wavelength. Therefore, optical propagation through a holographic element will be governed by the laws of diffraction rather than those of refraction or reflection. This diffractive optics technology is an emerging area which has potential for important new optical devices.

When the spatial variations of refractive index and conductivity within the material are known, it is then necessary to determine the field diffracted from the holographic element given some arbitrary, incident optical field. For completely general spatial variations of refractive index and conductivity, this diffraction problem is extremely difficult. Many researchers have put forth a considerable amount of effort toward finding a solution to this diffraction problem for limited classes of refractive index and conductivity variations. As part of this report, we solve the diffraction problem for a particular class of refractive index and conductivity variations.

The classes previously considered all have, with a few exceptions to be noted later, the following characteristics:

1. The holographic element is of infinite extent in the x and y directions (see Figure 1-1).

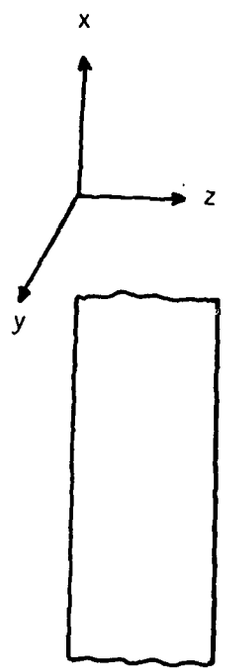

Refractive Index = $n(x, y, z) = n(x \sin \phi + z \cos \phi)$

Figure 1-1. Planar Holographic Optical Element

2. The element is flat, i.e., its front and rear surfaces are parallel.

3. The refractive index and conductivity variations can be written as a function of $(\cos \phi)z + (\sin \phi)x$ where ϕ is an arbitrary constant. This is equivalent to saying that the refractive index and conductivity varies only as a function of the distance measured along a line which lies in the x-z plane of the element. This line subtends an angle of ϕ with the z axis.

4. The refractive index and conductivity variations are periodic.

Thus, the structures which have been studied are planar, periodic (though not necessarily sinusoidal) gratings. The methods developed to date for analyzing such structures are of three types - rigorous modal, coupled-wave, and thin grating decomposition.

The rigorous modal approach was first applied by C.B. Burckhardt to an element having a sinusoidal refractive index variation along the x direction [2]. The approach leads to an eigenvalue problem formulated in terms of a matrix equation. The matrix is infinite but is truncated in order to make the problem solvable. By allowing the truncated matrix to be of sufficiently large size, good approximate results may be obtained. F.G. Kaspar showed that the modal approach could also be applied to periodic gratings having spatial variations of refractive index and conductivity along the x direction which are not sinusoidal [3]. Burckhardt's and Kasper's numerical methods are rigorous. They are, however, beset by a number of mathematical problems.

H. Kogelnik was the first to analyze holographic planar gratings using coupled-wave methods. In a classic paper, he drived closed form expressions for the field diffracted by an element having a spatial variation of refractive index and conductivity which is

sinudoidal, but arbitrary in direction, i.e., ϕ is arbitrary [4]. Kogelnik's coupled wave theory makes a number of approximations. These approximations are valid provided that the Bragg condition is approximately satisfied, and that the undiffracted field is strongly depleted. R. Magnusson and T.K. Gaylord have extended the coupled-wave theory approach to cases where the gratings are periodic but nonsinusoidal [5]. Their method results in an infinite system of coupled wave equations. The system is truncated to a finite size in order to obtain a solution. Kogelnik has also studied guided wave devices which have quasi-sinusoidal perturbations (i.e., the amplitude and frequency of the perturbations slowly change from one cycle to the next) along the guide in the direction of wave propagation [6].

The thin grating decomposition method was developed by R. Alferness [7]. In this technique, the holographic element is divided into thin slabs, parallel to the surface of the element. Each slab is treated as a thin transmission grating. A transfer matrix of infinite size relating the field at the front surface of the slab to that at the rear is postulated. When strong Bragg effects are present, a plausibility argument is presented for truncating the matrix to a finite size. The transfer matrix of the entire element is then obtained by multiplying together the truncated transfer matrices of the individual slabs. The theory is developed only for a TE polarized incident field, and a pure dielectric element (conductivity is zero). Alferness applies this technique to nonperiodic gratings as well as to multiple overlapping gratings having grating vectors in different directions (though still in the x-z plane). The theory is nonrigorous. W. Wang postulates that Alferness's approach can be extended to reflection gratings [8]. Prior to Alferness's work, D. Kermisch also studied a thin grating decomposition technique [9]. He applied his matrix method to structures having spatial variations of refractive index and conductivity along either the x or z directions. These variations were assumed to have the form of a slowly

amplitude modulated sinusoid. The method is only applicable at or near the Bragg angle and under the conditions that strong Bragg effects dominate the diffraction process. All of the above theories require that the incident field have no spatial variations in the y direction.

D. Young has developed a coupled-wave theory for analyzing the diffracted field from a holographic element having arbitrary spatial variations of refractive index and conductivity [10]. In his approach, infinite sets of variable coefficient coupled wave equations are obtained. He retains only a single pair under the assumption that strong Bragg effects dominate the diffraction process, and solves them using the WKJB approximations. No restriction is placed on the incident field.

In summary, we make the following observations. Rigorous modal methods are applicable only to periodic structures. They entail the numerical solution of a complicated eigenvalue problem. Furthermore, the eigenvalue problem is of infinite dimension and must be truncated to a finite size in order to obtain a solution.

Coupled wave methods have been applied to both periodic and non-periodic structures. In the case of periodic structures, an infinite set of constant coefficient coupled wave equations is obtained. This set is truncated to a finite size and the resulting equations are solved numerically. For non-periodic structures, an infinite set of variable coefficient coupled wave equations is obtained. Under the assumption that strong Bragg effects dominate the diffraction process, this set is truncated to just two equations. The two variable coefficient coupled wave equations are solved using the WKJB approximation.

Thin grating decomposition methods have little theoretical justification. The technique requires the truncation of an infinite transfer matrix to a finite size. The method does not consider the case of TM polarization.

This report only considers structures which have the properties listed below:

1. The structure is a pure dielectric (conductivity is zero).
2. The structure is of infinite extent in the x and y dimensions.
3. The refractive index of the structures varies spatially only as a function of z. (Structures of this type are said to be horizontally stratified.)
4. The spatial variations of the refractive index are quasi-sinusoidal.

Holographically produced dielectric structures which are horizontally stratified are a type of phase reflection gratings. We wish to determine the field diffracted from such a structure given an arbitrary incident optical field. It is desirable to develop an analysis technique which is rigorous, computationally simple, and allows one to deduce general properties of these structures. The modal technique cannot be applied to quasi-sinusoidal structures. Although the coupled wave theory approach can be applied to quasi-sinusoidal structures and is semi-rigorous, it is only justified under the condition that strong Bragg effects dominate the diffraction process. It is not immediately apparent whether general properties of the quasi-sinusoidal structures can be deduced by this coupled-wave approach. The thin layer decomposition method is non-rigorous. Furthermore, it is restricted to the case where the incident field has TE polarization. Thus, none of the existing grating theory techniques are well suited for determining the diffracted field from the structure being considered here.

Electromagnetic propagation through horizontally stratified media has been studied extensively [11]. A general theory was first published in 1950 by Abelés [12]. The theory has been successfully applied to a number of areas including radio wave propagation through

the ionosphere and multilayer dielectric stacks. Researchers in the area of holographic gratings have neglected Abele's theory for the most part. W.W. Rigrod did, however, draw an analogy between thick hologram gratings and multilayer dielectric stacks [13], while H. Kogelnik has mentioned the possibility of using the theory of stratified media to study thick, holographic, reflection gratings [6].

Research has not been pursued in this area for fundamental reasons. First, and perhaps foremost is the fact that fabrication of holographic reflection gratings is considerably more difficult than fabricating other types of holographic gratings. This is because fabricating reflection gratings requires recording materials of very high resolution (>5000 line pairs/mm). Secondly, applications of holographic reflection gratings have developed more slowly than those of other other holographic gratings. Reflection gratings are, however, becoming increasingly more important. They are now an integral part of distributed feedback lasers and are also used as selective wavelength filters in integrated optics devices and aircraft head-up displays [14-15]. Thirdly, the theory of stratified media is only applicable to a limited class of gratings, whereas the emphasis today tends to be on developing general theories which have broader ranges of applicability. Finally, no serious consideration has been given to the problem of producing holographic reflection gratings having tailored quasi-sinusoidal refractive index profiles. There exists the possibility of designing such gratings so that they have specified spectral and angular characteristics. The ability to design these gratings would require extremely accurate analysis techniques. Since the grating design problem has not been seriously considered to date, such analysis techniques have not been necessary.

The theory of stratified media provides a completely rigorous method of determining, to any degree of accuracy, the field diffracted by the structures under consideration. Therefore, it provides a means for checking the validity and accuracy of all other

theories as they apply to these structures. We will show how it may also be used to gain a fundamental understanding of the spectral and angular characteristics of reflection gratings. Furthermore, it will aid in the development of approximate design techniques. A design technique is a procedure which allows one to determine the refractive index profile of a reflection grating given its spectral and angular characteristics. This is an inverse scattering problem.

This report is organized into nine chapters. Chapter two discusses the applicability of frequency domain concepts to the analysis of holographic reflection gratings. The use of these gratings as position-invariant frequency domain filters is discussed.

Chapter three reviews the general theory of electromagnetic propagation through horizontally stratified media. This material is not new and is presented only in the interest of completeness. A computer routine is written to calculate the field diffracted from a horizontally stratified media. Two examples are given, one of a multilayer dielectric stack and the other of a holographic grating having a sinusoidal refractive index profile. The field diffracted from the holographic reflection grating is also calculated using coupled wave theory. The two results are compared.

Chapter four uses techniques from the theory of horizontally stratified media to develop an efficient method, based on matrix multiplication, for calculating the field diffracted from holographic reflection gratings.

Chapter five applies the theory of the previous chapter to derive analytic expressions for the field diffracted from holographic reflection gratings having quasi-sinusoidal refractive index profiles. These expressions are used in three examples to determine the complex reflection and transmission coefficients of gratings. A closed form expression is also derived for the complex reflection and transmission coefficients of a holographic reflection grating having a

sinusoidal refractive index profile. This expression is universally valid. It does not require that the Bragg condition be satisfied either exactly or approximately, nor does it require strong Bragg effects to dominate the diffraction process.

Chapter six discusses some general properties of holographic reflection gratings. The mutual interaction of two reflection gratings placed in contact is investigated, as is the connection between the spectral and angular characteristics of a grating. A theorem on polarization effects is stated and proved. Using the matrix multiplication technique developed in chapters four and five combined with a mathematical induction argument, general expressions for the complex reflection and transmission coefficients are derived which do not require matrix multiplications for their evaluation. These expressions are used in the following chapter to develop approximate techniques for solving the inverse scattering problem.

Chapter seven considers the inverse scattering (design) problem. Given the spectral and angular characteristics of a holographic reflection grating, first and second order approximate techniques are developed for determining the corresponding refractive index variation. Examples of the procedure are given.

Chapter eight develops and analyzes interferometric techniques for fabricating holographic reflection gratings having quasi-sinusoidal refractive index profiles.

Chapter nine contains our conclusion, and a discussion of areas for future research.

Notes to Chapter 1

[1] We consider here only volume recordings, surface relief recordings are not discussed.

[2] C.B. Burckhardt, "Diffraction of a Plane Wave at a Sinusoidally Stratified Dielectric Grating," Journal of the Optical Society of America, Vol. 56, No. 11, November 1966.

[3] F.G. Kaspar, "Diffraction by Thick, Periodically Stratified Gratings with Complex Dielectric Constant," Journal of the Optical Society of America, Vol. 63, No. 1, January 1973.

[4] H. Kogelnik, "Coupled Wave Theory for Thick Hologram Gratings," The Bell System Technical Journal, Vol. 48, No. 9, November 1969.

[5] R. Magnusson and T.K. Gaylord, "Analysis of Multiwave Diffraction of Thick Gratings," Journal of the Optical Society of America, Vol. 67, No. 9, September 1977.

[6] H. Kogelnik, "Filter Response of Nonuniform Almost-Periodic Structures," Vol. 55, No. 1, January 1976.

[7] R. Alferness, "Optical Propagation in Holographic Gratings," Ph.D. Thesis (The University of Michigan, 1976).

[8] W. Wang, "Optical Propagation in Periodic Medium: Theory and Applications, Ph.D. Thesis (The University of Michigan 1977).

[9] D. Kermisch, "Nonuniform Sinusoidally Modulated Dielectric Gratings," Journal of the Optical Society of Americal, Vol. 59, No. 11, November 1969.

[10] D. Young, "The Theory of Diffraction from a Holographic Lens," Ph.D. Thesis (Air Force Institute of Technology, 1976).

[11] J.R. Wait, Electromagnetic Waves in Stratified Media, Macmillan Publishing Co., New York, 1962.

[12] F. Abeles, Ann. d. Phys., 5, 596 (1950).

[13] W.W. Rigrod, "Diffraction Efficiency of Nonsinusoidal Bragg Reflection Gratings," Journal of the Optical Society of America, Vol. 64, No. 1, January 1974.

[14] A. Yariv, Introduction to Optical Electronics (2nd Edition), Chapter 13, Holt Rinehart and Winston, New York, 1976.

[15] Holographic Combiners for Head-Up Displays, Final Technical Report No. AFAL-TR-77-110, Radar and Optics Division, Environmental Research Institute of Michigan, Ann Arbor, Michigan, 1977.

2
FREQUENCY DOMAIN CONCEPTS

In this chapter, we demonstrate the applicability of frequency domain concepts to the analysis of flat, holographic, reflection gratings. We restrict our discussion to gratings which have refractive index variations only in the z direction (see Figure 2-1).

The field transmitted by such a grating, when it is illuminated by a plane wave, will be another plane wave propagating in the same direction as the incident plane wave [1]. The phase and amplitude of this transmitted plane wave will, however, differ from the incident one. The field reflected by such a grating, when it is illuminated by a plane wave, will be another plane wave. Its x and y directional cosines will be identical with those of the incident plane wave, and its z directional cosine will be of opposite sign. As in the case of transmission, the phase and amplitude of the reflected plane wave will differ from the incident one.

Any monochromatic wavefront can be described, through a Fourier transform decomposition, as the superposition of plane waves. A flat, holographic, reflection grating is a linear device, therefore the field scattered by it (i.e., the transmitted and reflected fields) can be written as the sum of the scattered fields resulting from each plane wave component of the incident field. Thus, linear system theory can be applied, and the input-output transfer function of a flat, holographic, reflection grating derived.

From the above discussion, we note that the characteristics of the holographic grating can be completely described by two frequency domain transfer functions, $H_T(f_x, f_y)$ and $H_R(f_x, f_y)$. $H_T(f_x, f_y)$ is the transfer function for the transmission case, and $H_R(f_x, f_y)$ is the transfer function for the reflection case. Both $H_R(f_x, f_y)$ and $H_T(f_x, f_y)$ are complex and may be written as

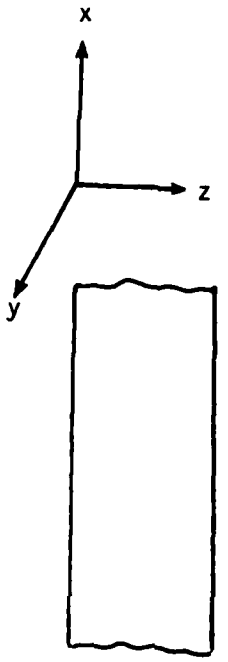

Refractive Index = n(z)

Figure 2-1. Holographic Reflection Grating

$$H_T(f_x, f_y) = |H_T(f_x, f_y)| \exp(i\phi_T(f_x, f_y)) \quad (2\text{-}1)$$

$$H_R(f_x, f_y) = |H_R(f_x, f_y)| \exp(i\phi_R(f_x, f_y)) \quad (2\text{-}2)$$

$H_T(f_x, f_y)$ is the ratio of the complex electric field amplitude of the transmitted wave to the complex electric field amplitude of the incident wave. $H_R(f_x, f_y)$ is the ratio of the complex electric field amplitude of the reflected wave to the complex electric field amplitude of the incident wave. λf_x and λf_y are the x and y directional cosines, respectively, of the incident wave (λ is the wavelength of the incident wave).

Initially, our discussion will be restricted to the transmission case, the reflection case is analogous. It is also assumed that we are working in spatially and temporally coherent light. Consider the situation shown in Figure 2-2. A wavefront is propagating to the right. In plane one, this wavefront has a spatial distribution of amplitude and phase given by

$$a_I(x, y) = |a_I(x, y)| \exp(i\phi_I(x, y)) \quad (2\text{-}3)$$

In plane one this wavefront can be equivalently described in the frequency domain by [2]

$$A_I(f_x, f_y) = |A_I(f_x, f_y)| \exp(i\Phi_I(f_x, f_y)) \quad (2\text{-}4)$$

where

$$A_I(f_x, f_y) = \int_{-\infty}^{\infty}\int_{-\infty}^{\infty} a_I(x, y) \exp[-i2\pi(f_x x + f_y y)]dxdy \quad (2\text{-}5a)$$

$$a_I(x, y) = \int_{-\infty}^{\infty}\int_{-\infty}^{\infty} A_I(f_x, f_y) \exp[i\frac{2\pi}{\lambda}(\lambda f_x x + \lambda f_y y)df_x df_y \quad (2\text{-}5b)$$

The wavefront in propagating between plane one and the front surface of the holographic grating traverses free space. The transfer function describing free space propagation between two planes separated by a distance d is [2]

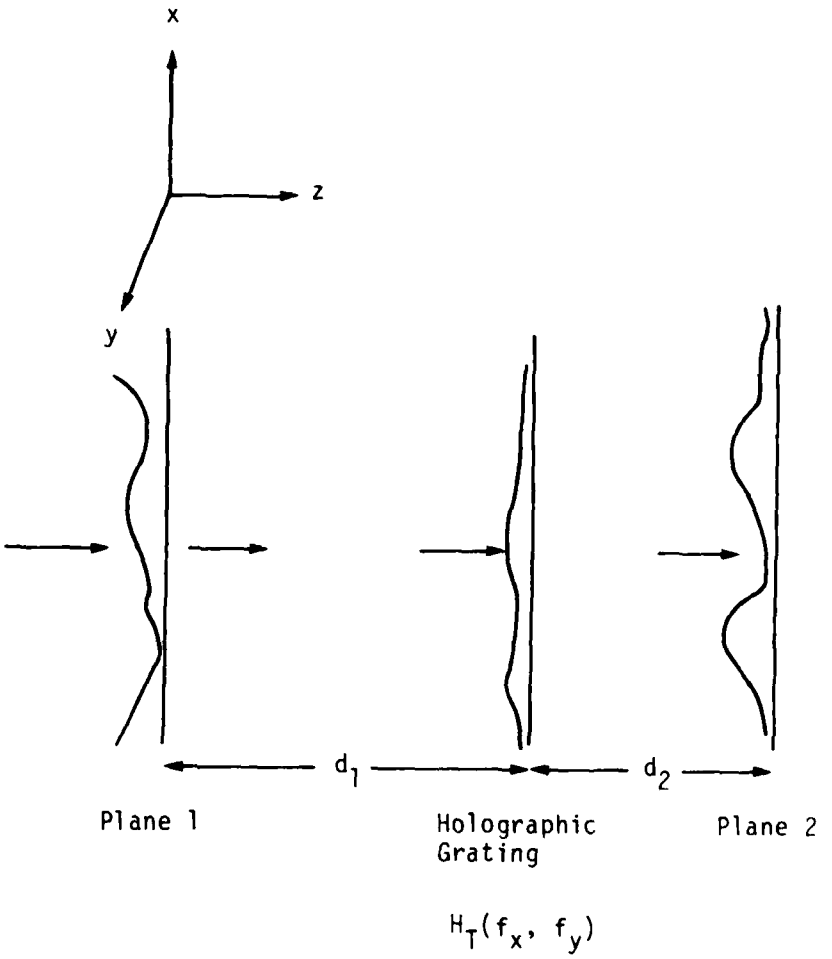

Figure 2-2. Transmission through a Holographic Reflection Grating

$$\mathfrak{H}(f_x, f_y; d) = \exp[-i\pi\lambda d(f_x^2 + f_y^2)] \qquad (2\text{-}6)$$

Thus, the wavefront at the front surface holographic grating is given in the frequency domain by

$$A_I(f_x, f_y)\mathfrak{H}(f_x, f_y; d_1) \qquad (2\text{-}7)$$

and at the back surface by

$$A_I(f_x, f_y)\mathfrak{H}(f_x, f_y; d_1)H_T(f_x, f_y) \qquad (2\text{-}8)$$

The wavefront once again propagates through free space between the back surface of the holographic grating and plane two. The wavefront at plane two is described in the frequency domain by

$$A_I(f_x, f_y)\mathfrak{H}(f_x, f_y; d_1)H_T(f_x, f_y)\mathfrak{H}(f_x, f_y; d_2) \qquad (2\text{-}9)$$

We note that

$$\mathfrak{H}(f_x, f_y; d_1)\mathfrak{H}(f_x, f_y; d_2) = \mathfrak{H}(f_x, f_y; d_1 + d_2) \qquad (2\text{-}10)$$

Thus Eq. (2-9) can be rewritten as

$$A_I(f_x, f_y)H_T(f_x, f_y)\mathfrak{H}(f_x, f_y; d_1 + d_2) \qquad (2\text{-}11)$$

Eq. (2-11) indicates that the transfer function relating plane one to plane two is

$$\mathfrak{H}(f_x, f_y; d_1 + d_2)H_T(f_x, f_y) \qquad (2\text{-}12)$$

The following conclusions can be drawn from Eq. (2-12)

1. The holographic grating acts as a frequency domain filter. It changes both the amplitude and phase of the incident frequency components.
2. The relationship between the wavefront at plane two and the wavefront at plane one depends <u>only</u> upon $H_T(f_x, f_y)$ and the distance d_1+d_2 between plane one and plane two.

This relationship does not depend upon the value of d_1 or d_2 alone. For example, consider the two systems shown in Figure 2-3. If the wavefront at plane one is identical in both systems, then both systems will have identical wavefronts at plane two.

We investigate the use of the holographic grating as a frequency domain filter. Suppose the holographic grating is placed immediately behind plane one (i.e., $d_1 = 0$), then by Eqs. (2-6), (2-7) and (2-8) the frequency domain description of the wavefront at the back surface of the element will be

$$A_I(f_x, f_y)H_T(f_x, f_y) \tag{2-13}$$

The back surface of the holographic grating can be imaged using conventional refractive optics onto a distant plane [3]. The frequency domain relationship between the wavefront at plane one and the wavefront at this distant image is given by Eq. (2-14)

$$A_I^*(-f_x, -f_y)H_T^*(-f_x, -f_y) \tag{2-14}$$

We note that in the spatial domain the wavefronts given by Eqs. (2-13) and (2-14) are conjugates. This conjugation always results from conventional refractive optics of imaging systems. The distinction is actually meaningless in the image plane where the intensity of conjugate wavefronts are identical. Thus, $H_T^*(-f_x, -f_y)$ is the transfer function between plane one and the image plane. A system for performing frequency domain filtering is shown in Figure 2-4, where we represent the conventional refractive optics imaging system by a single lens. It should be noted that conclusion two above implies that the holographic grating can be located anywhere between plane one and the refractive optics imaging system without changing the system transfer function. Therefore, the system in Figure 2-5 has the same transfer function as the system in Figure 2-4.

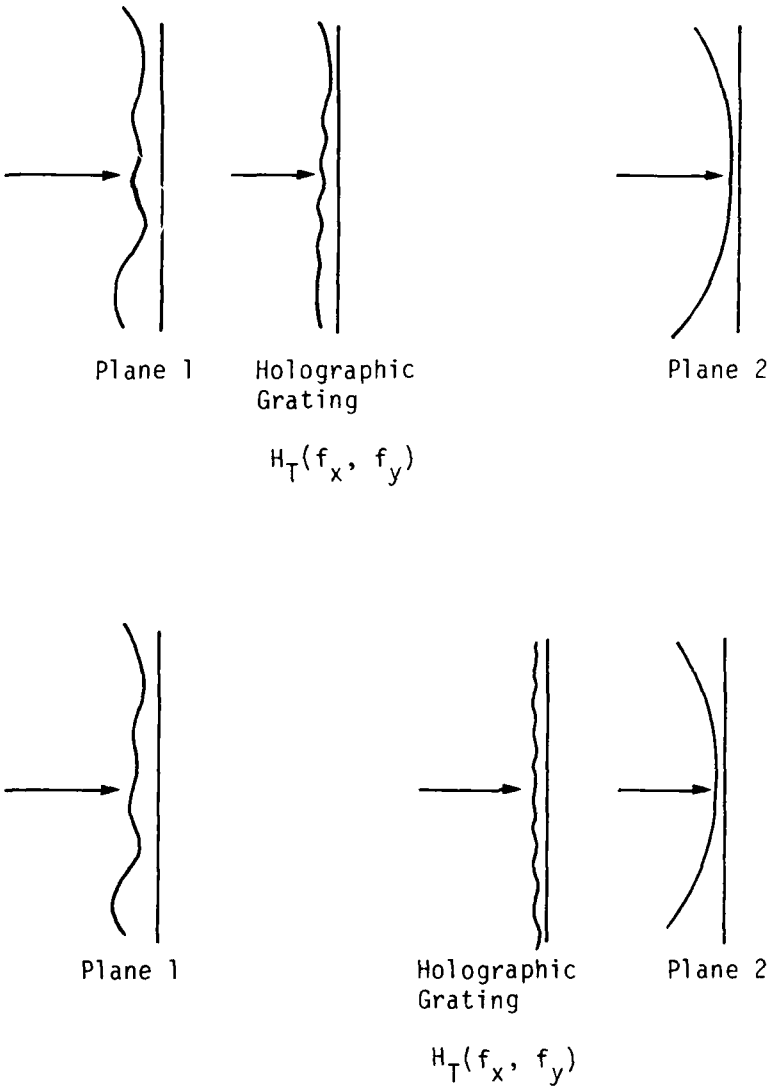

Figure 2-3. Position Invariant Property

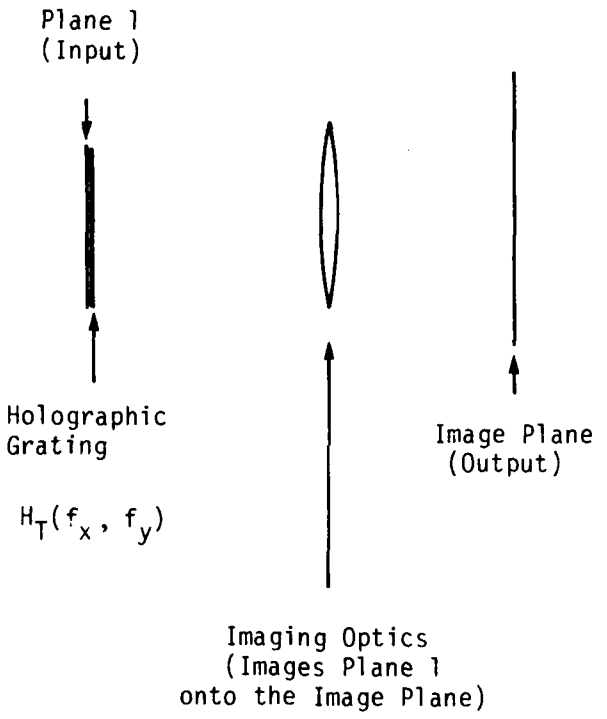

Figure 2-4. Single Grating Frequency Domain Filtering System

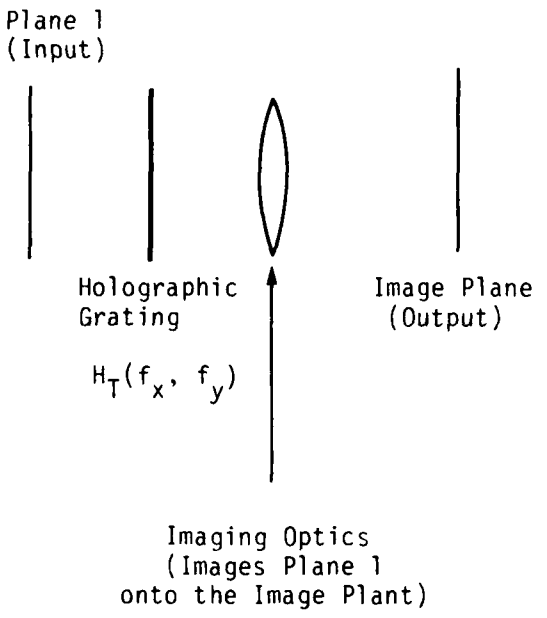

Figure 2-5. **Position Invariant Property of Frequency Domain Filtering System**

We have described a system which is capable of performing frequency domain filtering. The principal component of this system is a flat, holographic, reflection grating which has a refractive index variation only in a direction normal to its surface. The transfer function of this system is given by $H_T^*(-f_x, -f_y)$. It is natural then to investigate the characteristics of $H_T(f_x, f_y)$.

From symmetry considerations it is clear that $H_T(f_x, f_y)$ is circularly symmetric, i.e.,

$$H_T(f_x, f_y) = H_T\left(\sqrt{f_x^2 + f_y^2}\right) \tag{2-15}$$

Also, it should be noted that $H_T(f_x, f_y)$ is a complex quantity as is indicated by Eq. (2-1). Given the refractive index profile, $n(z)$, it is possible to determine $H_T(f_x, f_y)$. We have performed such a calculation (actually we computed $H_R(f_x, f_y)$ for the case where $n(z)$ is sinusoidal). A holographic grating having such a refractive index profile can be fabricated by recording the interference pattern of two plane waves as shown in Figure 2-6. The $H_R(f_x, f_y)$ corresponding to this element is shown in Figures 2-7 and 2-8. The relationship between the θ given in Figures 2-7 and 2-8 and (f_x, f_y) is

$$\cos \theta_0 = \sqrt{1 - (\lambda f_x)^2 - (\lambda f_y)^2} \tag{2-16}$$

Eq. (2-15) can therefore be written as

$$H_T(f_x, f_y) = H_T(\lambda_1, \theta_0) \tag{2-17}$$

Consider the setup shown in Figure 2-9. An input transparency is illuminated by a collimated beam at normal incidence. The light transmitted by the transparency passes through a beamsplitter and then strikes the holographic grating shown earlier in Figure 2-6. The light reflected by the holographic grating is redirected by the

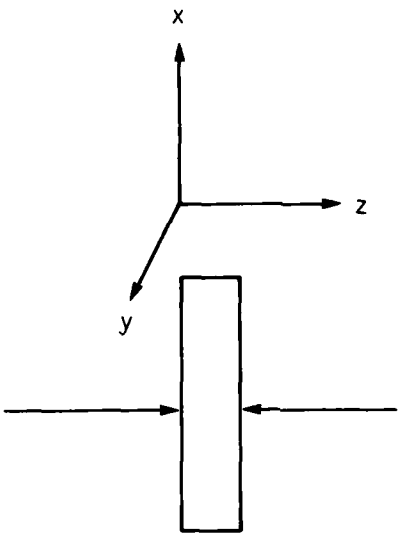

$$n(z) = n_0 + n_1 \sin 2\pi fz$$

Figure 2-6. Geometry for Fabricating a Holographic Reflection Grating

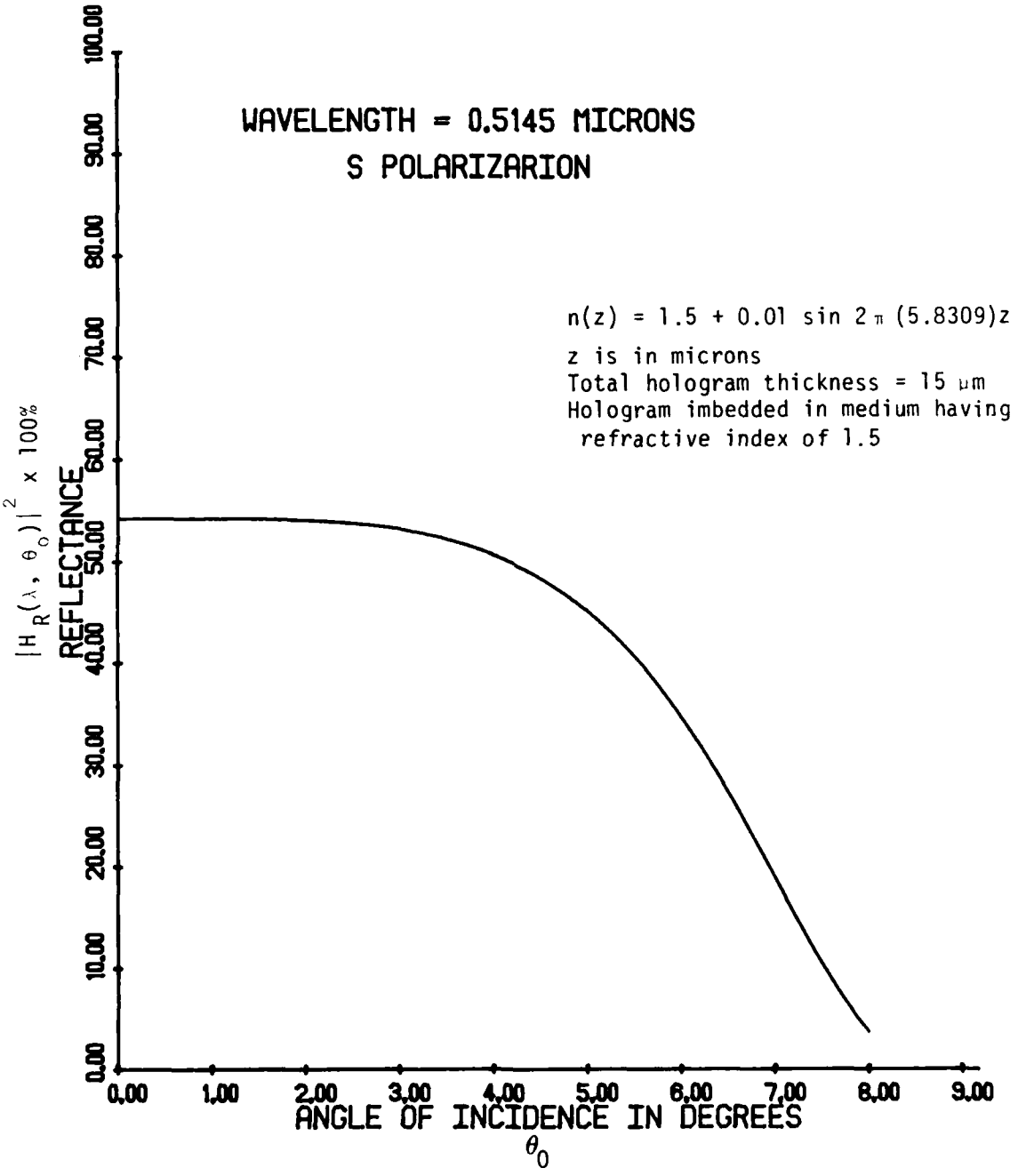

Figure 2-7. Reflectance vs. Angle of Incidence Characteristic

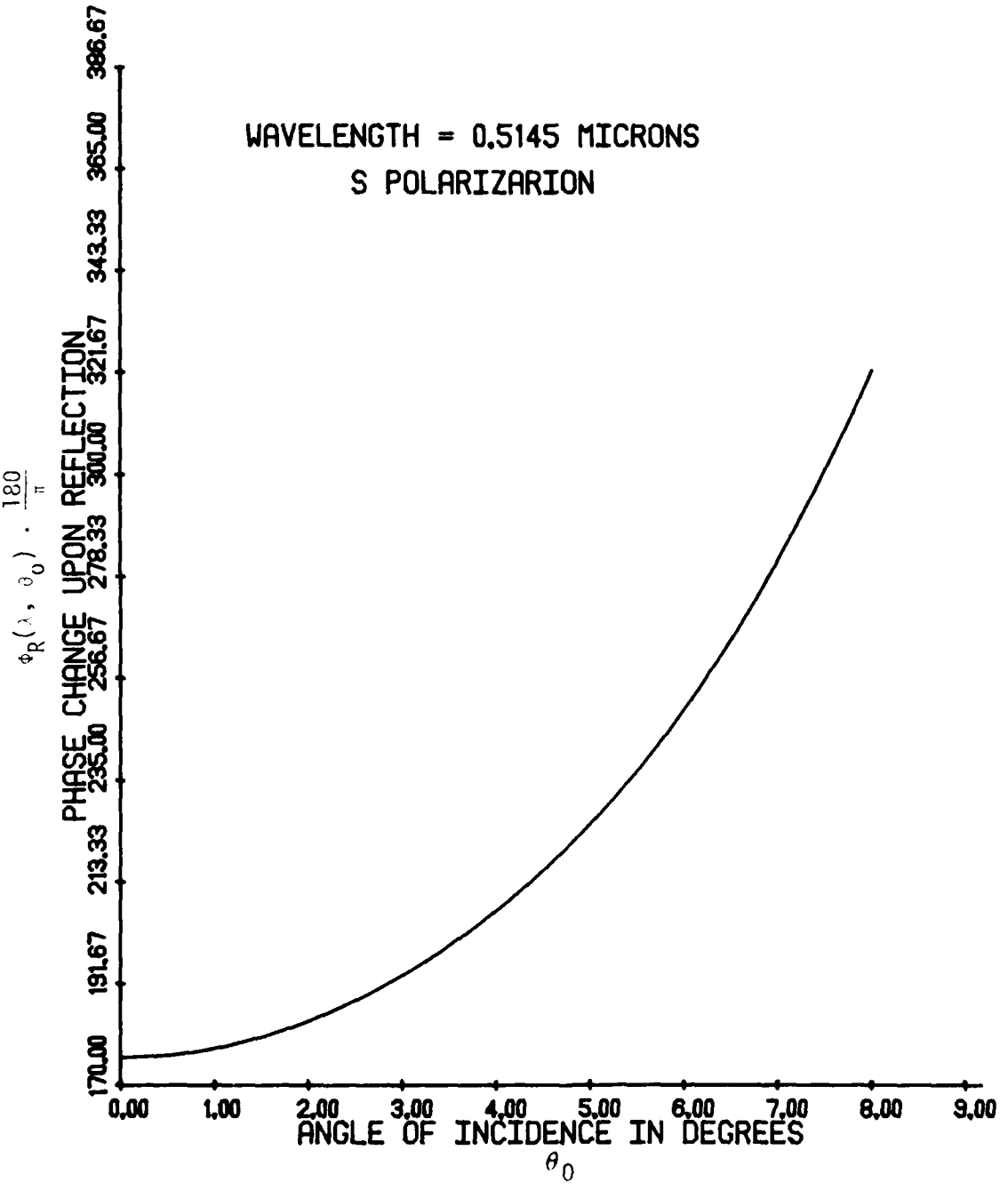

Figure 2-8. Phase Change Upon Reflection vs. Angle of Incidence Characteristic

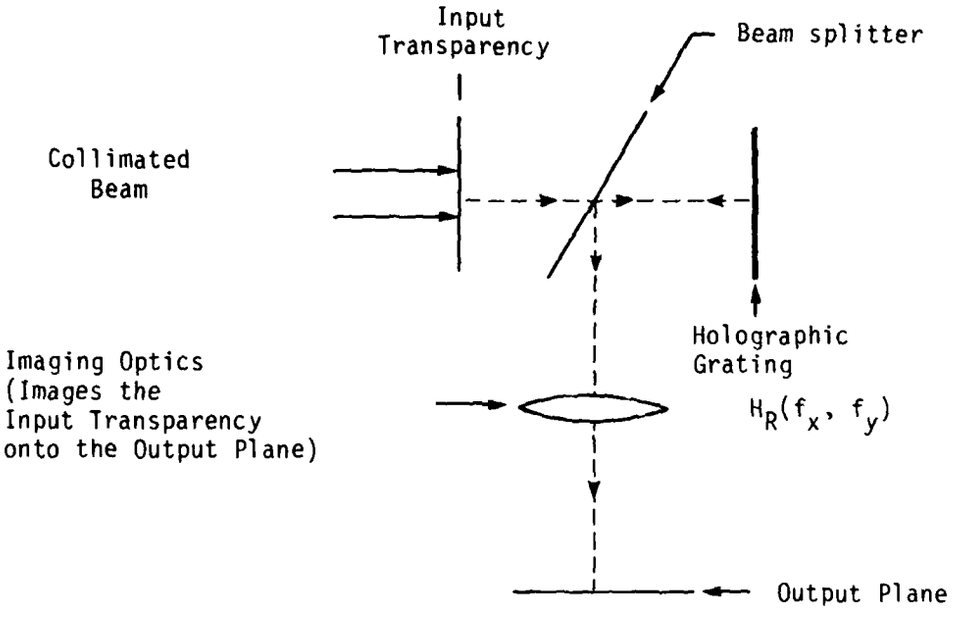

Figure 2-9. Holographic Mirror System

beamsplitter to pass through some refractive optics which image the input transparency onto an output plane. Following our earlier analysis, we designate the spatial distribution of amplitude and phase of the wavefront at the back surface of the transparency by $a_I(x, y)$. The frequency domain description of this wavefront is $A_I(f_x, f_y)$. In the output plane the frequency domain description of the wavefront is

$$A_I^*(-f_x, -f_y)H_R^*(-f_x, -f_y) \tag{2-18}$$

where $H_R(f_x, f_y)$ is the transfer function of the holographic grating. Typically a transparency will have spatial frequency components up to 100 ℓ/mm. Thus we can write

$$A_I(f_x, f_y) = 0 \text{ for } f_x > 100 \text{ ℓ/mm or } f_y > 100 \text{ ℓ/mm} \tag{2-19}$$

If $\lambda = 5145\text{Å}$, then by Eqs. (2-16) through (2-19) it is clear that the only segment of $H_R(\lambda, \theta_o)$ which will affect the wavefront in the output plane is the segment described by

$$0^\circ \leq \theta \leq \cos^{-1}\left(\sqrt{1 - (0.5145)^2(0.1)^2 - (0.5145)^2(0.1)^2}\right) \simeq 4.2^\circ \tag{2-20}$$

From Figure 2-7, it can be seen that $|H_R(\lambda, \theta_o)|$ is reasonably flat between 0° and 4.2°. Thus, this particular holographic grating does not change the relative amplitudes of the input transparencies frequency components. Next we examine the exp $[i\Phi_R(\lambda, \theta_o)]$ term of the frequency response. Φ_R vs θ_o varies by about 30° (or 0.083 wavelengths) in the range between $0^\circ \leq \theta_o \leq 4.2^\circ$. For θ small, we note for completeness that Eq. (2-16) can be written approximately as

$$\theta = \lambda f_x + \lambda f_y \tag{2-21}$$

where θ_o is in radians. Small variations in the phase change upon reflection as a function of (f_x, f_y) will introduce aberrations

into the image, though these may not be readily discernible. A linear phase shift upon reflection, measured as a function of (f_x, f_y) has no effect on the image formed in the output plane except that of translation.

Most individuals familar with holographic optical elements would expect the system shown in Figure 2-9 to behave as a mirror. It should be noted however this result is actually very surprising. It is surprising because this mirror like behavior requires the holographic grating to display as a function of f_x and f_y a very small or a nearly linear phase change upon reflection over the principal reflection band of the filter. We note that a similar situation occurs in the case of multilayer dielectric mirrors [4]. These mirrors are observed to form virtually unaberrated images upon reflection. This requires that the phase change upon reflection of such a mirror be a very small or nearly linear function of f_x and f_y over the principal range of frequencies which the mirror reflects. For an arbitrary refractive index profile, $n(z)$, $\Phi_R(f_x, f_y)$ and $\Phi_T(f_x, f_y)$ are neither very small nor linear functions of f_x and f_y over the entire range of f_x and f_y. Under what conditions and over what ranges are they are linear This question remains to be answered. This is an important consideration when filtering is to be performed using this type of holographic grating.

We explore further the use of flat holographic gratings which have refractive index variations only in a direction normal to their surface. In the previous discussion we have assumed that the holographic grating is oriented so that its surface is parallel to the input plane. This, we recall, guaranteed that the grating response be circularly symmetric in (f_x, f_y).

Now suppose that the grating is rotated by α degrees about its y-axis and by β degrees about the x-axis (+ degrees indicates

clockwise rotation while - degrees indicates counterclockwise rotation). Then we can write

$$H_T^{\alpha,\beta}(f_x,f_y) = H_T\left(\sqrt{1-\sin^2(\sin^{-1}(\lambda f_x)-\alpha)-\sin^2(\sin^{-1}(\lambda f_y)+\beta)}\right) \quad (2\text{-}22)$$

where $H_T^{\alpha,\beta}(f_x, f_y)$ is the transfer function of the grating when it is rotated by α degrees about the y axis and by β degrees about the x axis. $H_T(f_x, f_y)$ is the transfer function of the grating when it is not rotated at all. It should be noted that the grating, when rotated, has a transfer function which is not circularly symmetric. Furthermore and perhaps more significantly, the response of the grating is not the same in the $f_x = 0$ plane as in the $f_y = 0$ plane.

Consider now the situation shown in Figure 2-10. An input plane is imaged onto an output plane by conventional refractive optics. A [illegible] grating having a system transfer function $H_T(f_x,$ [illegible] distance d_1 from the input plane. Another holo[illegible] having a system transfer function $H_{T_2}(f_x,$ f_y [illegible] a distance d_2 from the output plane. A wavefront is p[illegible] from left to right in this system. In the frequency domain, the wavefront at the input plane will be described by

$$A_I(f_x, f_y)$$

Let us imagine for the moment that $H_{T_2}(f_x, f_y) = 1$. This is equivalent to removing the second holographic grating from the system. Then at the output plane

$$A_I^*(-f_x, -f_y)H_{T_1}^*(-f_x,-f_y) \quad (2\text{-}23)$$

gives the frequency domain description of the wavefront. At a distance d_2 from the output plane, the wavefront is described by

$$A_I^*(-f_x, -f_y)H_T^*(-f_x, -f_y)\mathcal{G}^{-1}(f_x, f_y;d_2) \quad (2\text{-}24)$$

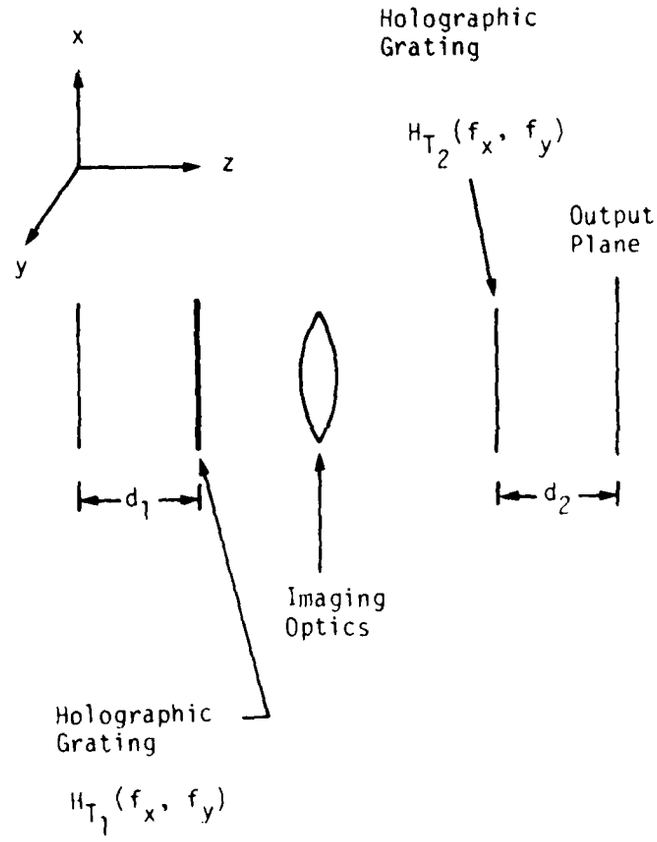

Figure 2-10. Two Grating Filtering System

Thus, with $H_{T_2}(f_x, f_y)$ not identically equal to 1, the wavefront at the output plane will be given by

$$A_I^*(-f_x, -f_y)H_{T_1}^*(-f_x,-f_y)\mathcal{F}^{-1}(f_x,f_y;d_2)H_{T_2}(f_x,f_y)\mathcal{F}(f_x, f_y;d_2) \quad (2\text{-}25)$$

Hence, we rewrite Eq. (2-25) as

$$A_I^*(-f_x, -f_y)H_{T_1}^*(-f_x, -f_y)H_{T_2}(f_x, f_y) \quad (2\text{-}26)$$

Therefore,

$$H_{T_1}^*(-f_x, -f_y)H_{T_2}(f_x, f_y) \quad (2\text{-}27)$$

is the frequency domain transfer function of the system.

Now if

$$H_{T_2}(f_x, f_y) = H_{T_1}(-f_x, -f_y) \quad (2\text{-}28)$$

Then Eq. (26) becomes

$$A_I^*(-f_x, -f_y)\left|H_{T_1}(-f_x, -f_y)\right|^2 \quad (2\text{-}29)$$

We note that:

1. Eq. (2-26) describes in the frequency domain the wavefront at the output plane.
2. This wavefront is independent of the longitudinal positions, i.e., d_1 and d_2, of the holographic gratings
3. The above equations remain valid in the case where the holographical optical elements are rotated about their x and y axes if $H_{T_1}(f_x, f_y)$ is replaced by $H_{T_1}^{\alpha,\beta}(f_x, f_y)$ and and replaced by $H_{T_2}^{\alpha,\beta}(f_x, f_y)$.

4. From Eqs. (2-22) and (2-27) it is seen that the frequency domain transfer function of the system will be real if the two holographic gratings are identical, and if they are rotated by equal amounts but in opposite directions. By rotation of equal amounts but in opposite directions, we mean that $\alpha_1 = -\alpha_2$ and $\beta_1 = -\beta_2$.

5. Comment (4) indicates that a real transfer function can always be realized by using two identical holographic optical elements which have an arbitrary and perhaps unknown phase transfer function characteristic.

6. A situation analogous to what has been described above exists when the holographic gratings are used in the reflection rather than the transmission mode.

Notes to Chapter 2

[1] For simplicity, we assume that the grating is imbedded in mediums which match it in refractive index at its front and rear surfaces.

[2] J.W. Goodman, Introduction to Fourier Optics, McGraw-Hill, New York, 1968.

[3] A telescope system could be used to perform the imaging.

[4] W.G. Driscoll, Handbook of Optics, Optical Society of America, McGraw-Hill Co., New York, 1978.

3
THE THEORY OF DISCRETE HORIZONTALLY STRATIFIED MEDIA

This chapter presents the theory of electromagnetic wave propagation through discrete horizontally stratified media. The theory was first published by Abeles in 1950 [1]. Our development is similar to one given by Knittl [2]. The theory is presented in an effort to make this report self-contained.

Given the description of a discrete, horizontally stratified, dielectric media, i.e., the number of layers, thickness of each layer and refractive index or each layer, we will determine the reflectance, phase change upon reflection, transmittance and phase change upon transmission of the media when illuminated by an s (TE) or p (TM) polarized plane wave of arbitrary frequency at an arbitrary angle of incidence. In the notation of chapter two, this is *equivalent to determining* $H_R(\lambda, \theta_o)$ *and* $H_T(\lambda, \theta_o)$.

Consider the structure shown in Figure 3-1. It consists of N parallel homogeneous, isotropic dielectric layers each assumed to be of infinite extent in the x and y directions. The j^{th} layer is of thickness d_j measured in microns and has refractive index $n_{(j)}$. The refractive index, $n_{(j)}$ is given by

$$\sqrt{\frac{\epsilon_{(j)}\mu_{(j)}}{\epsilon_o \mu_o}}$$

where $\epsilon_{(j)}$ and $\mu_{(j)}$ are the permittivity and permeability, respectively, of the j^{th} layer, and ϵ_o and μ_o are the permittivity and permeability, respectively, of free space. It is assumed that $\mu_{(j)}$ equals μ_o. For notational convenience the region above layer 1 will be designated as layer 0, while the region below N will be designated layer N+1. We make the following definitions

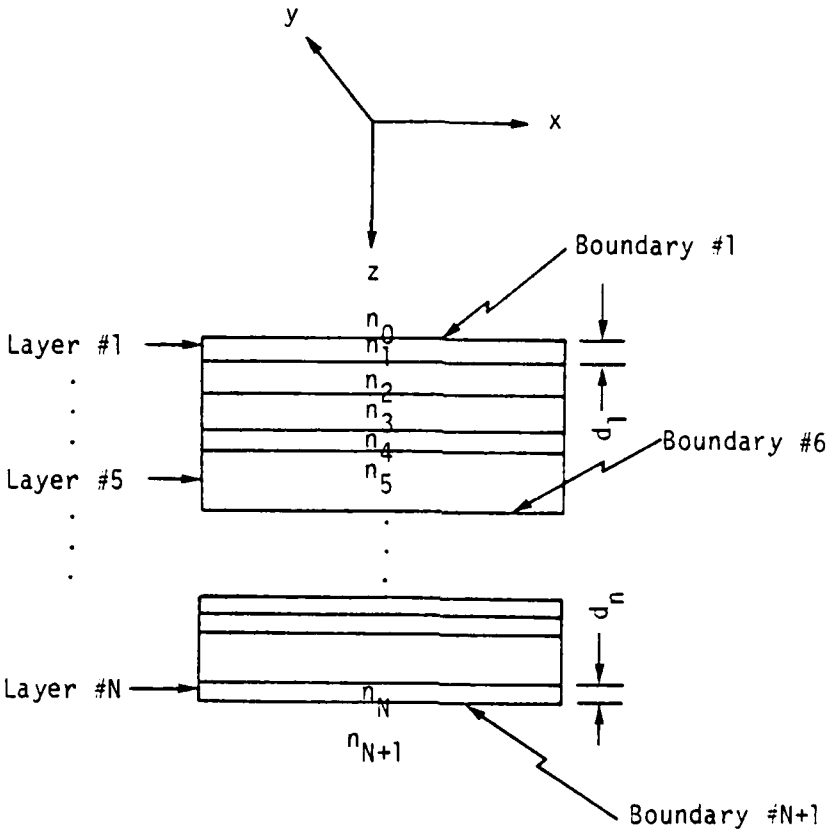

Figure 3-1. A Discrete Horizontally Stratified Dielectric Structure

$$\theta_{(j)} \overset{\Delta}{=} \sin^{-1}\left(\frac{n_0 \sin\theta_0}{n_{(j)}}\right)$$

$$Y_{(j)} \overset{\Delta}{=} \begin{cases} \dfrac{n_{(j)}\cos\theta_{(j)}}{\sqrt{\mu_0/\epsilon_0}}, & \text{for s polarization} \\ \dfrac{-n_{(j)}}{(\cos\theta_{(j)})\sqrt{\dfrac{\mu_0}{\epsilon_0}}}, & \text{for p polarization} \end{cases}$$

$$V_{(i)} \overset{\Delta}{=} \begin{bmatrix} 1 & 1 \\ Y_{(j)} & -Y_{(j)} \end{bmatrix}$$

$$\phi_{(j)} \overset{\Delta}{=} \frac{2\pi}{\lambda} n_{(j)} d_{(j)} \cos\theta_{(j)}$$

$$U_{(j)} \overset{\Delta}{=} \begin{bmatrix} \exp(i\phi_{(j)}) & 0 \\ 0 & \exp(-i\phi_{(j)}) \end{bmatrix}$$

$$U_{(o)} = U_{(N+1)} \overset{\Delta}{=} \begin{bmatrix} 1 & 0 \\ 0 & 1 \end{bmatrix}$$

$$M_{(j)} \overset{\Delta}{=} V_{(j)} U_{(j)} V^{-1}_{(j)}$$

$$S = \begin{bmatrix} S_{11} & S_{12} \\ S_{21} & S_{22} \end{bmatrix} \overset{\Delta}{=} \prod_{j=0}^{N+1} M_{(j)}$$

In the remaining portions of this chapter, it will be shown that

$$H_R(\lambda, \theta_0) = \begin{cases} \dfrac{S_{21}}{S_{11}}, & \text{for s polarization} \\ \dfrac{S_{21}}{S_{11}}, & \text{for p polarization} \end{cases}$$

and

$$H_T(\lambda, \theta_0) = \begin{cases} \frac{1}{S_{11}}, & \text{for s polarization} \\ \frac{1}{S_{11}} \frac{\cos \theta_0}{\cos \theta_{(N+1)}}, & \text{for p polarization} \end{cases}$$

where λ is the wavelength of the incident phase wave and θ_0 is the angle at which the incident plane wave is propagating with respect to the z axis.

Maxwell's phasor wave equation for the electric field in a homogeneous isotropic dielectric is given by Eq. (3-1) below

$$\frac{\partial^2 E_x}{\partial x^2} + \frac{\partial^2 E_x}{\partial y^2} + \frac{\partial^2 E_x}{\partial z^2} + K^2 E_x = 0 \qquad (3\text{-}1a)$$

$$\frac{\partial^2 E_y}{\partial x^2} + \frac{\partial^2 E_y}{\partial y^2} + \frac{\partial^2 E_y}{\partial z^2} + K^2 E_y = 0 \qquad (3\text{-}1b)$$

$$\frac{\partial^2 E_z}{\partial x^2} + \frac{\partial^2 E_z}{\partial y^2} + \frac{\partial^2 E_z}{\partial z^2} + K^2 E_z = 0 \qquad (3\text{-}1c)$$

where $K = \omega\sqrt{\mu\varepsilon}$. ω is the frequency in radians while ε and μ are the permittivity and permeability of the dielectric respectively. It is noted that

$$E_x = E_{xR} + E_{xL} \qquad (3\text{-}2a)$$

$$E_y = E_{yR} + E_{yL} \qquad (3\text{-}2b)$$

$$E_z = E_{zR} + E_{zL} \qquad (3\text{-}2c)$$

where

$$E_{XR} = ae^{iK((\sin\theta)y-(\cos\theta)z)} \tag{3-3a}$$

$$E_{YR} = 0 \tag{3-3b}$$

$$E_{ZR} = 0 \tag{3-3c}$$

$$E_{XL} = be^{ik((\sin\theta)y+(\cos\theta)z)} \tag{3-4a}$$

$$E_{YL} = 0 \tag{3-4b}$$

$$E_{ZL} = 0 \tag{3-4c}$$

with a, b, and θ arbitrary constants satisfies the wave equations. A solution of the wave equation (3-1) is a solution of Maxwell's Equations if it also satisfies $\nabla\cdot(E_x\hat{x} + E_y\hat{y} + E_z\hat{z}) = 0$ which is one of Maxwell's four equations. Thus, Eq. (3-2) is a solution of Maxwell's Equations. With reference to Figure 3-1, Eq. (3-2) represents the superposition of two s-polarized plane waves, one traveling in the direction of increasing z and the others traveling in the direction of decreasing z. Furthermore, the phasor components, H_x, H_y, and H_z of the magnetic field are related to the phasor components, E_x, E_y, and E_z of the electric field by one of Maxwell's Equations. The relationship is given below

$$H_x = \frac{i}{\omega\mu}\left(\frac{\partial E_z}{\partial y} - \frac{\partial E_y}{\partial z}\right) \tag{3-5a}$$

$$H_y = \frac{i}{\omega\mu}\left(\frac{\partial E_x}{\partial z} - \frac{\partial E_z}{\partial x}\right) \tag{3-5b}$$

$$H_z = \frac{i}{\omega\mu}\left(\frac{\partial E_y}{\partial x} - \frac{\partial E_x}{\partial y}\right) \tag{3-5c}$$

Therefore, the magnetic field corresponding to the electric field given by Eqs. (3-2), (3-3), and (3-4) is

$$H_x = H_{xR} + H_{xL} \tag{3-6a}$$

$$H_y = H_{yR} + H_{yL} \tag{3-6b}$$

$$H_z = H_{zR} + H_{zL} \tag{3-6c}$$

where

$$H_{xR} = 0 \tag{3-7a}$$

$$H_{yR} = \sqrt{\frac{\epsilon}{\mu}} \cos\theta\, E_{xR} \tag{3-7b}$$

$$H_{zR} = \sqrt{\frac{\epsilon}{\mu}} \sin\theta\, E_{xR} \tag{3-7c}$$

$$H_{xL} = 0 \tag{3-8a}$$

$$H_{yL} = -\sqrt{\frac{\epsilon}{\mu}} \cos\theta\, E_{xL} \tag{3-8b}$$

$$H_{zL} = \sqrt{\frac{\epsilon}{\mu}} \sin\theta\, E_{xL} \tag{3-8c}$$

Similarly Maxwell's phasor wave equation for the magnetic field in a homogeneous, isotropic dielectric is given by Eq. (3-9) below

$$\frac{\partial^2 H_x}{\partial x^2} + \frac{\partial^2 H_x}{\partial y^2} + \frac{\partial^2 H_x}{\partial z^2} + K^2 H_x = 0 \tag{3-9a}$$

$$\frac{\partial^2 H_y}{\partial x^2} + \frac{\partial^2 H_y}{\partial y^2} + \frac{\partial^2 H_y}{\partial z^2} + K^2 H_y = 0 \tag{3-9b}$$

$$\frac{\partial^2 H_z}{\partial x^2} + \frac{\partial^2 H_z}{\partial y^2} + \frac{\partial^2 H_z}{\partial z^2} + K^2 H_z = 0 \tag{3-9c}$$

where $K = \omega\sqrt{\mu\epsilon}$ as before. A solution of the wave equation is

$$H_x = H_{xR} + H_{xL} \tag{3-10a}$$

$$H_y = H_{yR} + H_{yL} \tag{3-10b}$$

$$H_z = H_{zR} + H_{zL} \tag{3-10c}$$

where

$$H_{xR} = ae^{iK((\sin\theta)y - (\cos\theta)z)} \tag{3-11a}$$

$$H_{yR} = 0 \tag{3-11b}$$

$$H_{zR} = 0 \tag{3-11c}$$

$$H_{xL} = be^{iK((\sin\theta)y + (\cos\theta)z)} \tag{3-12a}$$

$$H_{yL} = 0 \tag{3-12b}$$

$$H_{zL} = 0 \tag{3-12c}$$

with a, b, and e arbitrary constants. With reference to Figure 1, Eq. (3-10) represents the superposition of two p-polarized plane waves, one traveling in the direction of increasing z and the other traveling in the direction of decreasing z. A solution of the wave equation (3-9) is a solution of Maxwell's Equations if in addition it also satisfies

$$\nabla \cdot (H_x\hat{x} + H_y\hat{y} + H_z\hat{z}) = 0$$

which is one of Maxwell's four equations. Furthermore, the phasor components, E_x, E_y, and E_z, of the electric field are related to the phasor components, H_x, H_y, and H_z, of the magnetic field by one of Maxwell's equations. The relationship is given below

$$E_x = \frac{-i}{\omega\epsilon}\left(\frac{\partial H_z}{\partial y} - \frac{\partial H_y}{\partial z}\right) \tag{3-13a}$$

$$E_y = \frac{-i}{\omega\epsilon}\left(\frac{\partial H_x}{\partial z} - \frac{\partial H_z}{\partial x}\right) \tag{3-13b}$$

$$E_z = \frac{-i}{\omega\epsilon}\left(\frac{\partial H_y}{\partial x} - \frac{\partial H_x}{\partial y}\right) \tag{3-13c}$$

Therefore, the electric field corresponding to the magnetic field given by Eqs. (3-10), (3-11), and (3-12) is

$$E_x = E_{xR} + E_{xL} \tag{3-14a}$$

$$E_y = E_{yR} + E_{yL} \tag{3-14b}$$

$$E_z = E_{zR} + E_{zL} \tag{3-14c}$$

where

$$E_{xR} = 0 \tag{3-15a}$$

$$E_{yR} = -\sqrt{\frac{\mu}{\epsilon}}\cos\theta\, H_{xR} \tag{3-15b}$$

$$E_{zR} = -\sqrt{\frac{\mu}{\epsilon}}\sin\theta\, H_{xR} \tag{3-15c}$$

$$E_{xL} = 0 \tag{3-16a}$$

$$E_{yL} = \sqrt{\frac{\mu}{\epsilon}}\cos\theta\, H_{xL} \tag{3-16b}$$

$$E_{zL} = -\sqrt{\frac{\mu}{\epsilon}}\sin\theta\, H_{xL} \tag{3-16c}$$

Eqs. (3-2), (3-3), (3-4), (3-6), (3-7), and (3-8) constitute an s-polarized two plane wave solution of Maxwell's Equations within each layer of the dielectric stack shown in Figure 3-1, while Eqs. (3-10), (3-11), (3-12) (3-14), (3-15), and (3-16) constitute a p-polarized two plane wave solution of Maxwell's Equations within each layer of the dielectric stack. In order for the corresponding sets of equations to be valid solutions for the electromagnetic fields existing within the entire stack, Maxwell's boundary conditions must be satisfied at the interfaces between the layers. We wish to show that Maxwell's boundary conditions can be satisfied

by these equations by choosing appropriate values for a, b, and θ in each layer. Consider the i^{th} boundary and translate the coordinate system so that z = 0 at this boundary. Maxwell's six boundary conditions, i.e., continuity of the tangential components of E and H and continuity of the normal components of the D and B are given below:

$$E_x^{(j)} = E_x^{(j)'} \tag{3-17a}$$

$$E_y^{(j)} = E_y^{(j)'} \tag{3-17b}$$

$$H_x^{(j)} = H_x^{(j)'} \tag{3-17c}$$

$$H_y^{(j)} = H_y^{(j)'} \tag{3-17d}$$

$$\varepsilon_{(j)} E_z^{(j)} = \varepsilon_{(j+1)} E_z^{(j)} \tag{3-17e}$$

$$H_z^{(j)} = H_z^{(j)'} \tag{3-17f}$$

where superscript (j) denotes at the j^{tn} boundary on the $(j-1)^{th}$ layer side

superscript (j)' denotes at the j^{th} boundary on the j^{th} layer side

subscript (j) denotes in the j^{th} layer

Consider first the s-polarized case. Eqs. (3-17b), (3-17c), and (3-17e) are trivially satisfied for arbitrary $a_{(j-1)}$, $b_{(j-1)}$, $\theta_{(j-1)}$, $a_{(j)}$, $b_{(j)}$ and $\theta_{(j)}$. Boundary condition (3-17a) can be explicitly written as

$$a_{(j-1)} e^{iK_{(j-1)} \sin\theta_{(j-1)} y} + b_{(j-1)} e^{iK_{(j-1)} \sin\theta_{(j-1)} y} = a_{(j)} e^{iK_{(j)} \sin\theta_{(j)} y} + b_{(j)} e^{iK_{(j)} \sin\theta_{(j)} y} \tag{3-18}$$

Equation (3-18) implies

$$K_{(j-1)}\sin\theta_{(j-1)} = K_{(j)}\sin\theta_{(j)} \tag{3-19}$$

or equivalently

$$n_{(j-1)}\sin\theta_{(j-1)} = n_{(j)}\sin\theta_{(j)} \tag{3-20}$$

and

$$a_{(j-1)} + b_{(j-1)} = a_{(j)} + b_{(j)} \tag{3-21}$$

Equation (3-20) will be recognized as Snell's Law of Refraction. Boundary condition (3-17d) can be explicitly written as

$$\begin{aligned} &-\sqrt{\frac{\epsilon_{(j-1)}}{\mu_0}}\cos\theta_{(j-1)}\, a_{(j-1)} e^{iK_{(j-1)}\sin\theta_{(j-1)}y} \\ &+\sqrt{\frac{\epsilon_{(j-1)}}{\mu_0}}\cos\theta_{(j-1)}\, b_{(j-1)} e^{iK_{(j-1)}\sin\theta_{(j-1)}y} = \\ &-\sqrt{\frac{\epsilon_{(j)}}{\mu_0}}\cos\theta_{(j)}\, a_{(j)}\, e^{iK_{(j)}\sin\theta_{(j)}y} \\ &+\sqrt{\frac{\epsilon_{(j)}}{\mu_0}}\cos\theta_{(j)} b_{(j)} e^{iK_{(j)}\sin\theta_{(j)}y} \end{aligned} \tag{3-22}$$

Equation (3-22) implies, Eq. (3-19) above and also

$$n_{(j-1)}\cos\theta_{(j-1)}\left(a_{(j-1)} - b_{(j-1)}\right) = n_{(j)}\cos\theta_{(j)}\left(a_{(j)} - b_{(j)}\right) \tag{3-23}$$

By explicitly writing out boundary conditions (3-17f), it would be seen to be equivalent to boundary condition (3-17a). Solving Eqs. (3-21) and (3-23) simultaneously yields

$$a_{(j)} = \frac{\left[n_{(j)}\cos\theta_{(j)} + n_{(j-1)}\cos\theta_{(j-1)}\right]a_{(j-1)} + \left[n_{(j)}\cos\theta_{(j)} - n_{(j-1)}\cos\theta_{(j-1)}\right]b_{(j-1)}}{2n_{(j)}\cos\theta_{(j)}} \tag{3-24}$$

$$b_{(j)} = \frac{\left[n_{(j)}\cos\theta_{(j)} - n_{(j-1)}\cos\theta_{(j-1)}\right]a_{(j-1)} + \left[n_{(j)}\cos\theta_{(j)} + n_{(j-1)}\cos\theta_{(j-1)}\right]b_{(j-1)}}{2n_{(j)}\cos\theta_{(j)}} \qquad (3\text{-}25)$$

Thus, given $a_{(j-1)}$, $b_{(j-1)}$, and $\theta_{(j-1)}$, Eqs. (3-20), (3-24), and (3-25) determine the $a_{(j)}$, $b_{(j)}$, and $\theta_{(j)}$ necessary in order to satisfy the boundary conditions.

We repeat the above procedure for the p-polarized cases. Eqs. (3-17a), (3-17d), and (3-17f) are trivially satisfied for arbitrary $a_{(j-1)}$, $b_{(j-1)}$, $\theta_{(j-1)}$, $a_{(j)}$, $b_{(j)}$, and $\theta_{(j)}$. Boundary condition (3-17c) can be explicitly written as

$$a_{(j-1)}e^{iK_{(j-1)}\sin\theta_{(j-1)}y} + b_{(j-1)}e^{iK_{(j-1)}\sin\theta_{(j-1)}y} = \qquad (3\text{-}26)$$

$$a_{(j)}e^{iK_{(j)}\sin\theta_{(j)}y} + b_{(j)}e^{iK_{(j)}\sin\theta_{(j)}y}$$

Eq. (3-26) implies

$$K_{(j-1)}\sin\theta_{(j-1)} = K_{(j)}\sin\theta_{(j)} \qquad (3\text{-}27)$$

or equivalently

$$n_{(j-1)}\sin\theta_{(j-1)} = n_{(j)}\sin\theta_{(j)} \qquad (3\text{-}28)$$

and

$$a_{(j-1)} + b_{(j-1)} = a_{(j)} + b_{(j)} \qquad (3\text{-}29)$$

Boundary condition (3-17b) can be explicitly written as

$$-\sqrt{\frac{\mu_0}{\epsilon_{(j-1)}}}\cos\theta_{(j-1)}a_{(j-1)}e^{iK_{(j-1)}\sin\theta_{(j-1)}y} + \sqrt{\frac{\mu_0}{\epsilon_{(j-1)}}}\cos\theta_{(j-1)}b_{(j-1)}e^{iK_{(j-1)}\sin\theta_{(j-1)}y} =$$

$$-\sqrt{\frac{\mu_0}{\epsilon_{(j)}}}\cos\theta_{(j)}a_{(j)}e^{iK_{(j)}\sin\theta_{(j)}y} \qquad (3\text{-}30)$$

(Equation continued on next page)

$$+\sqrt{\frac{\mu_0}{\epsilon_{(j)}}}\cos\theta_{(j)}b_{(j)}e^{iK_{(j)}\sin\theta_{(j)}y}$$

Eq. (3-30) implies, Eq. (3-27) above and also

$$\frac{1}{n_{(j-1)}}\cos\theta_{(j-1)}\left[a_{(j-1)} - b_{(j-1)}\right] =$$

$$\frac{1}{n_{(j)}}\cos\theta_{(j)}\left[a_{(j)} - b_{(j)}\right] \qquad (3\text{-}31)$$

By explicitly writing out boundary condition (3-17e), it would be seen to be equivalent to boundary condition (3-17c). Solving equations (3-29) and (3-31) simultaneously yields

$$a_{(j)} = \frac{n_{(j)}\cos\theta_{(j-1)} + n_{(j-1)}\cos\theta_{(j)}}{2n_{(j-1)}\cos\theta_{(j)}}a_{(j-1)} + \frac{n_{(j-1)}\cos\theta_{(j)} - n_{(j)}\cos\theta_{(j-1)}}{2n_{(j-1)}\cos\theta_{(j)}}b_{(j-1)} \qquad (3\text{-}32)$$

$$b_{(j)} = \frac{n_{(j-1)}\cos\theta_{(j)} - n_{(j)}\cos\theta_{(j-1)}}{2n_{(j-1)}\cos\theta_{(j)}}a_{(j-1)} + \frac{n_{(j-1)}\cos\theta_{(j)} + n_{(j)}\cos\theta_{(j-1)}}{2n_{(j-1)}\cos\theta_{(j)}}b_{(j-1)} \qquad (3\text{-}33)$$

Thus, given $a_{(j-1)}$, $b_{(j-1)}$, and $\theta_{(j-1)}$, Eqs. (3-29), (3-32), and (3-33) determine the $a_{(j)}$, $b_{(j)}$, and $\theta_{(j)}$ necessary in order to satisfy the boundary conditions.

We have given a solution of Maxwell's Equations and the associated boundary conditions in the multilayer dielectric stack and the adjoining free space regions shown in Figure 3-1. The fields in each layer and the adjoining free space regions can be described by the superposition of two s or two p polarized plane waves. These plane waves propagate in the y-z plane and have directional cosines which are the same in the y direction and equal in magnitude but opposite in sign in the z direction. The amplitudes of these plane waves and their directional cosines will vary from layer to layer.

Define $Y_{(j)}$ by Eq. (3-34)

$$Y_{(j)} \triangleq \begin{cases} \dfrac{H_{YR_{(j)}}}{E_{XR_{(j)}}} & \text{, for s polarization} \\ \dfrac{H_{XR_{(j)}}}{E_{YR_{(j)}}} & \text{, for p polarization} \end{cases} \tag{3-34}$$

Then by Eqs. (3-7b) and (3-15b)

$$Y_{(j)} = \begin{cases} \dfrac{n_{(j)}\cos_{(j)}}{\sqrt{\mu_o/\varepsilon_o}} & \text{, for s polarization} \\ \dfrac{-n_{(j)}}{\cos\theta_{(j)}\sqrt{\mu_o/\varepsilon_o}} & \text{, for p polarization} \end{cases} \tag{3-35}$$

We also note from Eqs. (3-8b) and (3-16b) that

$$Y_{(j)} = \begin{cases} -\dfrac{H_{YL_{(j)}}}{E_{XL_{(j)}}} & \text{, for s polarization} \\ -\dfrac{H_{XL_{(j)}}}{E_{YL_{(j)}}} & \text{, for p polarization} \end{cases} \tag{3-36}$$

Next define

$$V_{(j)} \triangleq \begin{bmatrix} 1 & 1 \\ Y_{(j)} & -Y_{(j)} \end{bmatrix} \tag{3-37}$$

Then

$$V_{(j)}^{-1} = \frac{1}{2}\begin{bmatrix} 1 & Y_{(j)}^{-1} \\ 1 & -Y_{(j)}^{-1} \end{bmatrix} \tag{3-38}$$

For s polarization, the boundary conditions (3-17a) and (3-17d), which are the only nontrivial independent ones as we saw earlier, can be written as

$$V_{(j-1)} \begin{bmatrix} E_{XR}^{(j)} \\ E_{XL}^{(j)} \end{bmatrix} = V_{(j)} \begin{bmatrix} E_{XR}^{(j)'} \\ E_{XL}^{(j)'} \end{bmatrix} \tag{3-39}$$

For p polarization, the boundary conditions (3-17b) and (3-17c), which are the only nontrivial independent ones as we saw earlier, can be written as

$$V_{(j-1)} \begin{bmatrix} E_{YR}^{(j)} \\ E_{YL}^{(j)} \end{bmatrix} = V_{(j)} \begin{bmatrix} E_{YR}^{(j)'} \\ E_{YL}^{(j)'} \end{bmatrix} \tag{3-40}$$

Furthermore, for s-polarization we can write

$$\begin{bmatrix} E_{XR}^{(j)'} \\ E_{XL}^{(j)'} \end{bmatrix} = \begin{bmatrix} e^{i\phi_{(j)}} & 0 \\ 0 & e^{-i\phi_{(j)}} \end{bmatrix} \begin{bmatrix} E_{XR}^{(j+1)} \\ E_{XL}^{(j+1)} \end{bmatrix} \tag{3-41}$$

by Eqs. (3-3a) and (3-4a), while for the p-polarization case we can write

$$\begin{bmatrix} E_{YR}^{(j)'} \\ E_{YL}^{(j)'} \end{bmatrix} = \begin{bmatrix} e^{i\phi(j)} & 0 \\ 0 & e^{-i\phi(j)} \end{bmatrix} \begin{bmatrix} E_{YR}^{(j)} \\ E_{YL}^{(j)} \end{bmatrix} \tag{3-42}$$

by Eqs. (3-11a), (3-12a), (3-15b) and (3-16b). In both cases

$$\phi_{(j)} \triangleq K_{(j)}\, d_j \cos\theta_{(j)} \tag{3-43}$$

or equivalently

$$\phi_{(j)} = \frac{2\pi}{\lambda} n_{(j)}\, d_{(j)} \cos\theta_{(j)} \tag{3-44}$$

where λ is the free space wavelength corresponding to frequency ω. Combining Eqs. (3-39) and (3-41) yields in the case of s-polarization

$$\begin{bmatrix} E_{XR}^{(j)} \\ E_{XL}^{(j)} \end{bmatrix} = V_{(j-1)}^{-1}\, V_{(j)} U_{(j)} \begin{bmatrix} E_{XR}^{(j+1)} \\ E_{XL}^{(j+1)} \end{bmatrix} \tag{3-45}$$

where

$$U_{(j)} \triangleq \begin{bmatrix} e^{i\phi(j)} & 0 \\ 0 & e^{-i\phi(j)} \end{bmatrix} \tag{3-46}$$

Combining Eqs. (3-40) and (3-42) yields in the case of p-polarization

$$\begin{bmatrix} E_{YR}^{(j)} \\ E_{YL}^{(j)} \end{bmatrix} = V_{(j-1)}^{-1}\, V_{(j)}\, U_{(j)} \begin{bmatrix} E_{YR}^{(j+1)} \\ E_{YL}^{(j+1)} \end{bmatrix} \tag{3-47}$$

Using Eqs. (3-45) and (3-47) repeatedly, we can write

$$\begin{bmatrix} E_{XR}^{(0)} \\ E_{XL}^{(0)} \end{bmatrix} = V_{(0)}^{-1}(V_{(1)}U_{(1)}V_{(1)}^{-1})(V_{(2)}U_{(2)}V_{(2)}^{-1}) \cdots (V_{(N-1)}U_{(N-1)}V_{(N-1)}^{-1})(V_{(N)}U_{(N)}) \begin{bmatrix} E_{XR}^{(N+1)} \\ X_{XL}^{(N+1)} \end{bmatrix}$$

for s polarization (3-48)

and

$$\begin{bmatrix} E_{YR}^{(0)} \\ E_{YL}^{(0)} \end{bmatrix} = V_{(0)}^{-1}(V_{(1)}U_{(1)}V_{(0)}^{-1})(V_{(2)}U_{(2)}V_{(2)}^{-1}) \cdots (V_{(N-1)}U_{(N-1)}V_{(N-1)})(V_{(N)}U_{(N)}) \begin{bmatrix} E_{YR}^{(N+1)} \\ E_{XL}^{(N+1)} \end{bmatrix}$$

for p polarization (3-49)

Now with the aid of Eq. (3-40), Eqs. (3-48) and (3-49) become

$$\begin{bmatrix} E_{XR}^{(0)} \\ E_{XL}^{(0)} \end{bmatrix} = V_{(0)}^{-1}(V_{(1)}U_{(1)}V_{(1)}^{-1})(V_{(2)}U_{(2)}V_{(2)}^{-1}) \cdots (V_{(N)}U_{(N)}V_{(N)}^{-1})V_{(N+1)} \begin{bmatrix} E_{XR}^{(N+1)'} \\ E_{XL}^{(N+1)'} \end{bmatrix}$$

for s polarization (3-50)

$$\begin{bmatrix} E_{YR}^{(0)} \\ \\ E_{YL}^{(0)} \end{bmatrix} = V_{(0)}^{-1} \; (V_{(1)}U_{(1)}V_{(1)}^{-1})(V_{(2)}U_{(2)}V_{(2)}^{-1})$$

$$\cdots (V_{(N)}U_{(N)}V_{(N)}^{-1}) \; V_{(N+1)} \begin{bmatrix} E_{YR}^{(N+1)'} \\ \\ E_{YL}^{(N+1)'} \end{bmatrix}$$

for p polarization (3-51)

We define

$$M_{(j)} \triangleq V_{(j)}U_{(j)}V_{(j)}^{-1} \tag{3-52}$$

$$M \triangleq \prod_{j=1}^{N} M_{(j)} \tag{3-53}$$

$$S \triangleq V_{(0)}^{-1} \; M \; V_{(N+1)} \tag{3-54}$$

The components of the 2 x 2 matrices S, $M_{(\ell)}$, and M will be designated by S_{jK}, $M_{(\ell)jK}$ and M_{jK} respectively (j, K=1, 2).

It is noted that Eqs. (3-50) and (3-51) relate the tangential electric field components of the two propagating plane waves in the free space region at the first boundary, to the tangential electric field components of the two propagating plane waves in the free space region at the $N + 1^{th}$ boundary. Eqs. (3-50) and (3-51) can be rewritten as

$$E_{XR}^{(0)} = S_{11}E_{XR}^{(N+1)'} + S_{12}E_{XL}^{(N+1)'}$$

$$E_{XL}^{(0)} = S_{21}E_{XR}^{(N+1)'} + S_{22}E_{XL}^{(N+1)'}$$

for s polarization (3-55)

$$E_{YR}^{(0)} = S_{11}E_{YR}^{(N+1)'} + S_{12}E_{YL}^{(N+1)'}$$

$$E_{YL}^{(0)} = S_{21}E_{YR}^{(N+1)} + S_{22}E_{YL}^{(N+1)'}$$

for p polarization (3-56)

If a plane wave is incident on layer No. 1, then it is easy to see that $E_{XR}^{(N+1)'}$ and $E_{YL}^{(N+1)'}$ must be identically zero. Thus, for s polarization Eq. (3-55) yields

$$\frac{E_{XL}^{(0)}}{E_{XR}^{(0)}} = \frac{S_{21}}{S_{11}} \tag{3-57}$$

and

$$\frac{E_{XR}^{(N+1)'}}{E_{XR}^{(0)}} = \frac{1}{S_{11}} \tag{3-58}$$

Similarly, for p polarization

$$\frac{E_{YL}^{(0)}}{E_{YR}^{(0)}} = \frac{S_{21}}{S_{11}} \tag{3-59}$$

and

$$\frac{E_{YR}^{(N+1)'}}{E_{YR}^{(0)}} = \frac{1}{S_{11}} \tag{3-60}$$

We define

$$r \triangleq \begin{cases} \dfrac{E_{XL}^{(0)}}{E_{XR}^{(0)}}, & \text{for s-polarization} \\ \dfrac{E_{YL}^{(0)}}{E_{YR}^{(0)}}, & \text{for p-polarization} \end{cases} \tag{3-61}$$

$$t \triangleq \begin{cases} \dfrac{E_{XR}^{(N+1)'}}{E_{XR}^{(0)}}, & \text{for s polarization} \\ \dfrac{E_{YR}^{(N+1)'}}{E_{YR}^{(0)}} \dfrac{\cos\theta_0}{\cos\theta_{(N+1)}}, & \text{for p polarization} \end{cases} \tag{3-62}$$

It will be noted that r, which we'll call the reflection coefficient, is the ratio of the electric field of the plane wave reflected from the multilayer stack to the electric field of the plane wave incident upon the first layer of the stack. t, which we'll call the transmission coefficient, is the ratio of the electric field of the plane wave which leaves the last layer of the stack to the electric field of the plane wave incident upon the first layer of the stack. Both r and t are complex quantities, each having a magnitude and a phase. This is noted explicitly by writing

$$r = |r| e^{j\gamma_r}$$

$$t = |t| e^{j\gamma_t} \tag{3-63}$$

Using Poynting's Theorem, the power density across the x-y plane due to the incident, reflected and transmitted plane waves is given by Eqs. (3-64), (3-65), and (3-66) respectively

$$P_I = \begin{cases} \left| E_{XR}^{(0)} \cdot H_{YR}^{(0)} \right|, & \text{for s polarization} \\ \left| E_{YR}^{(0)} \cdot H_{XR}^{(0)} \right|, & \text{for p polarization} \end{cases} \tag{3-64}$$

$$P_\rho = \begin{cases} \left| E_{XL}^{(0)} \cdot H_{YL}^{(0)} \right|, & \text{for s polarization} \\ \left| E_{YL}^{(0)} \cdot H_{XL}^{(0)} \right|, & \text{for p polarization} \end{cases} \tag{3-65}$$

$$P_T = \begin{cases} \left| E_{XR}^{(N+1)'} \cdot H_{YR}^{(N+1)'} \right|, & \text{for s polarization} \\ \left| E_{YR}^{(N+1)'} \cdot H_{XR}^{(N+1)'} \right|, & \text{for p polarization} \end{cases} \tag{3-66}$$

Eq. (3-64) is rewritten with the aid of Eqs. (3-7b) and (3-15b) as

$$P_I = \begin{cases} \sqrt{\frac{\epsilon(0)}{\mu_0}} \cos\theta_0 \left| E_{XR}^{(0)} \right|^2, & \text{for s polarization} \\ \sqrt{\frac{\epsilon(0)}{\mu_0}} \frac{\left| E_{YR}^{(0)} \right|^2}{\cos\theta_0}, & \text{for p polarization} \end{cases} \tag{3-67}$$

Eq. (3-65) is rewritten with the aid of Eqs. (3-8b) and (3-16b) as

$$P_R = \begin{cases} \sqrt{\frac{\epsilon(0)}{\mu_0}} \cos\theta_0 \left| E_{XL}^{(0)} \right|^2, & \text{for s polarization} \\ \sqrt{\frac{\epsilon(0)}{\mu_0}} \frac{\left| E_{YL}^{(0)} \right|^2}{\cos\theta_0}, & \text{for p polarization} \end{cases} \tag{3-68}$$

Eq. (3-66) is rewritten with the aid of Eqs. (3-7b) and (3-15b) as

$$P_T = \begin{cases} \sqrt{\frac{\epsilon(N+1)}{\mu_0}} \cos\theta_{(N+1)} \left| E_{XR}^{(N+1)'} \right|^2, & \text{for s polarization} \\ \sqrt{\frac{\epsilon(N+1)}{\mu_0}} \frac{\left| E_{YR}^{N+1)'} \right|^2}{\cos\theta_{(N+1)}}, & \text{for p polarization} \end{cases} \tag{3-69}$$

Defining the reflectance, ρ, by

$$\rho \triangleq \frac{P_\rho}{P_I} \tag{3-70}$$

and the transmittance, T, by

$$T \triangleq \frac{P_T}{P_I} \tag{3-71}$$

Eqs. (3-67), (3-68), and (3-69) yield

$$\rho = \begin{cases} \left| \dfrac{E_{XL}^{(0)}}{E_{XR}^{(0)}} \right|^2, & \text{for s polarization} \\ \left| \dfrac{E_{YL}^{(0)}}{E_{YR}^{(0)}} \right|^2, & \text{for p polarization} \end{cases} \tag{3-72}$$

$$T = \begin{cases} \dfrac{n_{(N+1)}}{n_{(o)}} \dfrac{\cos\theta_{(N+1)}}{\cos\theta_0} \left| \dfrac{E_{XR}^{(N+1)'}}{E_{XR}^{(o)}} \right|^2, & \text{for s polarization} \\ \dfrac{n_{(N+1)}}{n_{(o)}} \dfrac{\cos\theta_0}{\cos\theta_{(N+1)}} \left| \dfrac{E_{YR}^{(N+1)}}{E_{YR}^{(o)}} \right|^2, & \text{for p polarization} \end{cases} \tag{3-73}$$

Combining Eqs. (3-61), (3-62), (3-72), and (3-73), we have

$$\rho = |r|^2 \tag{3-74}$$

$$T = \begin{cases} \dfrac{n_{(N+1)}}{n_{(o)}} \dfrac{\cos\theta_{(N+1)}}{\cos\theta_0} |t|^2, & \text{for s polarization} \\ \dfrac{n_{(N+1)}}{n_{(o)}} \dfrac{\cos\theta_{(N+1)}}{\cos\theta_0} |t|^2, & \text{for p polarization} \end{cases} \tag{3-75}$$

Thus, we have derived the reflectance, phase change upon reflection, transmittance and phase change upon transmission of the multilayer

dielectric stack shown in Figure 3-1 when illuminated by an s or p polarized plane wave of arbitrary frequency at an arbitrary angle of incidence. Any plane wave incident upon the stack can be written as the sum of an s-polarized and a p-polarized plane wave. Due to the linearity of Maxwell's Equations, each of these plane waves can be treated separately using the above procedure.

Below, we give an algorithm for computing the reflectance, phase change upon reflection, transmittance and phase change upon transmission of the multilayer dielectric stack shown in Figure 3-1 when illuminated by an s or p polarized plane wave of arbitrary frequency at an arbitrary angle of incidence is detailed.

1. An s-polarized or p-polarized plane wave having a wavelength λ in layer No. 0 is incident at an angle θ_0 upon the multilayer dielectric stack
2. Eq. (3-20), which is a statement of Snell's Law of Refraction, is used to compute $\theta_{(j)}$ for each layer of the stack.
3. Eq. (3-35) is used to compute $Y_{(j)}$ for each layer of the stack
4. Eqs. (3-37) and (3-38) are used to compute $V_{(j)}$ and $V_{(j)}^{-1}$ for each layer of the stack
5. Eqs. (3-44) and (3-46) are used to compute $\Phi_{(j)}$ and $U_{(j)}$ for each layer of the stack
6. Eq (3-52) is used to compute $M_{(j)}$ for each layer of the stack
7. Eq. (3-53) is used to compute M
8. Eq. (3-54) is used to compute S
9. r and t are computed by Eqs. (3-59) through (3-62)
10. ρ and T are computed by Eqs. (3-74) and (3-75)

It is customary to refer to $Y_{(j)}$ as the admittance of the j^{th} layer, $V_{(j)}$ as the admittance matrix of the j^{th} layer, $U_{(j)}$ as the phase transformation matrix of the j^{th} layer, M as the interference matrix of the entire stack and S as the stack system transfer matrix.

Later on, we will use a number of results contained in this chapter. It would be more convenient at that time if these results were in a somewhat different form that which they appear in here. Anticipating this, we will present the alternate forms now.

Consider a single layer stack. Then Eqs. (3-50) and (3-51) become

$$\begin{bmatrix} E_{XR}^{(0)} \\ E_{XL}^{(0)} \end{bmatrix} = V_{(0)}^{-1} V_{(1)} U_{(1)} V_{(1)}^{-1} V_{(2)} \begin{bmatrix} E_{XR}^{(2)'} \\ E_{XL}^{(2)'} \end{bmatrix}, \text{ for s polarization} \tag{3-76}$$

$$\begin{bmatrix} E_{YR}^{(0)} \\ E_{YL}^{(0)} \end{bmatrix} = V_{(0)}^{-1} V_{(1)} U_{(1)} V_{(1)}^{-1} V_{(2)} \begin{bmatrix} E_{YR}^{(2)'} \\ E_{YL}^{(2)'} \end{bmatrix}, \text{ for p polarization} \tag{3-77}$$

The two by two system transfer matrix of this single layer stack will be designated L. Then

$$L = V_{(0)}^{-1} V_{(1)} U_{(1)} V_{(1)}^{-1} V_{(2)} \tag{3-78}$$

Equations (3-43) and (3-46) indicate that $U_{(j)}$ approaches the identity matrix in the limit as d_1, the layer thickness, approaches zero. Thus

$$G \triangleq \lim_{d_1 \to 0} L = V_{(0)}^{-1} V_{(2)} \tag{3-79}$$

The theory developed in this chapter was used to determine the reflectance versus wavelength characteristic of a twelve layer

"high-low, high-low" multilayer dielectric stack. The refractive index profile and corresponding reflectance characteristic are shown in Figures 3-2 and 3-3 respectively. Similarly, we calculated the reflectance versus wavelength characteristic of a 15 μm thick reflection hologram. The hologram has a refractive index variation in the z-direction (see Figue 2-1) given by

$$n(z) = 1.5 + 0.01 \sin \left(2\pi \left(\frac{5.285}{}\right) z\right)$$

Furthermore, the hologram is assumed to be surrounded by a medium having a refractive index of 1.5. The solid line in Figure 3-3 shows the reflectance versus wavelength characteristic calculated by the theory of stratified media. The calculation was performed by dividing the hologram into 7927 slabs of equal thickness. The refractive index within each slab was assumed to be constant and equal to the refractive index of that slab at its front surface. The dotted line shows the reflectance versus wavelength calculated by Kogelnik's coupled wave theory. Although Kogelnik's theory is not exact, whereas the theory of stratified media is, Kogelnik's theory is seen to give reasonably good results in this particular case.

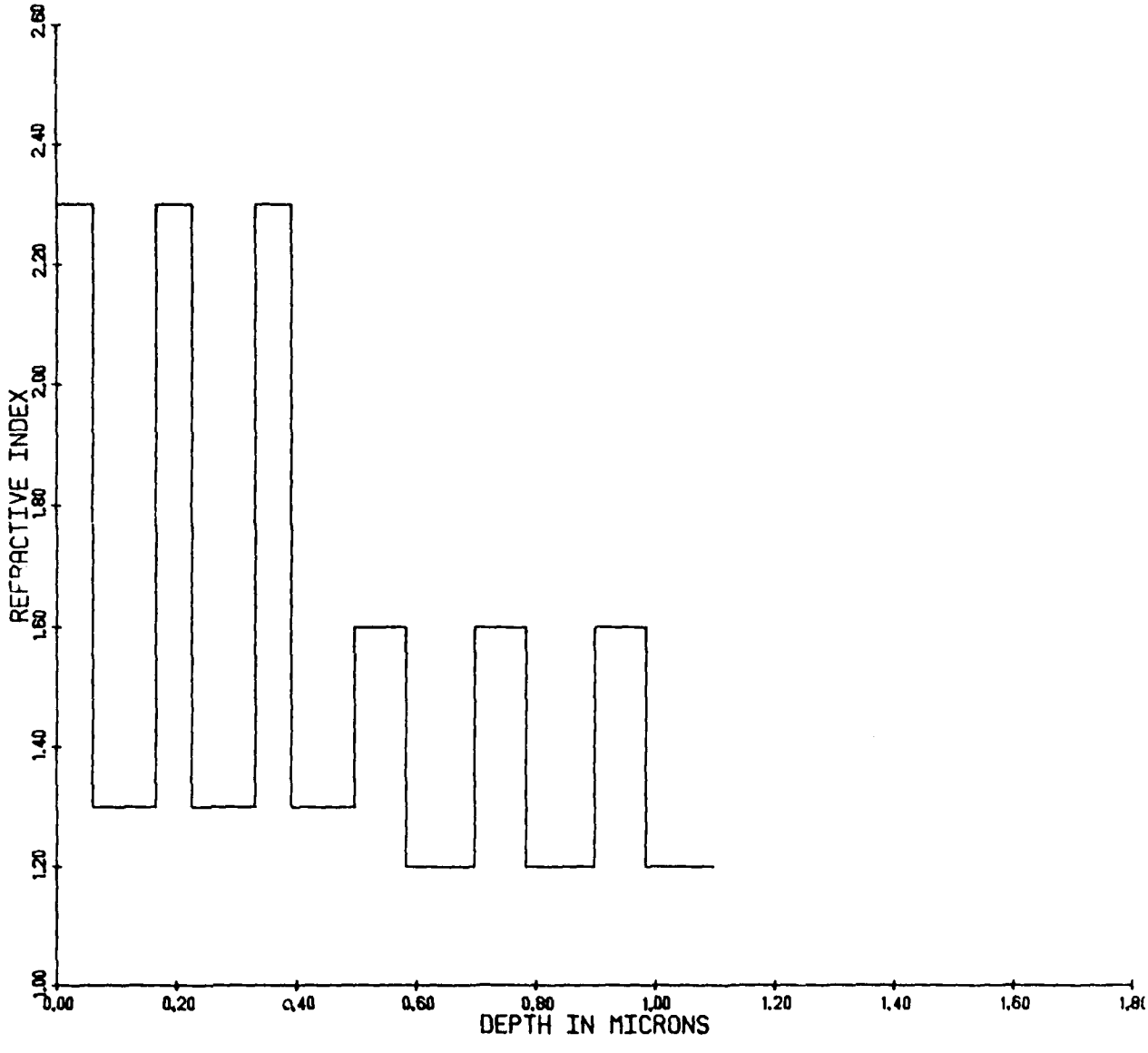

Figure 3-2. Twelve Layer High-Low High-Low Dielectric Stack

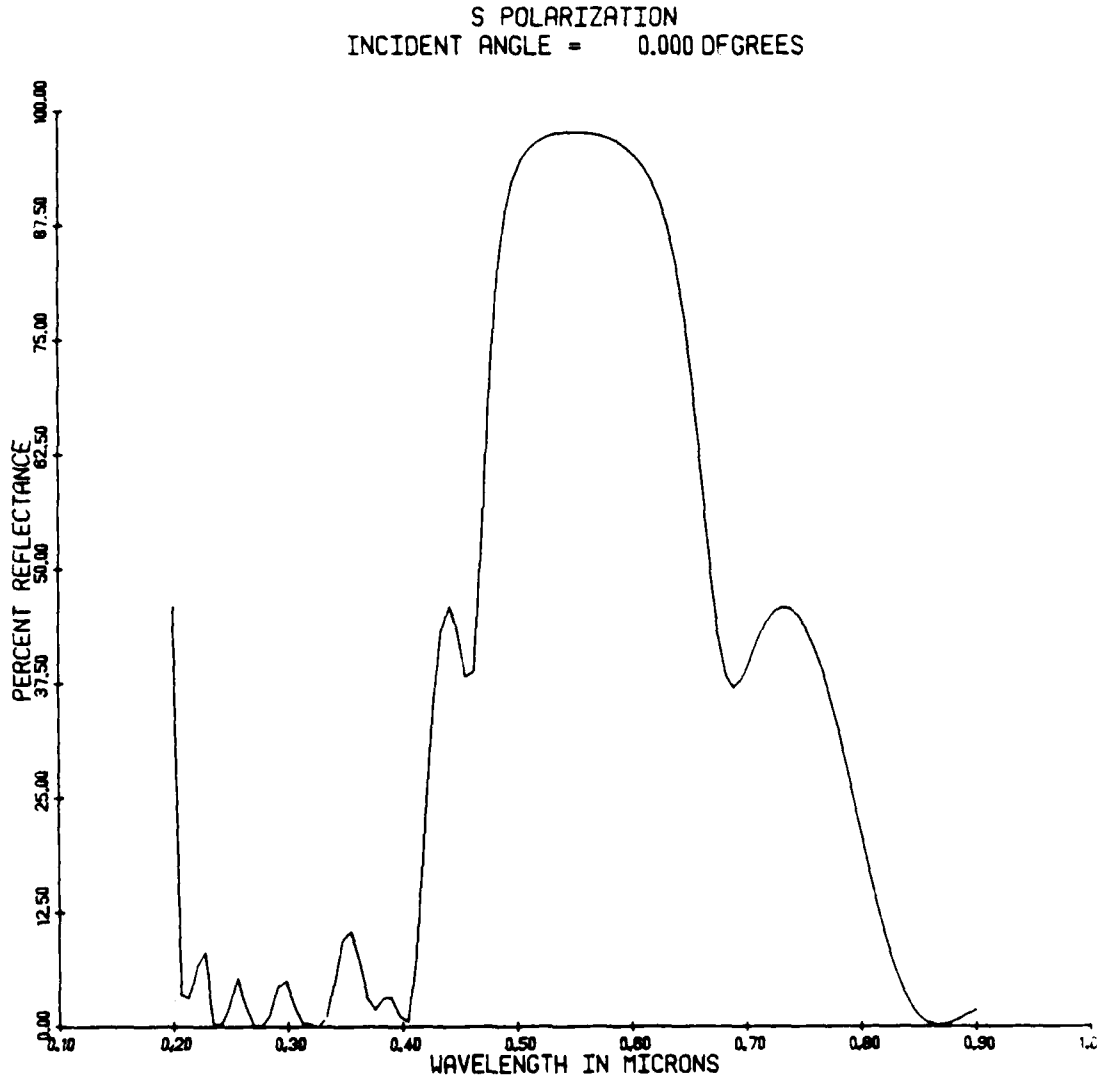

Figure 3-3. Reflectance vs. Wavelength Characteristic of a Twelve Layer High-Low High-Low Dielectric Stack

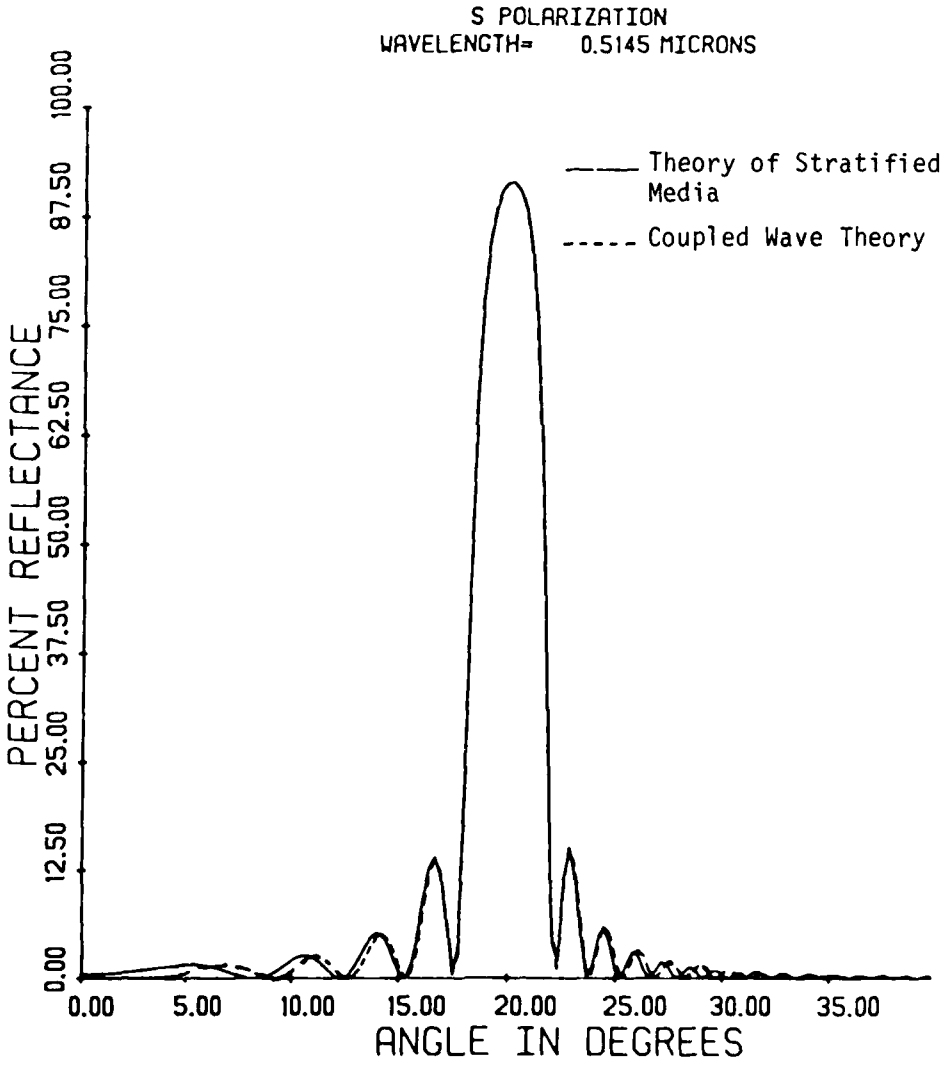

Figure 3-4. A Comparison between Coupled Wave Theory and the Theory of Stratified Media

Notes to Chapter 3

[1] F. Abelés, Ann. d. Phys., 5, 596 (1950).

[2] Z. Knittl, Optics of Thin Films, John Wiley & Sons, New York, 1976.

4
THE THEORY OF THICK SLAB DECOMPOSITION

In this chapter we develop a technique for determining the frequency domain transfer functions, $H_R(\lambda, \theta_o)$ and $H_T(\lambda, \theta_o)$, of a flat, holographic, phase reflection grating. As before, the grating is assumed to have a refractive index variation only in the direction normal to its surface. The technique will be referred to as the thick slab decomposition (TSD) method.

Consider the situation shown in Figure 4-1. A plane wave of wavelength λ is incident upon the front surface of a flat, holographic, phase, reflecting grating at an angle θ_o. Without loss of generality the plane of incidence is taken to be the x-z plane. The holographic grating is assumed to be of infinite extent in the x and y directions, and it has a refractive index which varies only as a function of z. The front surface of the holographic grating is adjacent to a homogeneous dielectric of refractive index n_f while the back surface is adjacent to a homogeneous dielectric of refractive index n_b. The complex electric field amplitude at $x = 0$, $z = 0^-$ of the incident wave is designated $\bar{E}_R$. There will be a field reflected from the holographic grating and a field transmitted through the grating. Both of these fields will be plane waves. The complex electric field amplitude at $x = 0$, $z = 0^-$ of the reflected plane wave is designated $\bar{E}_L$ while the complex electric field amplitude at $\bar{x} = 0$, $z = D^+$ of the transmitted plane wave is designated $\bar{E}_R'$. $\bar{E}_R$, $\bar{E}_L$ and $\bar{E}_R'$ are complex vector quantities having x, y and z components. The right going reflection coefficient, r_R, and the right going transmission coefficient, t_R, are defined below by Eqs. (4-1a) and (4-1b), respectively.

$$r_R \triangleq \begin{cases} \dfrac{E_{xL}}{E_{xR}}, & \text{for s polarization} \\ \dfrac{E_{yL}}{E_{yR}}, & \text{for p polarization} \end{cases} \qquad (4\text{-}1a)$$

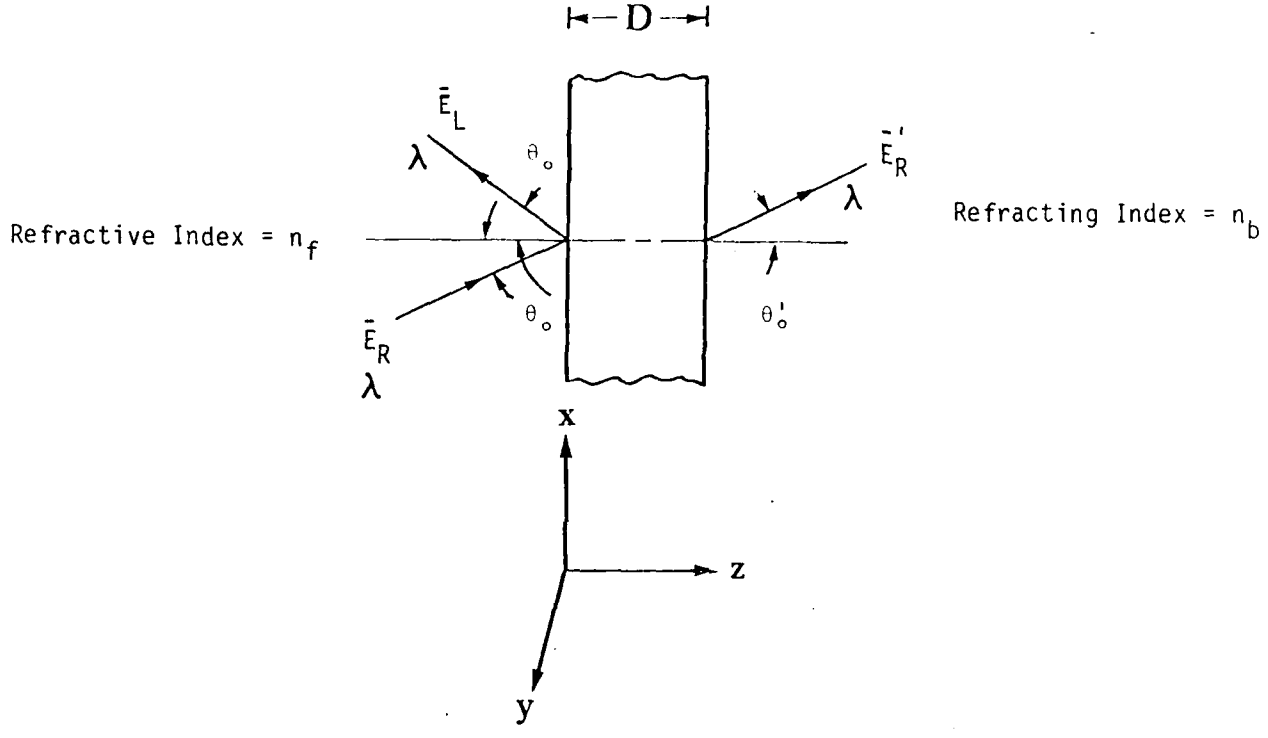

Figure 4-1. Holographic Grating, Definition of Reflection and Transmission Coefficients

$$t_R \triangleq \begin{cases} \dfrac{E_{xL}}{E_{xR}}, & \text{for s polarization} \\ \dfrac{E'_{yR}}{E_{yL}} \cdot \dfrac{\cos\theta_o}{\cos\theta'_o}, & \text{for p polarization} \end{cases} \tag{4-1b}$$

It immediately follows from the definitions of Chapter 2 that

$$H_R(\lambda,\theta_o) = r_R \tag{4-2a}$$

and

$$H_T(\lambda,\theta_o) = t_R \tag{4-2b}$$

If the grating is illuminated from the reverse side analogous left going reflection and transmission coefficient (r_L and t_L) can be defined. Furthermore, knowledge of r_R and r_L completely determines t_R and t_L This result follows from the reciprocity theorem of horizontally stratified media [1]. Thus, $H_R(\lambda,\theta_o)$ and $H_T(\lambda,\theta_o)$ can be determined if r_R and r_L are known.

The right going reflection coefficient (and consequently the left also) can be rigorously determined using Maxwell's Equations. To be more explicit, let us suppose that the section between $z = 0$ and $z = z_o$ ($z_o < D$) is removed from the holographic grating shown in Figure 4-1. We will designate the right going reflection coefficient of the remaining grating by $r_R(z_0)$. Then Maxwell's equations yield the following nonlinear differential equation and associated boundary condition for $r_R(z)$ [2].

$$\frac{dr_R(z)}{dz} = 2ik\gamma(z)r_R(z) + \frac{d\beta(z)}{dz}\frac{1}{2\beta(z)}[1 - r_R^2(z)], \qquad 0 < z < D \tag{4-3a}$$

$$r_R(D) = \frac{\beta(D^-) - \beta(D^+)}{\beta(D^-) + \beta(D^+)} \tag{4-3b}$$

where

$$\gamma(z) = n(z)\sqrt{1 - \frac{n_f^2 \sin^2\theta_o}{n^2(z)}} \tag{4-4}$$

$$\beta(z) = \begin{cases} \dfrac{Z_o}{n(z)\sqrt{1 - \dfrac{n_f^2 \sin^2\theta_o}{n^2(z)}}}, & \text{for s polarized illumination} \quad (4\text{-}5a) \\ \dfrac{n(z)}{Z_o\sqrt{1 - \dfrac{n_f^2 \sin^2\theta_o}{n^2(z)}}}, & \text{for p polarized illumination} \quad (4\text{-}5b) \end{cases}$$

$$K = \frac{2\pi}{\lambda} \tag{4-6}$$

Z_o = the characteristic impedance of free space $\left(\sqrt{\frac{\mu_o}{\varepsilon_o}}\right)$.

Equation (4-3a) can be solved for $r_R(0^+)$. r_R will then be given by [2]

$$r_R = \frac{\dfrac{\beta(0^+) - \beta(0^-)}{\beta(0^+) + \beta(0^-)} + r_R(0^+)}{1 + r_R(0^+)\dfrac{\beta(0^+) - \beta(0^-)}{\beta(0^+) + \beta(0^-)}} \tag{4-7}$$

Finding the solution of Eq. (4-3) will generally necessitate the use of numerical techniques.

Rather than solving Eq. (4-3a) directly, an alternate solution is to divide the grating shown in Figure 4-1 into a very large number of thin slabs parallel to the grating surface. The slabs are chosen to be sufficiently thin so that the refractive index across each thin slab is to a good approximation constant. Thus, each thin slab may be considered to be a homogeneous dielectric. The holographic reflection grating is being modeled as a multilayer dielectric stack. In a straightforward and rigorous manner the reflection coefficient of such a stack may be determined (using the theory of stratified media given in Chapter 3). The approach involves determining the two by two interference matrix associated with each slab and then multiplying together the inteference matrices for all the slabs. It can be shown that this multilayer dielectric stack approach is, in effect, a numerical technique for solving Eq. (4-3a) [2].

The approach discussed above has three principal drawbacks. First, it does not result in a compact solution; second, it does not yield insight into the problem; and third, it requires extensive "number crunching." Consider a 15 μm thick, holographic, reflection grating having a sinusoidal refractive index variation with a period of 0.1715 μm. Such a hologram can be recorded in dichromated gelatin from the interference pattern of two normally incident plane waves of wavelength 0.5145 μm. The recording geometry is shown in Figure 4-2. The refractive index of dichromated gelatin is nominally 1.5. We wish to determine the reflecction coefficient of this element by using the multilayer decomposition approach. Into how many thin slabs should each period of the refractive index profile be divided in order to get a good approximation of the reflection coefficient? The answer to this question will of course depend upon the magnitude of the refractive index modulation. Typically, this might be on the order of 0.02. It would probably be unwise to choose less than ten slabs/period and fifty slabs/period seems more reasonable. Ten slabs/period corresponds to 875 matrix multiplications for each

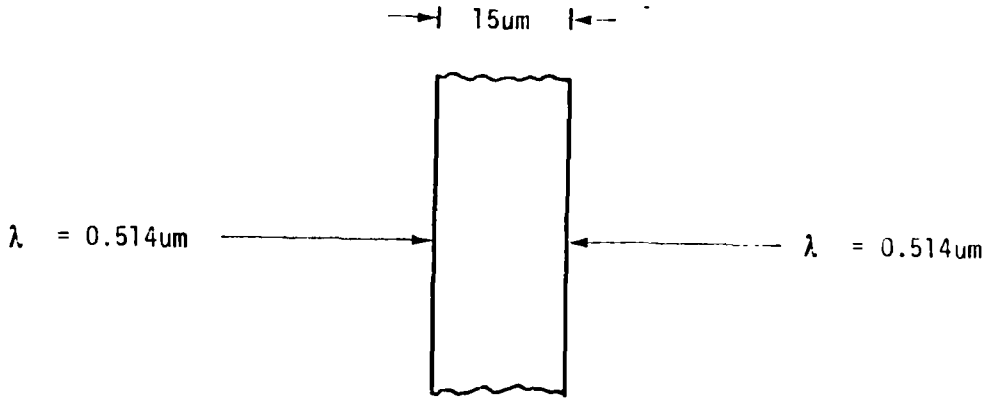

Figure 4-2. Holographic Reflection Grating Recording Geometry

value of θ_0 and λ while forty slabs/period corresponds to 4375 matrix multiplications for each value of θ_0 and λ. This is a rather large number of calculations.

For some refractive index profiles one may have to resort to the multilayer decomposition approach in order to determine the reflection coefficient. We, however, are interested in refractive index profiles which are holographically produced. Let $n(z)$ denote the refractive index profile. $n(z)$ is assumed to be a continuous function of z and its Fourier transform will be designted $N(f_z)$. We restrict our analysis to refractive index profiles which satisfy the conditions below.

$$|n(z) - n_0| \leq 0.03 \quad \text{where } n_0 \text{ is nominally } 1.5 \tag{4-8a}$$

and

$$N(f_z) \equiv 0 \quad \text{for } 4\ \mu m^{-1} \leq f_z \leq 6\ \mu m^{-1} \tag{4-8b}$$

These conditions are not artificial, they are reasonably consistent with currently available holographic recording materials and recording techniques. We will elaborate on this point in Chapter 8.

The technique we have developed for determining the reflection coefficient of a flat, holographic, reflection grating will be referred to as the thick slab decomposition (TSD) method. In principle its quite simple. The holographic grating is divided into a relatively small number of slabs each parallel to the surface of the holographic grating. The slabs, however, are chosen to be sufficiently thin so that the reflection coefficient of each slab by itself, when adjacent to dielectric mediums which index match the slab at its front and rear surfaces, is small. Next, it is shown that for our case of interest $\gamma(z)$ in Eq. (4-3a) can to a good approximation be considered constant. The reflection coefficient of each slab is now calculated using Eq. (4-3a) and the

approximation that $1 - r_R^2(z) \simeq 1$. It should be noted that this approximation together with the approximation that $\gamma(z)$ is constant reduces Eq. (4-3a) to a first order, linear differential equation which can be solved in closed form by integration.

With the reflection coefficient of each slab in hand, the reciprocity theorem of stratified media is applied in order to determine the two by two transfer matrix of each slab. The matrices for all the slabs are then multiplied together to yield the transfer matrix of the entire grating. The reflection coefficient of the grating, as well as $H_R(\lambda, \theta_0)$ and $H_T(\lambda, \theta_0)$, are easily determined from this matrix. The technique is described in detail below.

We begin by considering a slab between z = a and z = b of the grating shown in Figure 4-1. Our immediate goal is to derive the right going reflection of this slab. The slab thickness Δ

$$\Delta \triangleq b - a$$

is assumed to be sufficiently small so that the magnitude of the right going reflection coefficient of this slab is much less than one when it is adjacent to dielectric mediums which match the slab in refractive index at its front and back surfaces. The discussion which follows will be restricted to this slab under such conditions. The coordinate system for the slab will be as shown in Figure 4-3. The slabs refractive index profile will be designated n(z).

With the approximation

$$1 - r_R^2(z) \simeq 1 \qquad 0 \leq z \leq \Delta \tag{4-9}$$

Equations (4-3a) and (4-3b) become

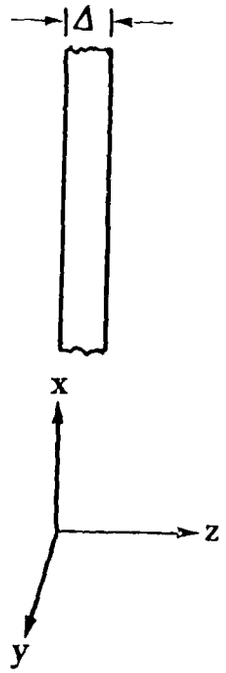

Refractive Index = n(z)

Figure 4-3. Holographic Grating Slab

$$\frac{dr_R(z)}{dz} = 2ik\gamma(z)r_R(z) + \frac{d\beta(z)}{dz}\frac{1}{2\beta(z)}, \qquad 0 < z < \Delta \tag{4-10a}$$

$$r_R(\Delta) = 0 \tag{4-10b}$$

This equation can also be written as

$$\frac{d}{dz}\left[r_R(z)\exp\left(-2ik\int_{0^+}^{z}\gamma(\xi)\,d\xi\right)\right] = \frac{d\beta(z)}{dz}\frac{1}{2\beta(z)}\exp\left(-2ik\int_{0^+}^{z}\gamma(\xi)\,d\xi\right) \tag{4-11}$$

Integrating both sides of Eq. (4-11) yields

$$\int_{0^+}^{\Delta}\left[\frac{d}{dz}\left[r_R(z)\exp\left(-2ik\int_{0^+}^{z}\gamma(\xi)\,d\xi\right)\right]\right]dz = \int_{0^+}^{\Delta}\left[\frac{d\beta(z)}{dz}\frac{1}{2\beta(z)}\exp\left(-2ik\int_{0^+}^{z}\gamma(\xi)\,d\xi\right)\right]dz \tag{4-12}$$

$$r_R(\Delta)\exp\left(-2ik\int_{0^+}^{\Delta}\gamma(\xi)\,d\xi\right) - r_R(0^+)\exp\left(-2ik\int_{0^+}^{0^+}\gamma(\xi)\,d\xi\right) =$$

$$\int_{0^+}^{\Delta}\left[\frac{d\beta(z)}{dz}\frac{1}{2\beta(z)}\exp\left(-2ik\int_{0^+}^{Z}\gamma(\xi)\,d\xi\right)\right]dz \tag{4-13}$$

The boundary condition $r_R(\Delta) = 0$, Eq. (4-10b), is now applied and Eq. (4-13) becomes

$$r_R(0^+) = -\int_{0^+}^{\Delta}\left[\frac{d\beta(z)}{dz}\frac{1}{2\beta(z)}\exp\left(-2ik\int_{0^+}^{Z}\gamma(\xi)\,d\xi\right)\right]dz \qquad (4\text{-}14)$$

From Eq. (4-7), i.e., $r_R = r_R(0^+)$, one gets

$$r_R = -\int_{0^+}^{\Delta}\left[\frac{d\beta(z)}{dz}\frac{1}{2\beta(z)}\exp\left(-2ik\int_{0^+}^{Z}\gamma(\xi)\,d\xi\right)\right]dz$$

or equivalently

$$r_R = -\int_{0}^{\Delta}\left[\frac{d\beta(z)}{dz}\frac{1}{2\beta(z)}\exp\left(-2ik\int_{0}^{Z}\gamma(\xi)\,d\xi\right)\right]dz \qquad (4\text{-}15)$$

If we define $\theta(z)$ by Eq. (4-16) below

$$\sin\theta(z) = \frac{n(0-)\sin\theta_0}{n(z)} \qquad (4\text{-}16)$$

Then

$$\cos\theta(z) = \sqrt{1 - \frac{n^2(0-)\sin^2\theta_0}{n^2(z)}} \qquad (4\text{-}17)$$

Using Eq. (4-17) we rewrite Eqs. (4-4), (4-5a), and (4-5b) as given below.

$$\gamma(z) = n(z) \cos \theta(z) \tag{4-18}$$

$$\beta(z) = \begin{cases} \dfrac{z_0}{n(z) \cos \theta(z)} , & \text{for s polarized illumination} \quad (4\text{-}19a) \\ \dfrac{n(z)}{z_0 \cos \theta(z)} , & \text{for p polarized illumination} \quad (4\text{-}19b) \end{cases}$$

We wish to evaluate $\frac{d\beta(z)}{dz} / \beta(z)$. Consider first the s polarized case. Then from Eq. (4-19a)

$$\frac{d\beta(z)}{dz} / \beta(z) = \frac{1}{n(z) \cos \theta(z)} \left[\frac{dn(z)}{dz} \cos \theta(z) - n(z) \sin \theta(z) \frac{d\theta(z)}{dz} \right] \tag{4-20}$$

Differentiating Eq. (4-16) yields

$$\frac{dn(z)}{dz} \sin \theta(z) + n(z) \cos \theta(z) \frac{d\theta(z)}{dz} = 0 \tag{4-21}$$

or equivalently

$$\frac{d\theta(z)}{dz} = -\frac{dn(z)}{dz} \frac{\tan \theta(z)}{n(z)} \tag{4-22}$$

Combining Eqs. (4-20) and (4-21)

$$\begin{aligned} \frac{d\beta(z)}{dz} / \beta(z) &= \left[\frac{dn(z)}{dz} / n(z) \right] [1 + \tan^2 \theta(z)] \\ &= \frac{dn(z)}{dz} \frac{1}{n(z) \cos^2 \theta(z)} \\ &\simeq \frac{dn(z)}{dz} \frac{1}{n_0 \cos^2 \theta_0} \end{aligned} \tag{4-23}$$

The last line follows from the fact that $n(z) \simeq n_0$ (see Eq. (4-8a)) and so $\theta(z) \simeq \theta_0$ (Eq. (4-16)). For the p polarized case Eq. (4-19b) yields

$$\frac{d\beta(z)}{dz} / \beta(z) = \frac{\cos \theta(z) \frac{dn(z)}{dz} + n(z) \sin \theta(z) \frac{d\theta(z)}{dz}}{n(z) \cos \theta(z)} \qquad (4\text{-}24)$$

Next, Eqs. (4-22) and (4-24) are combined to yield

$$\frac{d\beta(z)}{dz} / \beta(z) = \left[\frac{dn(z)}{dz} / n(z)\right] [1 - \tan^2 \theta(z)]$$

$$\simeq \frac{dn(z)}{dz} \frac{(1 - \tan^2 \theta_0)}{n_0} \qquad (4\text{-}25)$$

The last line follows from the approximations $n(z) \simeq n_0$ and $\theta(z) \simeq \theta_0$. Eq. (4-15) now becomes

$$r_R \simeq -\alpha \int_0^{\Delta} \frac{dn(z)}{dz} \exp\left[-2ik \int_0^{Z} \gamma(\xi)\, d\xi\right] dz \qquad (4\text{-}26)$$

where

$$\alpha = \begin{cases} \dfrac{1}{n_0 \cos^2 \theta_0}, & \text{for s polarization} \qquad (4\text{-}27a) \\ \dfrac{1 - \tan^2 \theta_0}{n_0}, & \text{for p polarization} \qquad (4\text{-}27b) \end{cases}$$

We wish to show that

$$-2ik\int_0^z \gamma(\xi)\,d\xi \simeq -2ikn_0(\cos\theta_0)z, \qquad 0 \le z \le \Delta \tag{4-28}$$

Equation (4-4) is rewritten as shown below

$$\gamma(z) = \sqrt{[n_0 + \Delta n(z)]^2 - (n_0 + \Delta n(0))^2 \sin^2\theta_0} \tag{4-29}$$

$$\gamma(z) = \sqrt{n_0^2 - n_0^2\sin^2\theta_0 + 2n_0(\Delta n(z) - \Delta n(0)\sin^2\theta_0) + [\Delta n(z)]^2 - [\Delta n(0)]^2\sin^2\theta_0} \tag{4-30}$$

$$\gamma(z) \simeq \sqrt{n_0^2 - n_0^2\sin^2\theta_0 + 2n_0(\Delta n(z) - \Delta n(0)\sin^2\theta_0)} \tag{4-31}$$

where $n(z)$ has been expressed as $n_0 + \Delta n(z)$. Note that $|\Delta n(z)| \le 0.03$ from Eq. (4-8a). In Eq. (4-31), the second order terms in $\Delta n(z)$ and $\Delta n(0)$ have been neglected. Equation (4-31) is now expanded in a power series

$$\gamma(z) = (n_0^2 - n_0^2\sin^2\theta_0)^{1/2} + \frac{1}{2}\frac{2n_0(\Delta n(z) - \Delta n(0)\sin^2\theta_0)}{(n_0^2 - n_0^2\sin^2\theta_0)^{1/2}}$$

$$- \frac{1}{8}\frac{2n_0(\Delta n(z) - \Delta n(0)\sin^2\theta_0)^2}{(n_0^2 - n_0^2\sin^2\theta_0)^{3/2}} + \cdots \tag{4-32}$$

From Eq. (4-32) it can be seen that

$$|\gamma(z) - n_0 \cos \theta_0| \leq \frac{|2\Delta n(z)|}{\cos \theta_0}, \quad 0 \leq z \leq \Delta \tag{4-33}$$

and so

$$\left| 2K \int_0^z \gamma(\xi)\, d\xi - 2K \int_0^z n_0 \cos \theta_0\, d\xi \right| \leq \left| \frac{2K}{\cos \theta_0} \int_0^z 2\Delta n(\xi)\, d\xi \right|, \quad 0 \leq z \leq \Delta \tag{4-34}$$

We want to find a strong upper bound on

$$\left| \frac{2K}{\cos \theta_0} \int_0^z 2\Delta n(\xi)\, d\xi \right|, \quad 0 \leq z \leq \Delta$$

We have been unable to do this, but hasten to point out that it seems likely that a rather weak bound is given by Eq. (4-35) below.

$$\left| \frac{2K}{\cos \theta_0} \int_0^z 2\Delta n(\xi)\, d\xi \right| < 0.18, \quad 0 \leq z \leq \Delta \tag{4-35}$$

The following plausibility argument is presented to support this conjecture. Let us write

$$\Delta n(z) = A(z) \sin [2\pi f(z) z + \phi(z)]$$

Equation (4-8b) indicates that $\Delta n(z)$ is to an extent narrow band. Arbitrarily pick p such that

$$0 \leq p \leq \Delta$$

Since $\Delta n(z)$ is to an extent narrowband, we would expect that there exist some δz such that $A(z)$, $f(z)$ and $\phi(z)$ are reasonably constant in the interval $p \leq z \leq \delta z$ and such that $f(p)\delta z$ is some integer. Now partition the interval from $[0, z]$ into sub-intervals $[p_m, p_m + (\delta z)_m]$, $m = 1, \ldots L$ where $p_1 = 0$. $A(z)$, $f(z)$ and $\phi(z)$ are reasonably constant throughout each sub-interval and $f(p_m)(\delta z)_m$ is some integer for all m except $m = L$. For $m = L$, $f(p_L)(\delta z)_L$ is less than one. It is noted that

$$\int_0^z A(\xi) \sin [2\pi f(\xi)\xi + \phi(\xi)]\, d\xi = \sum_{m=1}^{L-1} \int_{p_m}^{p_m+(\delta z)_m} A(\xi) \sin [2\pi f(\xi)\xi + \phi(\xi)]\, d\xi$$

$$+ \int_{p_L}^{p_L+(\delta z)_L} A(\xi) \sin [2\pi f(\xi)\xi + \phi(\xi)]\, d\xi$$

$$\simeq \sum_{m=1}^{L-1} \int_{p_m}^{p_m+(\delta z)_m} A(p_m) \sin [2\pi f(p_m)\xi + \phi(p_m)]\, d\xi$$

$$+ \int_{p_L}^{p_L+(\delta z)_L} A(p_L) \sin [2\pi f(p_L)\xi + \phi(p_L)]\, d\xi$$

$$\simeq A(p_L) \int_{p_L}^{p_L+(\delta z)_L} \sin [2\pi f(p_L)\xi + \phi(p_L)]\, d\xi$$

(note that $\int_{p_m}^{p_m+(\delta z)_m} A(p_m) \sin [2\pi f(p_m)\xi + \phi(p_m)]\, d\xi = 0$)

$$\leq \frac{|A(p_L)|}{\pi f(p_L)}$$

Consequently

$$\left| \frac{2K}{\cos \theta_0} \int_0^z 2\Delta n(\xi)\, d\xi \right| \leq \frac{4K}{\pi f(p_L) \cos \theta_0} |A(p_L)|$$

$$= \frac{8}{\lambda\, f(p_L) \cos \theta_0} |A(p_L)|$$

$$0 \leq z \leq \Delta$$

From Eqs. (8a) and (8b)

$$|A(p_L)| \leq 0.03 , \quad f(p_L) \geq 4\ \mu m^{-1}$$

Restricting λ to the visible spectrum

$$0.45\ \mu m \leq \lambda \leq 0.65\ \mu m$$

and noting that $\theta_0 < 42°$ [3], we have

$$\left| \frac{2K}{\cos \theta_0} \int_0^z \Delta n(\xi)\, d\xi \right| \leq \frac{8}{(0.45)(4) \cos 42^\circ} (0.03) \simeq 0.18$$

In any case, the validity of Eq. (4-28) can always be checked by evaluating the integral on the right hand side of Eq. (4-34). We will assume that Eq. (4-28) is valid. Equation (4-26) then becomes

$$r_R \simeq -\alpha \int_0^{\Delta} \frac{dn(z)}{dz} \exp\left[(-2ikn_0 \cos \theta_0)z\right] dz \qquad (4\text{-}36)$$

The above equation is the desired result.

We briefly comment on Eq. (4-36). By rewriting Eq. (4-36) as given below

$$r_R \simeq -\alpha \int_{-\infty}^{\infty} \frac{dn(z)}{dz} \text{rect}\left(\frac{z}{\Delta}\right) \exp\left(-i2\pi f_z z\right) dz \qquad (4\text{-}37)$$

where

$$\text{rect}\left(\frac{z}{\Delta}\right) = \begin{cases} 1, & 0 \leq z \leq \Delta \\ 0, & \text{elsewhere} \end{cases} \qquad (4\text{-}38)$$

$$f_z = \frac{2}{\lambda_0} n_0 \cos \theta_0 \qquad (4\text{-}39)$$

It is seen that r_R is the Fourier transform of

$$\frac{dn(z)}{dz} \text{rect}\left(\frac{z}{\Delta}\right)$$

One can also give a physical interpretation of Eq. (4-36). Such an interpretation goes as follows. The slab can be thought of as being composed of a very large number of parallel sub-slabs each of thickness dz and constant refractive index. Now, if $n(z_0)$ is the refractive index of the sub-slab whose front surface lies in the plane $z = z_0$ then to a good approximation

$$n(z_0 + dz) \simeq n(z_0)\, dz$$

will be the refractive index of the sub-slab whose front surface lies in the plane $z_0 + dz$. As a ray having an amplitude of one propagates into the slab, some of it is reflectecd at each of the interfaces separating the sub-slabs. The amplitude of the reflected ray at the plane $z = z_0$ is given by Fresnel's formula [4].

$$\frac{n(z_0)\cos[\theta(z_0)] - n(z_0 + dz)\cos[\theta(z_0 + dz)]}{n(z_0)\cos\theta(z_0) + n(z_0 + dz)\cos[\theta(z_0 + dz)]}\ , \text{ for s polarization} \qquad (4\text{-}40a)$$

$$\frac{n(z_0 + dz)\cos[\theta(z_0)] - n(z_0)\cos[\theta(z_0 + dz)]}{n(z_0 + dz)\cos[\theta(z_0)] + n(z_0)\cos[\theta(z_0 + dz)]}\ , \text{ for p polarization} \qquad (4\text{-}40b)$$

It can be shown with the use of Snell's Law and a bit of algebra and trigonometry that Eqs. (40a and 40b) become

$$\left(-\alpha \frac{dn(z)}{dz}\bigg|_{z = z_0}\right) dz$$

in the limit as $dz \to 0$. It is assumed that the amplitude of the ray does not attenuate significantly as it propagates into the slab, and that multiple reflections at the sub-slab interfaces can be ignored.

Then the right going reflection coefficient of the slab will be the sum of the reflections from each of the sub-slab interfaces. The phase associated with the reflected ray from the sub-slab interface at $z = z_0$ is given by the total optical path length that ray travels in going to the plane $z = z_0$ and then returning to the front surface of the slab. This optical path length is approximately

$$2Kn_0(\cos\theta_0)z_0$$

Thus,

$$r_R \simeq -\sum_{dz_j}\left[\left(\alpha\frac{dn(z)}{dz}\bigg|_{z=z_j}\right)dz_j\exp\left[(-2iKn_0\cos\theta_0)z_j\right]\right]$$

which approaches Eq. (4-36) in the limit as $dz_j \to 0$.

We have succeeded in deriving a closed form expression for the right going reflection coefficient of a slab section of the grating. Below, the two by two transfer matrix of this slab is derived from knowledge of its right going reflection coefficient. Figure 4-4 shows the slab illuminated from the front side with a plane wave. Similarly, Figure 4-5 shows the slab illuminated from the back side with a plane wave. $\bar{E}_R$, $\bar{E}_L$, $\bar{E}'_R$ and $\bar{E}'_L$ are the complex electric field amplitudes. They are vector quantities having x, y and z components. In Figures 4-4 and 4-5, θ_0 is related to θ'_0 by Snell's Law

$$\theta'_0 = \sin^{-1}\left(\frac{n(0)\sin\theta_0}{n(\Delta)}\right) \qquad (4\text{-}41)$$

But $n(0) \simeq n(\Delta)$ by Eq. (4-8a) and so

$$\theta'_0 \simeq \theta_0 \qquad (4\text{-}42)$$

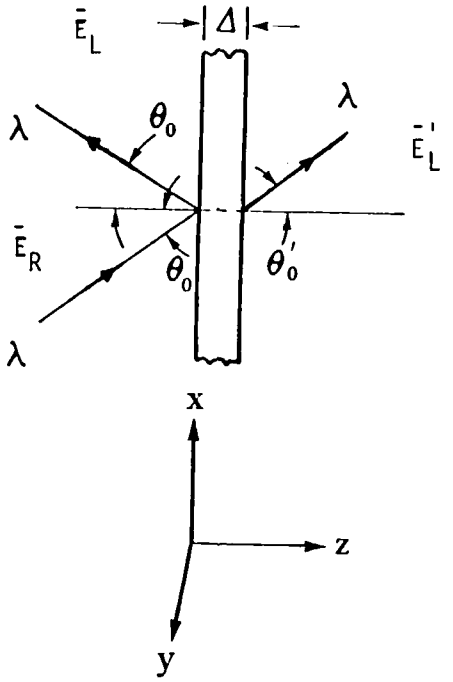

Figure 4-4. Grating Slab Illuminated from Front Side

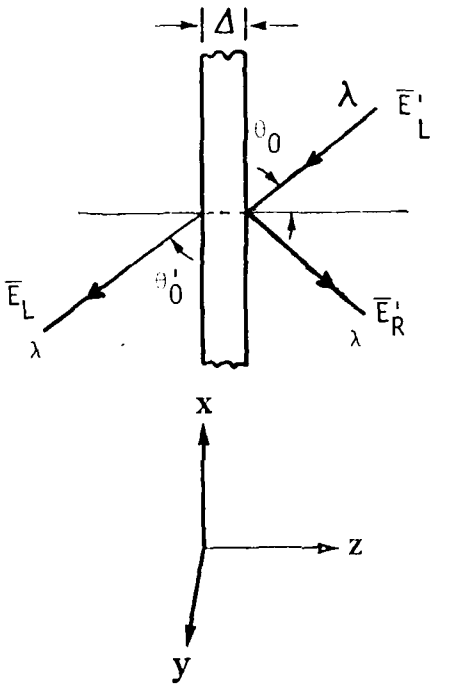

Figure 4-5. Grating Slab Illuminated from Rear Side

Suppose now that the holographic grating is illuminated simultaneously from both sides. The incident angles, θ_0 and θ_0', on the front and back sides respectively, are assumed to be related by Snell's Law (Eq. (4-41)). The principle of superposition applies. The situation is depicted as shown in Figure 4-6. $\bar{E}_R$ and $\bar{E}_L$ will be uniquely determined by $\bar{E}_R'$ and E_L'. The relationship can be written in matrix form as given below

$$\begin{bmatrix} E_{xR} \\ E_{xL} \end{bmatrix} = \begin{bmatrix} q_{11} & q_{12} \\ q_{21} & q_{22} \end{bmatrix} \begin{bmatrix} E'_{xR} \\ E'_{xL} \end{bmatrix}, \text{ for s polarization} \quad (4\text{-}43a)$$

and

$$\begin{bmatrix} E_{yR} \\ E_{yL} \end{bmatrix} = \begin{bmatrix} q_{11} & q_{12} \\ q_{21} & q_{22} \end{bmatrix} \begin{bmatrix} E'_{yR} \\ E'_{y_L} \end{bmatrix}, \text{ for p polarization} \quad (4\text{-}43b)$$

The q_{ij}'s in Eq. (4-43b) are not the same as those in Eq. (4-43a). The two by two matrix Q

$$Q \triangleq \begin{bmatrix} q_{11} & q_{12} \\ q_{21} & q_{22} \end{bmatrix} \quad (4\text{-}44)$$

is called the transfer matrix.

The right going reflection and transmission coefficients r_R and t_R, respectively, are defined as before

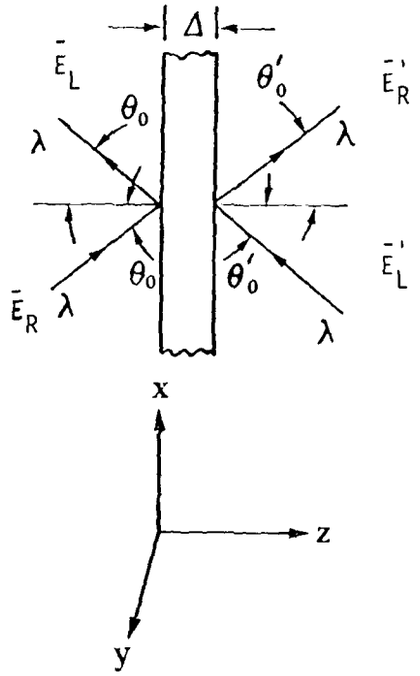

Figure 4-6. Grating Slab Illuminated from Front and Rear Sides

$$r_R \triangleq \begin{cases} \left.\dfrac{E_{xL}}{E_{xR}}\right|_{\bar{E}'_L = 0}, & \text{for s polarization} \\ \left.\dfrac{E_{yL}}{E_{yR}}\right|_{\bar{E}'_L = 0}, & \text{for p polarization} \end{cases} \tag{4-45}$$

$$t_R \triangleq \begin{cases} \left.\dfrac{E'_{xR}}{E_{xR}}\right|_{\bar{E}'_L = 0}, & \text{for s polarization} \\ \left.\dfrac{E'_{yR}}{E_{yR}}\right|_{\bar{E}'_L = 0} \cdot \dfrac{\cos\theta_0}{\cos\theta'_0}, & \text{for p polarization} \end{cases} \tag{4-46}$$

Similarly, the left going reflection and transmission coefficients, r_L and t_L, respectively, are defined by

$$r_L \triangleq \begin{cases} \left.\dfrac{E'_{xR}}{E'_{xL}}\right|_{\bar{E}_R = 0}, & \text{for s polarization} \\ \left.\dfrac{E'_{yR}}{E'_{yL}}\right|_{\bar{E}_R = 0}, & \text{for p polarization} \end{cases} \tag{4-47}$$

$$t_L \triangleq \begin{cases} \left.\dfrac{E_{xL}}{E'_{xL}}\right|_{\bar{E}_R = 0}, & \text{for s polarization} \\ \left.\dfrac{E_{yL}}{E'_{yL}}\right|_{\bar{E}_R = 0} \cdot \dfrac{\cos\theta_0}{\cos\theta'_0}, & \text{for p polarization} \end{cases} \tag{4-48}$$

We once again invoke the fact that $\theta_0' \simeq \theta_0$. Thus,

$$\frac{\cos \theta_0}{\cos \theta_0'} \simeq 1$$

With the use of Eq. (4-43a) and (4-43b) it is easy to show that

$$r_R = \frac{q_{21}}{q_{11}} \quad \text{, for s or p polarization} \tag{4-49}$$

$$t_R = \begin{cases} \dfrac{1}{q_{11}} & \text{, for s polarization} \\ \dfrac{1}{q_{11}} \cdot \dfrac{\cos \theta_0}{\cos \theta_0'} \simeq \dfrac{1}{q_{11}} & \text{, for p polarization} \end{cases} \tag{4-50}$$

$$r_L = \frac{-q_{12}}{q_{11}} \quad \text{, for s or p polarization} \tag{4-51}$$

$$t_L = \begin{cases} \dfrac{-q_{21}q_{12}}{q_{11}} + q_{22} & \text{, for s polarization} \\ \left(\dfrac{-q_{21}q_{12}}{q_{11}} + q_{22} \right) \cdot \dfrac{\cos \theta_0'}{\cos \theta_0} \simeq \dfrac{-q_{21}q_{12}}{q_{11}} - q_{22} & \text{, for p polarization} \end{cases} \tag{4-52}$$

Solving for q_{11}, q_{12}, q_{21} and q_{22} in terms of r_R, t_R, r_L and t_L one gets

$$q_{11} = \begin{cases} 1/t_R & \text{, for s polarization} \\ (1/t_R) \cdot \dfrac{\cos \theta_0}{\cos \theta_0'} \simeq 1/t_R & \text{, for p polarization} \end{cases} \tag{4-53}$$

$$q_{12} = \begin{cases} -r_L/t_R & \text{, for s polarization} \\ (-r_L/t_R) \cdot \dfrac{\cos\theta_0}{\cos\theta_0'} \simeq -r_L/t_R & \text{, for p polarization} \end{cases} \tag{4-54}$$

$$q_{21} = \begin{cases} r_R/t_R & \text{, for s polarization} \\ (r_R/t_R) \cdot \dfrac{\cos\theta_0}{\cos\theta_0'} \simeq r_R/t_R & \text{, for p polarization} \end{cases} \tag{4-55}$$

$$q_{22} = \begin{cases} \dfrac{t_L t_R - r_R r_L}{t_R} & \text{, for s polarization} \\ \left(\dfrac{t_L t_R - r_R r_L}{t_R}\right) \cdot \dfrac{\cos\theta_0}{\cos\theta_0'} \simeq \dfrac{t_L t_R - r_R r_L}{t_R} & \text{, for p polarization} \end{cases} \tag{4-56}$$

It will be shown below that t_R, t_L and r_L can be derived from knowleged of r_R. We start with r_R given by Eq. (4-36), which is repeated below

$$r_R \simeq -\alpha \int_0^{\Delta} \frac{dn(z)}{dz} \exp\left[(-2ikn_0 \cos\theta_0)z\right] dz \tag{4-57}$$

The left going reflection coefficient can be written as

$$r_L \simeq -\alpha' \int_0^{\Delta} \frac{dn(\Delta - z)}{dz} \exp\left[(-2ikn_0 \cos\theta_0')z\right] dz \tag{4-58}$$

where

$$\alpha' = \begin{cases} \dfrac{1}{n_0 \cos^2 \theta_0'} \text{ , s polarization} & (4\text{-}59a) \\ \dfrac{1 - \tan^2 \theta_0'}{n_0} \text{ , p polarization} & (4\text{-}59b) \end{cases}$$

With a simple change of variable, Eq. (4-58) becomes

$$r_L \simeq \alpha' \exp\left[(-2ikn_0 \cos \theta_0')\Delta\right] \int_0^{\Delta} \frac{dn(z)}{dz} \exp\left[(2ikn_0 \cos \theta_0')z\right] dz \quad (4\text{-}60)$$

Combining Eqs. (4-57) and(4-60) and noting that $\theta_0' = \theta_0$ yields

$$r_L \simeq -r_R^* \exp\left[(-2ikn_0 \cos \theta_0)\Delta\right] \quad (4\text{-}61)$$

where * denotes the conjugate.

Consider Figure 4-4. Energy conservation requires that the z component of the Poynting vector of the transmitted wave equal the z component of the Poynting vector of the incident wave plus the z component of the Poynting vector of the reflected wave. This condition is expressed mathematically by Eq. (4-62).

$$|r_R|^2 + |t_R|^2 g = 1 \quad (4\text{-}62)$$

Similarly from Figure 4-5, energy conservation dictates

$$|r_L|^2 + |t_L|^2/g = 1 \quad (4\text{-}63)$$

AD-A097 201 ENVIRONMENTAL RESEARCH INST OF MICHIGAN ANN ARBOR RA--ETC F/G 14/5
THICK PHASE HOLOGRAMS.(U)
JAN 81 K A WINICK F49620-78-C-0061
UNCLASSIFIED ERIM-134200-10-F AFOSR-TR-81-0196 NL

2 OF 3
AD A
097201

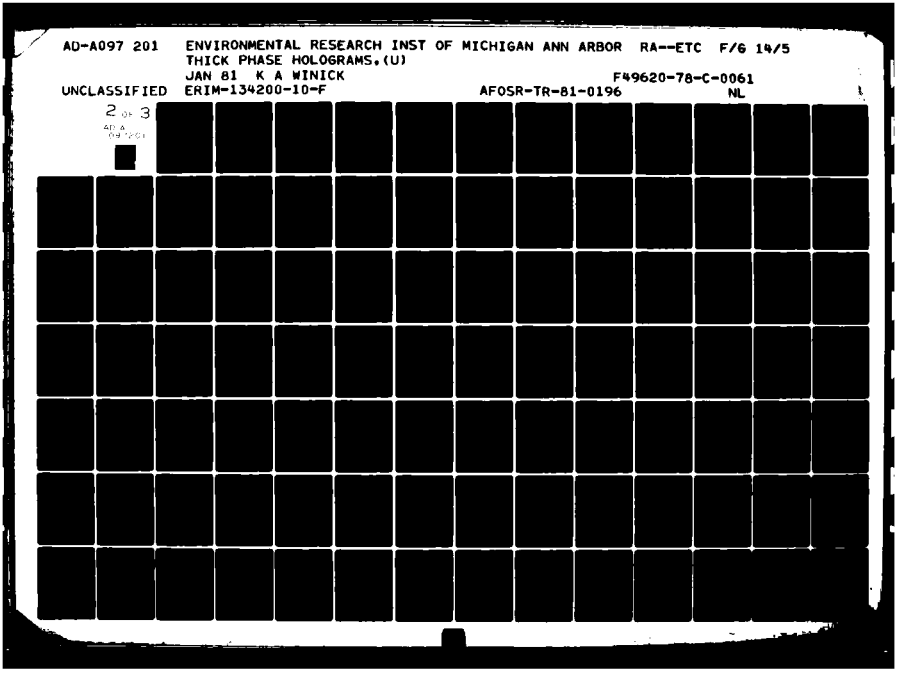

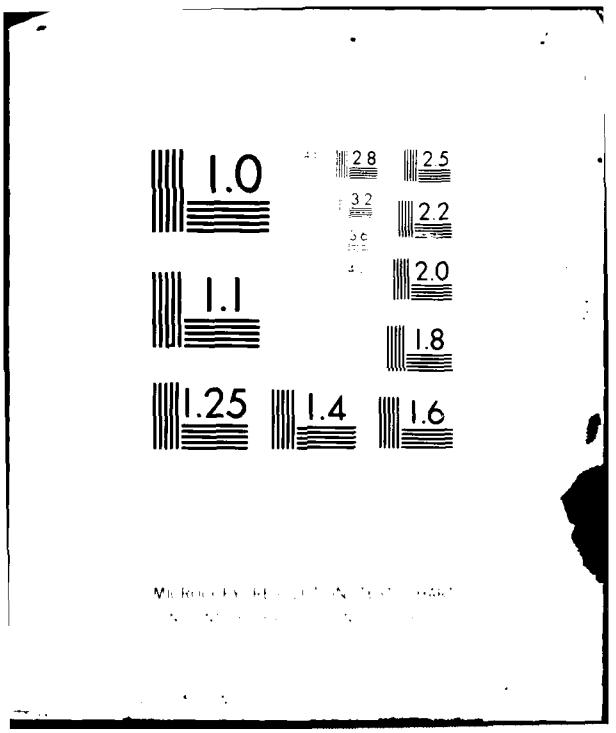
1.0
2.8
2.5
3.2
2.2
2.0
1.1
1.8
1.25
1.4
1.6

where

$$g = n(\Delta) \cos \theta_0' / n(0) \cos \theta_0, \text{ for s or p polarization}$$

But

$$n(0) \simeq n(\Delta) \quad \text{and} \quad \theta_0' \simeq \theta_0$$

[see Eqs. (4-8a) and (4-42)]. Thus Eqs. (4-62) and (4-63) reduce to

$$|t_R| \simeq \sqrt{1 - |r_R|^2} \tag{4-64}$$

$$|t_L| \simeq \sqrt{1 - |r_L|^2} \tag{4-65}$$

From Eq. (4-61) one gets

$$|r_L| \simeq |r_R| \tag{4-66}$$

Combining Eqs. (4-65) and (4-66)

$$|t_L| \simeq \sqrt{1 - |r_R|^2} \tag{4-67}$$

It remains only to determine the phases associated with t_R and t_L. We do this with the aid of the reversibility theorem of stratified media [1] which is given without proof in Eqs. (4-68a) and (4-68b).

$$r_R t_R^* + t_R r_L^* = 0 \tag{4-68a}$$

$$r_L t_L^* + t_L r_R^* = 0 \tag{4-68b}$$

Combining Eqs. (4-61), (4-68a) and (4-68b) immediately yields

$$t_R \simeq |t_R| \exp [(-ikn_0 \cos \theta_0)\Delta] \tag{4-69}$$

$$t_L \simeq |t_L| \exp [(-ikn_0 \cos \theta_0)\Delta] \tag{4-70}$$

From Eqs. (4-61), (4-64), (4-67), (4-69) and (4-70) it can easily be shown that

$$t_L t_R - r_R r_L \simeq \exp [(-2ikn_0 \cos \theta_0)\Delta] \tag{4-71}$$

We will use this result later.

From Eqs. (4-53) through (4-56) and Eq. (4-44) we have

$$Q \simeq \frac{1}{t_R} \begin{bmatrix} 1 & -r_L \\ r_R & t_L t_R - r_R r_L \end{bmatrix} \tag{4-72}$$

Equations (4-61), (4-71), and (4-72) can now be combined to yield

$$Q \simeq \frac{1}{t_R} \begin{bmatrix} 1 & r_R^* \exp [(-2ikn_0 \cos \theta_0)\Delta] \\ r_R & \exp [(-2ikn_0 \cos \theta_0)\Delta] \end{bmatrix} \tag{4-73}$$

where

$$r_R \simeq -\alpha \int_0^{\Delta} \frac{dn(z)}{dz} \exp [(-2ikn_0 \cos \theta_0)z] \, dz \tag{4-57}$$

$$t_R \simeq \sqrt{1 - |r_R|^2}\, \exp\,[(-ikn_0 \cos\theta_0)] \qquad (4\text{-}74)$$

Equation (4-74) is an immediate consequence of Eqs. (4-64) and (4-69).

In the previous section the two by two transfer matrix of a slab of thickness Δ adjacent to dielectrics which index match the slab at its front and rear surfaces was derived. The derivation required that the magnitude of the right going reflection coefficient r_R of that slab be small. Let us now divide the grating shown in Figure 4-1 into N slabs, each of which has a small right going reflection coefficient.

The slabs will be numbered 1 through N, with the slab at the front surface of the grating being the first and the slab at the rear surface being the N^{th}. The transfer matrix, Q_j, of the j^{th} slab is given by Eqs. (4-57), (4-73) and (4-74) which are repeated below.

$$Q_j \simeq \frac{1}{t_{R_j}} \begin{bmatrix} 1 & r^*_{R_j} \exp\,[(-2ikn_0 \cos\theta_{0j})\Delta_j] \\ r_{R_j} & \exp\,[(-2ikn_0 \cos\theta_{0j})\Delta j] \end{bmatrix} \qquad (4\text{-}73)$$

$$r_{R_j} \simeq -\alpha_j \int_0^{\Delta_j} \frac{dn_j(z)}{dz} \exp\,[(-2ikn_0 \cos\theta_{0j})z]\, dz \qquad (4\text{-}57)$$

$$t_{R_j} \simeq \sqrt{1 - |r_{R_j}|^2}\, \exp\,[(-ikn_0 \cos\theta_{0j})\Delta_j] \qquad (4\text{-}74)$$

The refractive index profile of the grating will be designated by n(z) as before. Thus

$$n_j(z) = n\left(z + \sum_{m=1}^{j-1} \Delta_m\right) \qquad (4\text{-}75)$$

$$n_1(z) = n(z)$$

Furthermore, from Snell's Law and Eq. (4-8a)

$$\theta_{0j} \simeq \sin^{-1}\left(\frac{n_f \sin\theta_0}{n_0}\right) \qquad j = 1, \ldots, N \qquad (4\text{-}76)$$

Recall that n_f is the refractive index of the dielectric in contact with the front surface of the grating while n_b is the refractive index of the dielectric in contact with the back surface of the grating. It should be noted that the transfer matrix, Q_1, of the first slab is given by Eq. (4-73) only when $n_f = n(0)$. This is because Eq. (4-73) was derived under the condition that the j^{th} slab is adjacent to a dielectric which index matches the slab at its front and rear surfaces. Similarly, the transfer matrix, Q_N, of the N^{th} slab is given by Equation (4-73) only when $n_b = n(D)$. We circumvent this problem by conceptually adding two additional "slabs" to the grating, one at its front surface and one at its back surface. These slabs are of thickness δ and have refractive indices $n(0)$ and $n(D)$, respectively. The situation is illustrated in Figure 4-7. In this case Q_1 and Q_N as given by Equation (4-73) are valid. As δ shrinks to zero the new grating shown in Figure 4-7 becomes indistinguishable from the original one shown in Figure 4-1. All that is necessary then is to determine the transfer matrices of the two additional layers shown in Figure 4-7 in the limit as $\delta \to 0$. This has already been done in Chapter 3 (see Eq. (3-79)). The transfer matrix of the front layer will be designated G_f while the transfer matrix of the back layer will be designated G_b.

The transfer matrix, Q, of the entire grating will then be

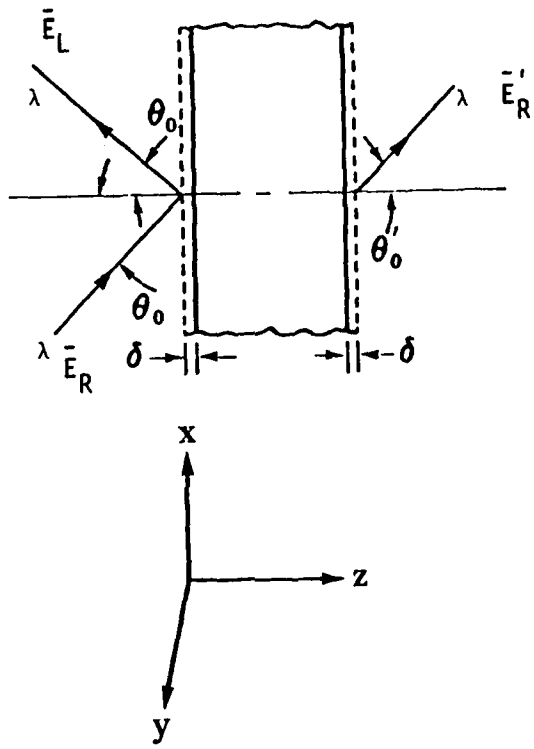

Figure 4-7. Holographic Grating with Front and Rear Extensions

$$Q = \begin{bmatrix} q_{11} & q_{12} \\ q_{21} & q_{22} \end{bmatrix} = G_f \left(\prod_{j=1}^{N} Q_j \right) G_b \qquad (4\text{-}77)$$

The right going reflection coefficient, r_R, of the grating is given by Eq. (4-49)

$$r_R = \frac{q_{21}}{q_{11}} \text{ , for s or p polarization} \qquad (4\text{-}49)$$

and the right going transmission coefficient by Eq. (4-50).

$$t_R = \begin{cases} \dfrac{1}{q_{11}} & \text{, for s polarization} \\ \dfrac{1}{q_{11}} \cdot \dfrac{\cos \theta_0}{\cos \theta_0'} & \text{, for p polarization} \end{cases} \qquad (4\text{-}50)$$

We have seen that the transfer matrix relates the right and left going electric field immediately outside of the front surface of a grating to the right and left going electric field immediately outside of the back surface of the same grating.

The transfer matrix will depend on the refractive index of the material which is adjacent to the front surface of the grating and the refractive index of the material which is adjacent to the back surface of the grating. It is more convenient to redefine the transfer matrix so that it relates the right and left going electric field immediately inside of the front surface of the grating to the right and left going electric field immediately inside of the back surface of the grating. Thus, the redefined transfer matrix no longer depends on the refractive indices of mediums which are adjacent to the grating. This redefined

transfer matrix is, of course, identical with the original transfer matrix if the two mediums which are adjacent to the grating match it in refractive index at the interfaces.

Now suppose that two gratings, called one and two, are placed together with their surfaces in contact. Gratings one and two have transfer matrices Q_1 and Q_2 respectively. What is the transfer matrix Q_1 and $_2$ of the combined grating? If the refractive index is continuous across the grating to grating interface, then the right and left going fields must be continuous across this interface. Thus, it immediately follows that

$$Q_{1 \text{ and } 2} = Q_1 \cdot Q_2 \tag{4-78}$$

If the refractive index is not continuous across the grating to grating interface, then the right and left going fields are not continuous across the interface. Therefore, Eq. (4-78) is no longer valid. Let $_1G_2$ denote a matrix which relates the right and left going fields immediately inside the back surface of optical element one to the right and left going fields immediately inside the front surface of optical element two. Then

$$Q_{1 \text{ and } 2} = Q_1 \cdot {}_1G_2 \cdot Q_2 \tag{4-79}$$

Clearly, $_1G_2$ relates the right and left going fields on one side of a dielectric to dielectric interface to those on the other side. The form of $_1G_2$ was derived in Chapter 3 (see Eq. (3-79)).

Note that in Eq. (4-77) the Q_j's can be multiplied directly together together without the use of $_jG_{j+1}$'s. This follows from the fact that there is no discontinuity in the refractive index at the inteface between the j^{th} and $j+1^{th}$ slabs.

Notes to Chapter 4

[1] Knittl, Optics of Thin Films, John Wiley & Sons, New York, 1976.

[2] E. Wolf, Progress in Optics, Vol. 5 (Chapter 5), North-Holland Publishing Co., Amsterdam, 1966.

[3] The propagation angle, θ_0 cannot excede the critical angle of the holographic material. This critical angle, θ_c, is given by

$$\theta_c \approx \sin^{-1}\left(\frac{1}{n_0}\right) \approx \sin^{-1}\left(\frac{1}{1.5}\right) \approx 42°$$

[4] A. Vašíček, Optics of Thin Films, North-Holland Publishing Co., Amsterdam, 1960.

5
QUASI-SINUSOIDAL REFRACTIVE INDEX PROFILES AND THE THICK SLAB DECOMPOSITION

In Chapter 4 a technique for determining the two by two transfer matrix [and consequently $H_R(\lambda, \theta_0)$ and $H_T(\lambda, \theta_0)$] of a flat, holographic grating having a refractive index variation only in a direction normal to the grating surface was presented. Here, we will apply this method, known as Thick Slab Decomposition (TSD), to several holographic gratings having quasi-sinusoidal refractive index profiles. The results will be compared with those obtained by the multilayer dielectric stack approach. We will also derive simple formulas for $H_R(\lambda, \theta_0)$ and $H_T(\lambda, \theta_0)$ when the refractive index profile of the grating is sinusoidal.

The following observations can be made concerning the TSD

1. The holographic grating is divided into N slabs. Each of these slabs must be sufficiently thin such that the modulus squared of the right going reflection coefficient is much less than one. This condition places a lower limit on the value of N.

2. The number of matrix multiplications required by the TSD method is proportional to N.

3. The TSD method offers computational advantages over the multilayer dielectric stack approach only when the right going reflection coefficient of each thick layer can be evaluated without substantial calculation.

4. The evaluation of the right going reflection coefficient of each slab generally becomes simpler as the number of slabs N, increases.

We assume that the refractive index profile, n(z) can be written as[1]

$$n(z) = n_0 + A(z) \sin [2\pi f(z)z + \Gamma(z)] \tag{5-1}$$

It was noted in Chapter 4 that refractive index profiles of reflection gratings which can be holographically fabricated will not have frequency components outside of the range 4 μm^{-1} to 6 μm^{-1}. Thus, n(z) is to an extent narrowband with f(z) nominally in the range 4 μm^{-1} to 6 μm^{-1}. Therefore, A(z), f(z) and $\Gamma(z)$ will be approximately constant over an interval of length, , where

$$\delta \simeq \frac{1}{f(z)} \tag{5-2}$$

If the grating is divided into N slabs, the j^{th} one being Δ_j μm thick ($\Delta_j \leq \delta$) then the refractive index profile within the j^{th} slab can to a reasonable approximation be written as

$$n_j(z) \simeq n_0 + A_j \sin (2\pi f_j z + \Gamma_j) \tag{5-3}$$

where A_j, f_j and Γ_j are constant.

Below, we derive the right going reflection coefficient r_{R_j}, of a slab Δ_j μm thick which has a refractive index profile given by Eq. (5-3). We assume for the moment that $|r_{R_j}^2| << 1$. From Eqs. (4-27a), (4-27b) and (4-57) of Chapter 4.

$$r_{R_j} \simeq -\alpha \int_0^{\Delta_j} \frac{dn_j(z)}{dz} \exp [(-2ikn_0 \cos \theta_0)z] dz \tag{5-4}$$

where

$$\alpha = \begin{cases} \dfrac{1}{n_0 \cos^2 \theta_0}, & \text{for s polarization} \quad (5\text{-}5a) \\ \dfrac{1 - \tan^2 \theta_0}{n_0}, & \text{for p polarization} \quad (5\text{-}5b) \end{cases}$$

Substituting Eq. (5-3) into Eq. (5-4) yields

$$r_{R_j} \simeq -\alpha \int_0^{\Delta_j} 2\pi f_j A_j \cos (2\pi f_j z + \Gamma_j) \exp [(-2ikn_0 \cos \theta_0)z] dz \quad (5\text{-}6)$$

$$= \frac{-2\pi f_j A_j \alpha}{2} \int_0^{\Delta_j} \Big[\exp (i\Gamma_j) \exp [i(2\pi f_j - 2kn_0 \cos \theta_o)z)$$

$$+ \exp (-i\Gamma_j) \exp [-i(2\pi f_j + 2kn_0 \cos \theta_0)z] \Big] dz$$

$$= \frac{-2\pi f_j A_j \alpha}{2} \exp (i\Gamma_j) \frac{\exp [i(2\pi f_j - 2kn_0 \cos \theta_0)\Delta_j] - 1}{i(2\pi f_j - 2kn_0 \cos \theta_0)}$$

$$- \frac{2\pi f_j A_j \alpha}{2} \exp (-i\Gamma_j) \frac{\exp [-i(2\pi f_j + 2kn_0 \cos \theta_0)\Delta_j] - 1}{-i(2\pi f_j + 2kn_0 \cos \theta_0)}$$

(Equation continued on next page)

$$= -\pi f_j A_j \alpha \Delta_j \exp\left(i[\Gamma_j + (\pi f_j - kn_0 \cos\theta_0)\Delta_j]\right) \operatorname{sinc}[(\pi f_j - kn_0 \cos\theta_0)\Delta_j]$$

$$-\pi f_j A_j \alpha \Delta_j \exp\left(-i[\Gamma_j + (\pi f_j + kn_0 \cos\theta_0)\Delta_j]\right) \operatorname{sinc}[(\pi f_j + kn_0 \cos\theta_0)\Delta_j]$$

The above equation is repeated below for reference

$$r_{R_j} \simeq -\pi f_j A_j \alpha \Delta_j \exp\left(i[\Gamma_j + (\pi f_j - kn_0 \cos\theta_0)\Delta_j]\right) \operatorname{sinc}[(\pi f_j - kn_0 \cos\theta_0)\Delta_j]$$

$$-\pi f_j A_j \alpha \Delta \exp\left(-i[\Gamma_j + (\pi f_j + kn_0 \cos\theta_0)\Delta_j]\right) \operatorname{sinc}[(\pi f_j + kn_0 \cos\theta_0)\Delta_j] \qquad (5\text{-}7)$$

From Eq. (5-7) we have

$$|r_{R_j}|^2 \lesssim (\pi f_j A_j \alpha \Delta_j)^2 \left\{\operatorname{sinc}^2[(\pi f_j - kn_0 \cos\theta_0)\Delta_j] + \operatorname{sinc}^2[(\pi f_j + kn_0 \cos\theta_0)\Delta_j]\right\} < 2(\pi f_j A_j \alpha \Delta_j)^2 \qquad (5\text{-}8)$$

As in Chapter 4, the index modulation, A_j, is assumed to be less than 0.03. Therefore, if Δ_j is chosen such that $\Delta_j = 1/f_j$ then

$$|r_{R_j}|^2 \lesssim 2\pi^2 (f_j)^2 (0.03)^2 \alpha^2 (1/f_j)^2 = 0.018\alpha^2 \qquad (5\text{-}9)$$

Since θ_0, the propagation angle within the grating, can never exceed the critical angle (42°) and since n_0 is nominally 1.5, Eqs. (5-5a) and (5-5b) indicate that

$$\alpha^2 < 1.46 \tag{5-10}$$

Combining Eqs. (5-9) and (5-10) yield

$$|r_{R_j}|^2 < 0.027 \tag{5-11}$$

Hence, our original assumption

$$|r_{R_j}|^2 << 1$$

was valid.

We combine Eq. (5-7) with Eqs. (4-73) and (4-74) of Chapter 4. The results is

$$Q_j \simeq \frac{1}{t_{R_j}} \begin{bmatrix} 1 & & B \\ & & \\ C & \exp\left[(-2ikn_0 \cos\theta_0)\Delta_j\right] \end{bmatrix} \tag{5-12}$$

where

$$C = -\pi f_j \alpha \Delta_j A_j \exp\left(i[\Gamma_j + (\pi f_j - kn_0 \cos\theta_0)\Delta_j]\right) \cdot$$

$$\operatorname{sinc}\left[(\pi f_j - kn_0 \cos\theta_0)\Delta_j\right] -$$

$$\pi f_j A_j \alpha \Delta_j \exp\left(-i[\Gamma_j + (\pi f_j + kn_0 \cos\theta_0)\Delta_j]\right) \cdot$$

$$\operatorname{sinc}\left[(\pi f_j + kn_0 \cos\theta_0)\Delta_j\right] \tag{5-13a}$$

$$B = -\pi f_j A_j \alpha \Delta_j \exp\left(-i[\Gamma_j + (\pi f_j + kn_0 \cos\theta_0)\Delta_j]\right) \cdot$$

$$\text{sinc}\,[(\pi f_j - kn_0 \cos\theta_0)\Delta_j] -$$

$$\pi f_j A_j \alpha \Delta_j \exp\left(i[\Gamma_j + (\pi f_j - kn_0 \cos\theta_0)\Delta_j]\right) \cdot$$

$$\text{sinc}\,[(\pi f_j + kn_0 \cos\theta_0)\Delta_j] \qquad (5\text{-}13b)$$

$$t_{R_j} \simeq \sqrt{1 - |C|^2}\, \exp\,[(-ikn_0 \cos\theta_0)\Delta_j] \qquad (5\text{-}13c)$$

Equations (5-12), (5-13a), (5-13b) and (5-13c) give the transfer matrix, Q_j, of a slab Δ_j microns thick which has a refractive index profile $n_j(z)$ described by

$$n(z) = n_0 + A_j \sin(2\pi f_j z + \Gamma_j)$$

$$|A_j| \leq 0.03 \text{ and } 4\ \mu m^{-1} \leq f_j \leq 6\ \mu m^{-1} \qquad (5\text{-}14)$$

The results obtained so far are summarized below. We consider a flat, holographic grating of thickness D microns which has a refractive index that varies only in a direction normal to the grating surface. It is assumed that the refractive index can, to a good approximation, be written as

$$n(z) = n_0 + A_j \sin(2\pi f_j z + \Gamma_j) \text{ for } \sum_{m=1}^{j-1} \Delta_m \leq z < \sum_{m=1}^{j} \Delta_m \qquad (5\text{-}15)$$

$$(\text{note} \sum_{m=1}^{0} \Delta_m \triangleq 0)$$

where n_0 is nominally 1.5

$|A_j| < 0.03$

$4\ \mu m^{-1} \leq f_j \leq 6\ \mu m^{-1}$

Then Eq. (5-12) is, to a good approximation, the transfer matrix of the section of the HOE between

$$\sum_{m=}^{j-1} \Delta_m \leq z < \sum_{m=1}^{j} \Delta_m$$

The two by two transfer matrix, Q, of the grating as well as r_R . $H_R(\lambda, \theta_0)$, t_R and $H_T(\lambda, \theta_0)$ of the HOE will be given by Eqs. (4-77), (4-49), (4-2a), (4-50) and (4-2b) of Chapter 4. These equations are repeated below.

$$Q = \begin{bmatrix} q_{11} & q_{12} \\ q_{21} & q_{22} \end{bmatrix} = G_f \left(\prod_j Q_j \right) G_b \qquad (5\text{-}16)$$

$$H_R(\lambda, \theta_0) = r_R = \frac{q_{21}}{q_{11}} \text{ , for s or p polarization} \qquad (5\text{-}17)$$

$$H_T(\lambda, \theta_0) = t_R = \begin{cases} \dfrac{1}{q_{11}}, & \text{for s polarization} \\ \dfrac{1}{q_{11}} \cdot \dfrac{\cos \theta_0}{\cos \theta_0'}, & \text{for p polarization} \end{cases} \qquad (5\text{-}18)$$

It should be noted that Eq. (5-12) is valid regardless of how large Δ_j is provided that $|r_{R_j}|^2 << 1$. Recall that Eq. (5-8) gives an upper bound for $|r_{R_j}|^2$ which can be used to determine the maximum allowable Δ_j.

It can be shown that calculation of $H_R(\lambda, \theta_0)$ and $H_T(\lambda, \theta_0)$ for ten or, more different values of θ_0 or λ via Eqs. (5-12), (5-16), (5-17) and (5-18) will be at least an order of magnitude faster than performing the same caluclations using the multilayer dielectric stack approach. Equation (5-12) can be further simplified under the following conditions:

1. Δ_j is chosen such that $f_j\Delta_j$ is an integer

Note that for $f_j\Delta_j$ an integer, Γ_j must be 0 or π since $n(z)$ is a continuous function of z. When the above condition is satisifed Eq. (5-12) becomes

$$Q_j \quad \frac{1}{\sqrt{1 - a_j^2}} \exp\left[(ikn_0 \cos \theta_0)\Delta_j\right] \begin{bmatrix} 1 & a_j \exp\left[(-ikn_0 \cos \theta_0)\Delta_j\right] \\ a_j \exp\left[(-ikn_0 \cos \theta_0)\Delta_j\right] & \exp\left[(-2ikn_0 \cos \theta_0)\Delta_j\right] \end{bmatrix}$$

(5-19)

where

$$a_j = \pm \pi f_j A_j \alpha \Delta_j \left(\text{sinc}\,[(\pi f_j - kn_0 \cos\theta_0)\Delta_j] + \text{sinc}\,[(\pi f_j + kn_0 \cos\theta_0)\Delta_j]\right) \tag{5-20}$$

The plus sign corresponds to $f_j\Delta_j$ an odd integer and $\Gamma_j = 0$, or $f_j\Delta_j$ an even integer and $\Gamma_j = \pi$. The minus sign corresponds to $f_j\Delta_j$ an odd integer and $\Gamma_j = \pi$, or $f_j\Delta_j$ and even integer and $\Gamma_j = 0$. In the remainder of this report we'll assume that

$$\Delta_j = 1/f_j \tag{5-21}$$

Then Eqs. (5-19) and (5-20) can be rewritten as

$$Q_j \simeq \frac{\exp(i\phi_j)}{\sqrt{1 - a_j^2}} \begin{bmatrix} 1 & a_j \exp(-i\phi_j) \\ a_j \exp(-i\phi_j) & \exp(-2i\phi_j) \end{bmatrix} \tag{5-22}$$

where

$$\phi_j = (kn_0 \cos\theta_0)/f_j \tag{5-23}$$

$$a_j = \pi A_j \alpha \left(\sin\,[(\pi f_j - kn_0 \cos\theta_0)/f_j] + \text{sinc}\,[(\pi f_j + kn_0 \cos\theta_0)/f_j]\right) \tag{5-24}$$

The above three equations are the principal result of this chapter.

On the following pages plots are given of the reflectance, ($|H_R(\lambda, \theta_0)|^2$, phase change upon reflection

$$\frac{H_R(\lambda, \theta_0)}{|H_R(\lambda, \theta_0)|}$$

transmittance ($|H_T(\lambda, \theta_0)|^2$), and phase change upon transmission

$$\frac{H_T(\lambda, \theta_0)}{|H_T(\lambda, \theta_0)|}$$

vs. angle of incidence for three flat holographic optical elements under s polarized plane wave illumination. All of the gratings considered have a refractive index which varies only in a direction normal to the surface of the grating, and for simplicity, they are assumed to be surrounded by a homogeneous dielectric of refractive index 1.5. The plots were generated using both the multilayer dielectric stack and thick layer decomposition techniques.

Each of the elements has a refractive index profile which to a good approximation can be given by Eq. (5-15) with the Γ_j's = 0 and n_0 = 1.5. Figures 5-1, 5-6 and 5-11 are plots of the refractive index modulation A_j (solid line), and the frequency f_j (dashed line) as a function of the cycle number j. Figures 5-2 through 5-5 are plots of the reflectance, phase change upon reflection, transmission and phase change upon transmission vs. angle of incidence for the element whose refractive index profile is given in Figure 5-1. The refractive index profile of this element can be analytically described by Eq. (5-25) below

$$n(z) = 1.5 + 0.02 \sin (2\pi \cdot 5.14237 \cdot z) \qquad (5\text{-}25)$$

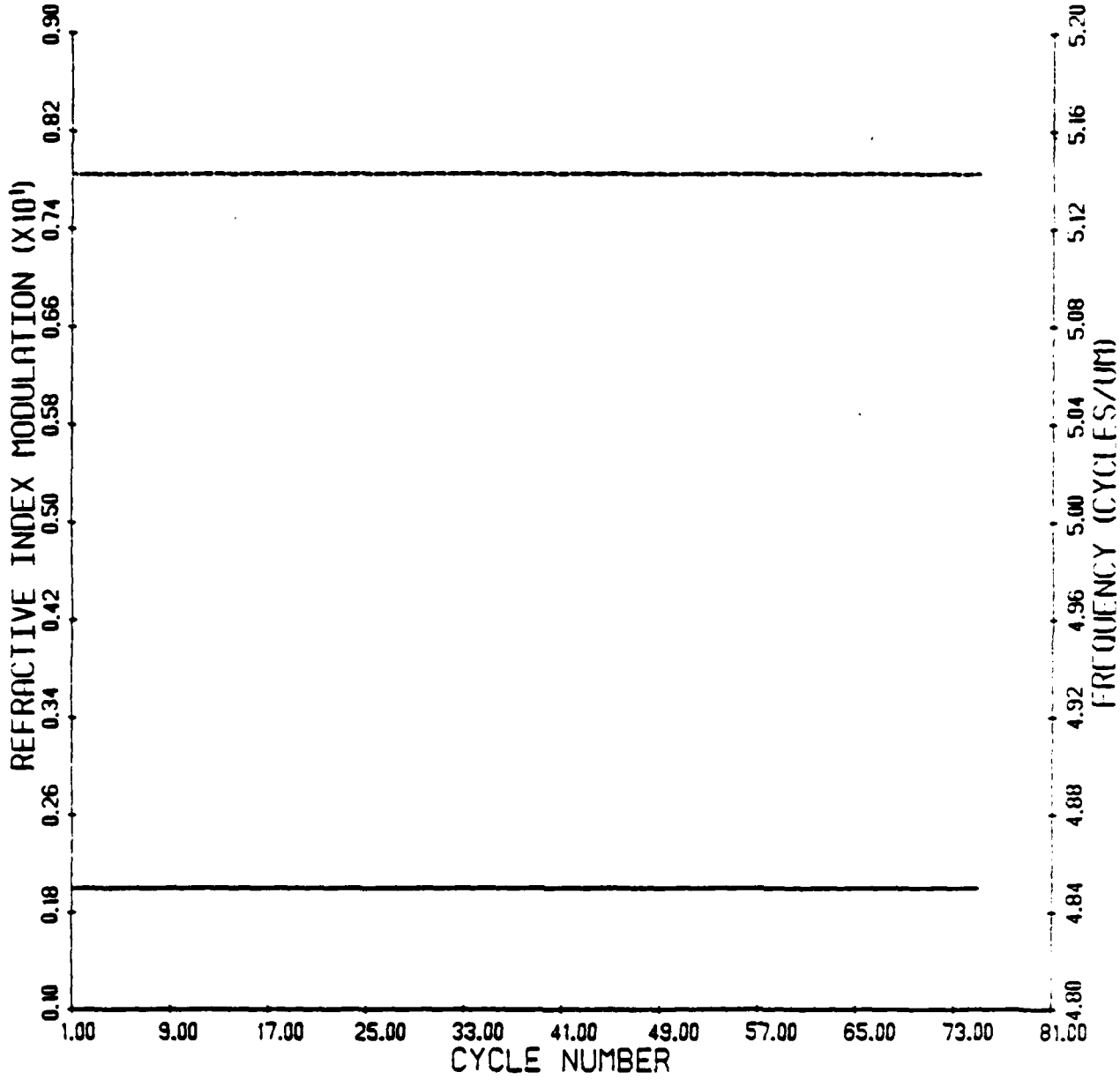

Figure 5-1. Refractive Index Modulation and Frequency vs. Cycle Number (Example 1)

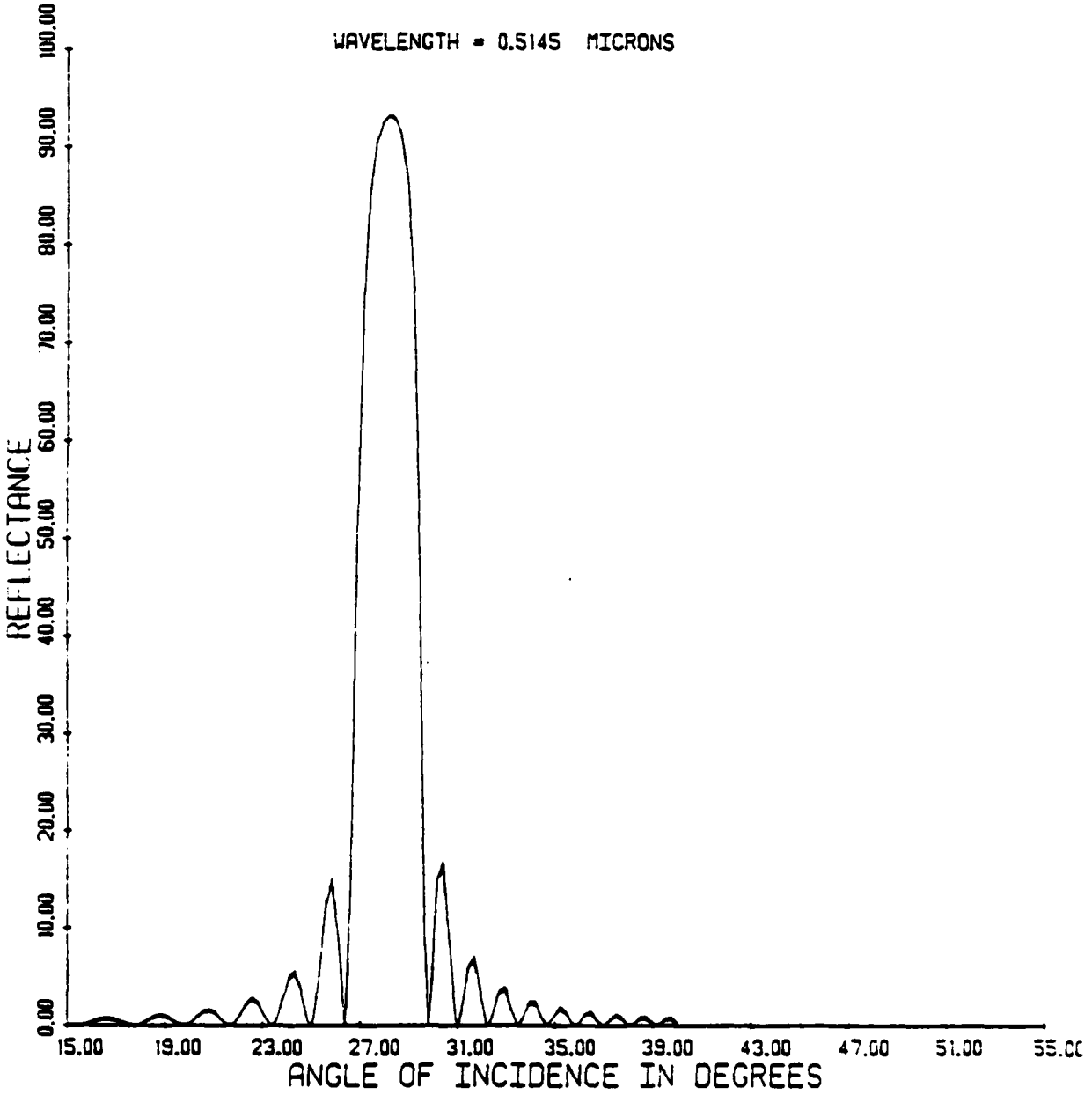

Figure 5-2. Comparison of Reflectance vs. Angle of Incidence Characteristics Computed by the TSD Method and the Multilayer Dielectric Stack Method (Example 1)

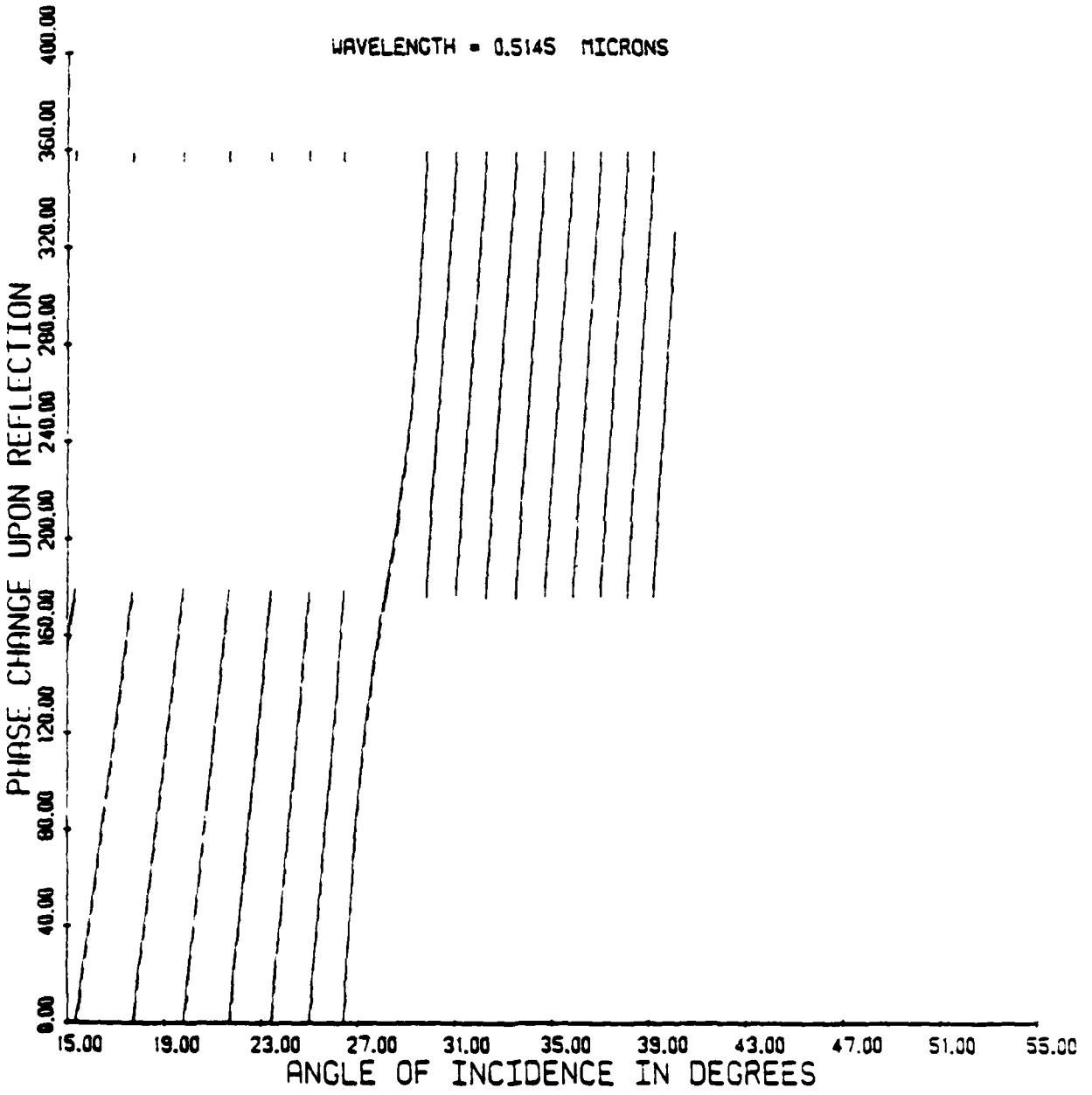

Figure 5-3. Comparison of Phase Change Upon Reflectance vs. Angle of Incidence Characteristics Computed by the TSD Method and the Multilayer Dielectric Stack Method (Example 1)

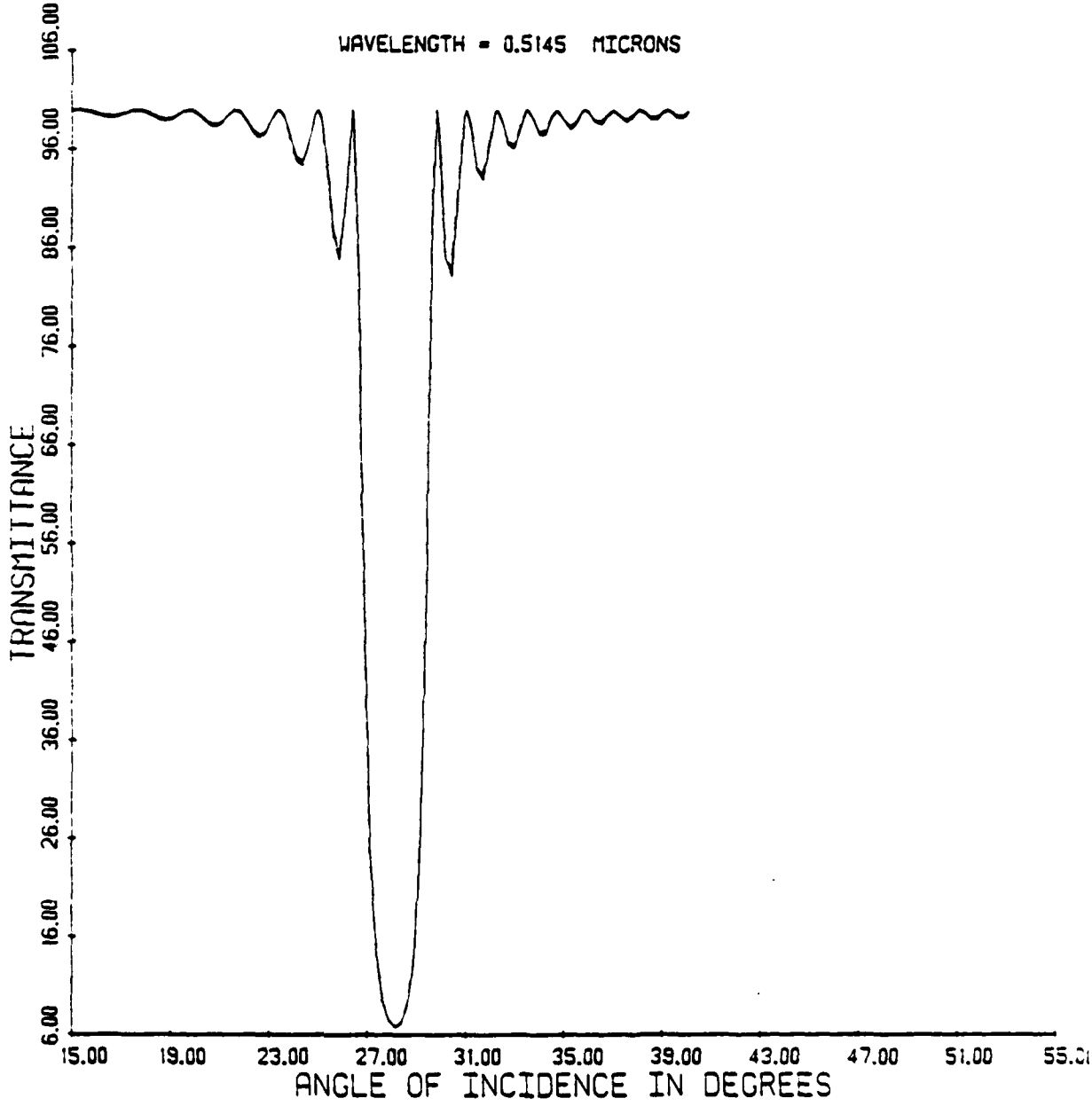

Figure 5-4. Comparison of Transmittance vs. Angle of Incidence Characteristics Computed by the TSD Method and the Multilayer Dielectric Stack Method (Example 1)

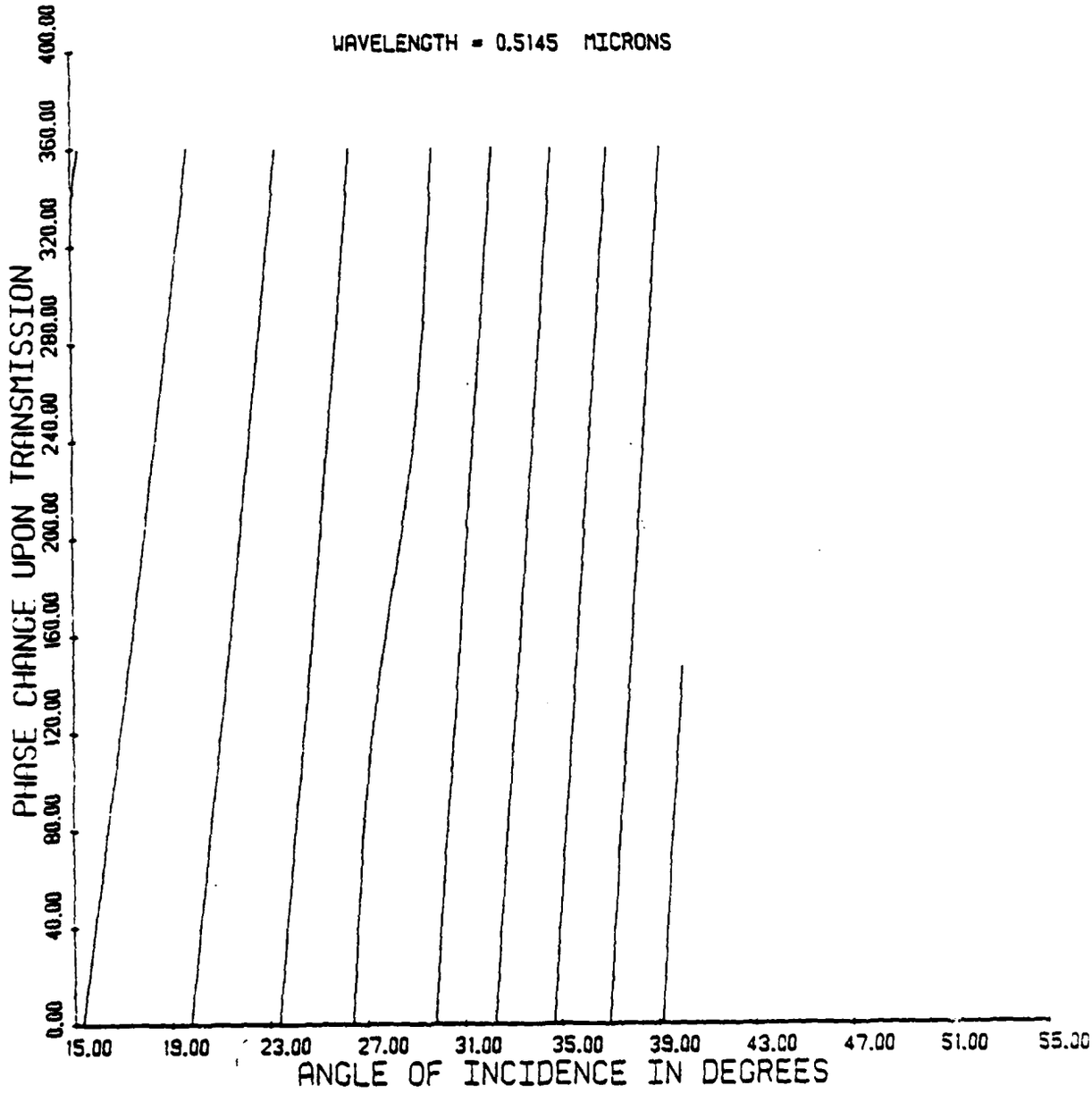

Figure 5-5. Comparison of Phase Change Upon Transmission vs. Angle of Incidence Characteristics Computed by the TSD Method and the Multilayer Dielectric Stack Method (Example 1)

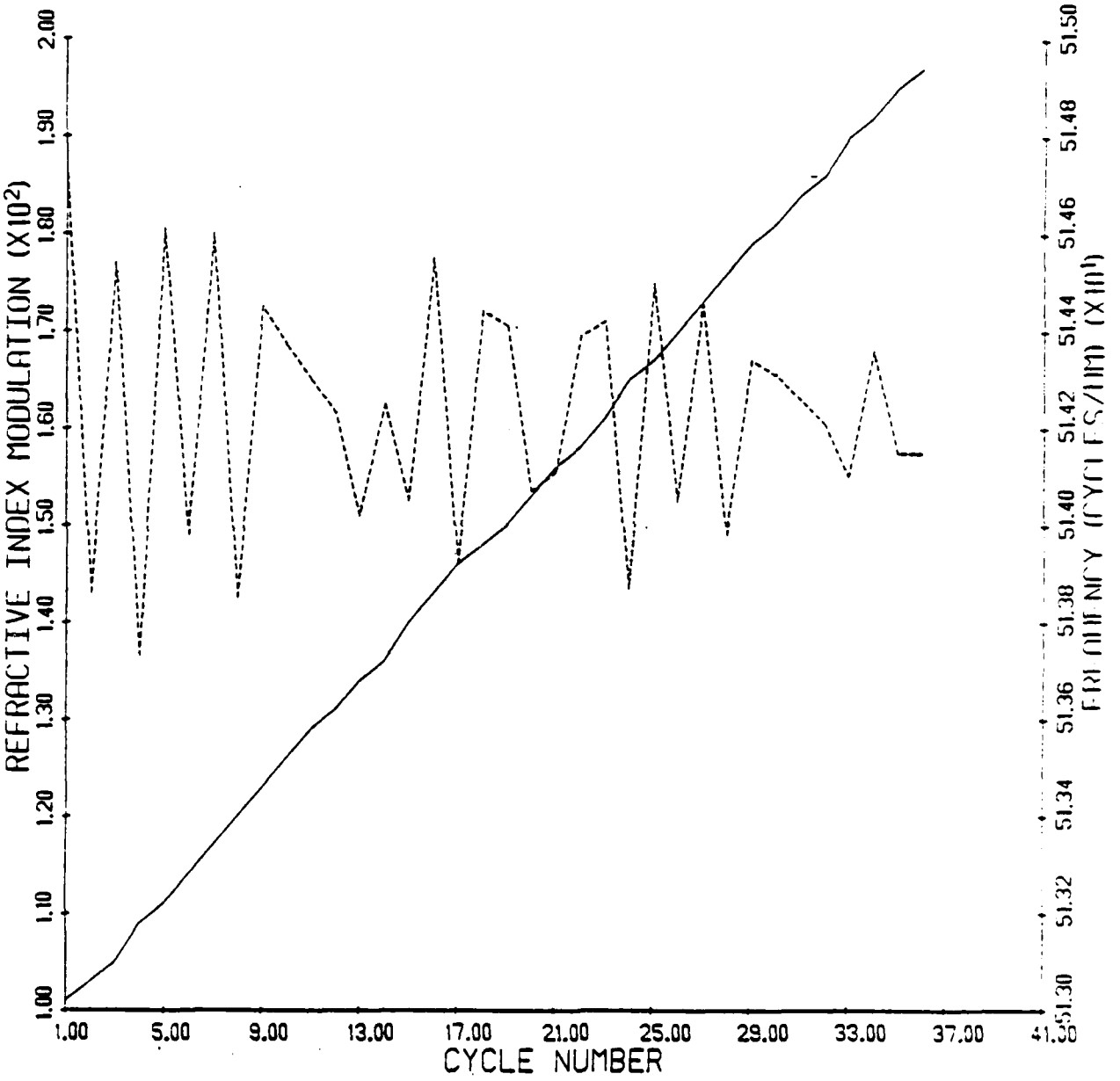

Figure 5-6. Refractive Index Modulation and Frequency vs. Cycle Number (Example 2)

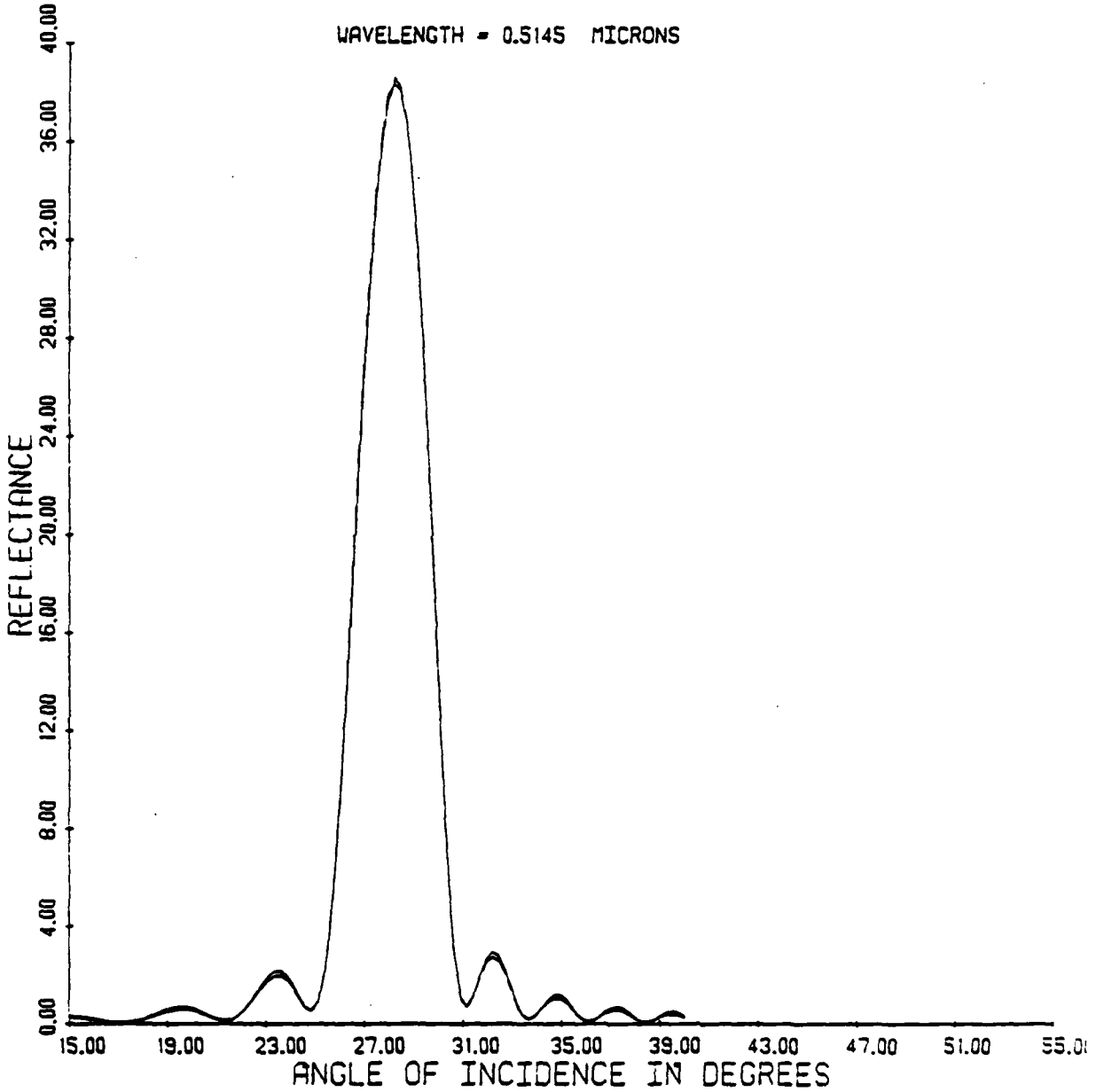

Figure 5-7. Comparison of Reflectance vs. Angle by Incidence Characteristics Computed by the TSD Method and the Multilayer Dielectric Stack Method (Example 2)

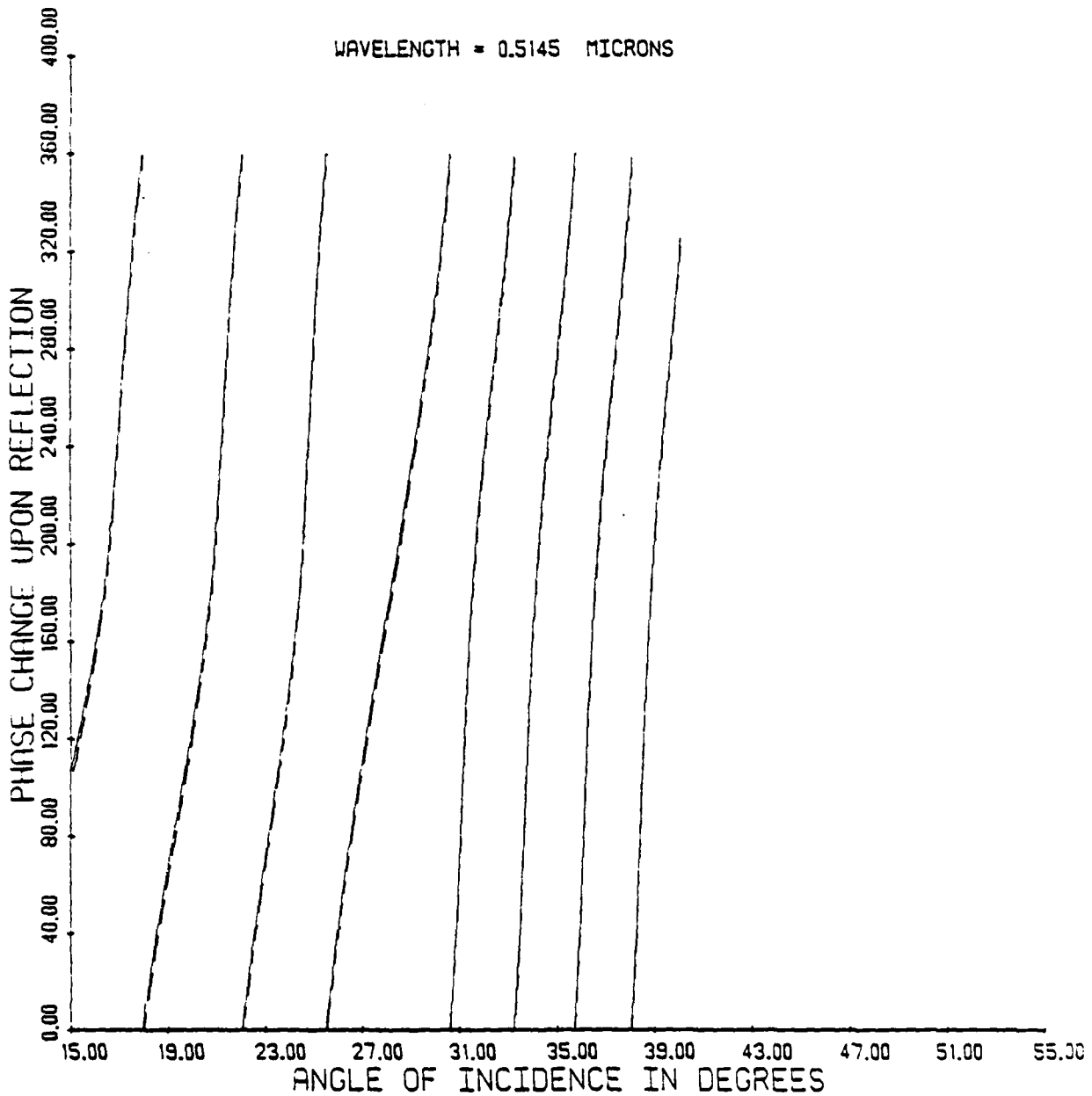

Figure 5-8. Comparison of Phase Change Upon Reflection vs. Angle of Incidence Characteristic Computed by the TSD Method and the Multilayer Dielectric Stack Method (Example 2)

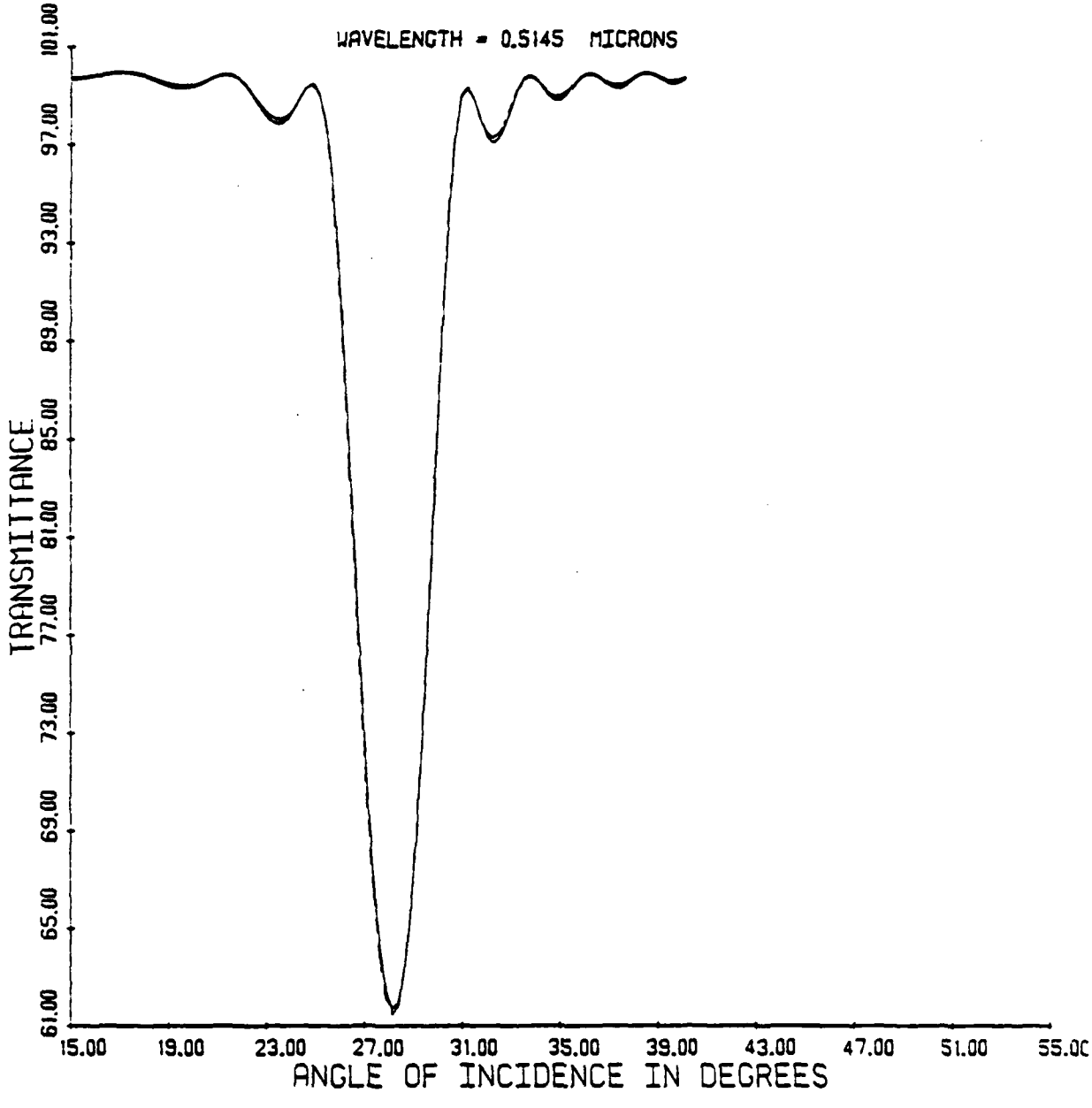

Figure 5-9. Comparison of Transmittance vs. Angle of Incidence Characteristic Computed by the TSD Method and the Multilayer Dielectric Stack Method (Example 2)

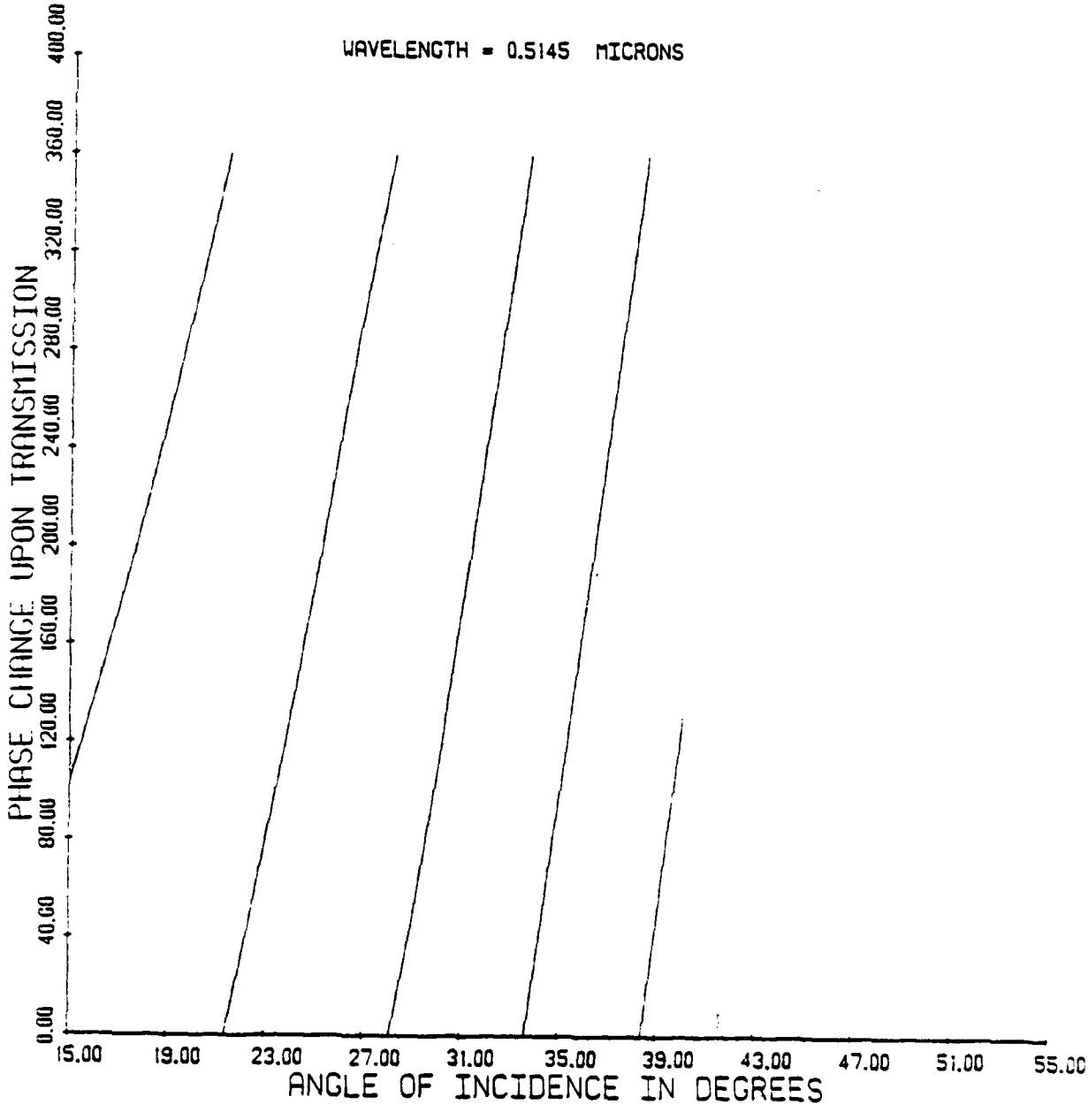

Figure 5-10. Comparison of Phase Change Upon Transmission vs. Angle of Incidence Characteristics Computed by the TSD Method and the Multilayer Dielectric Stack Method (Example 2)

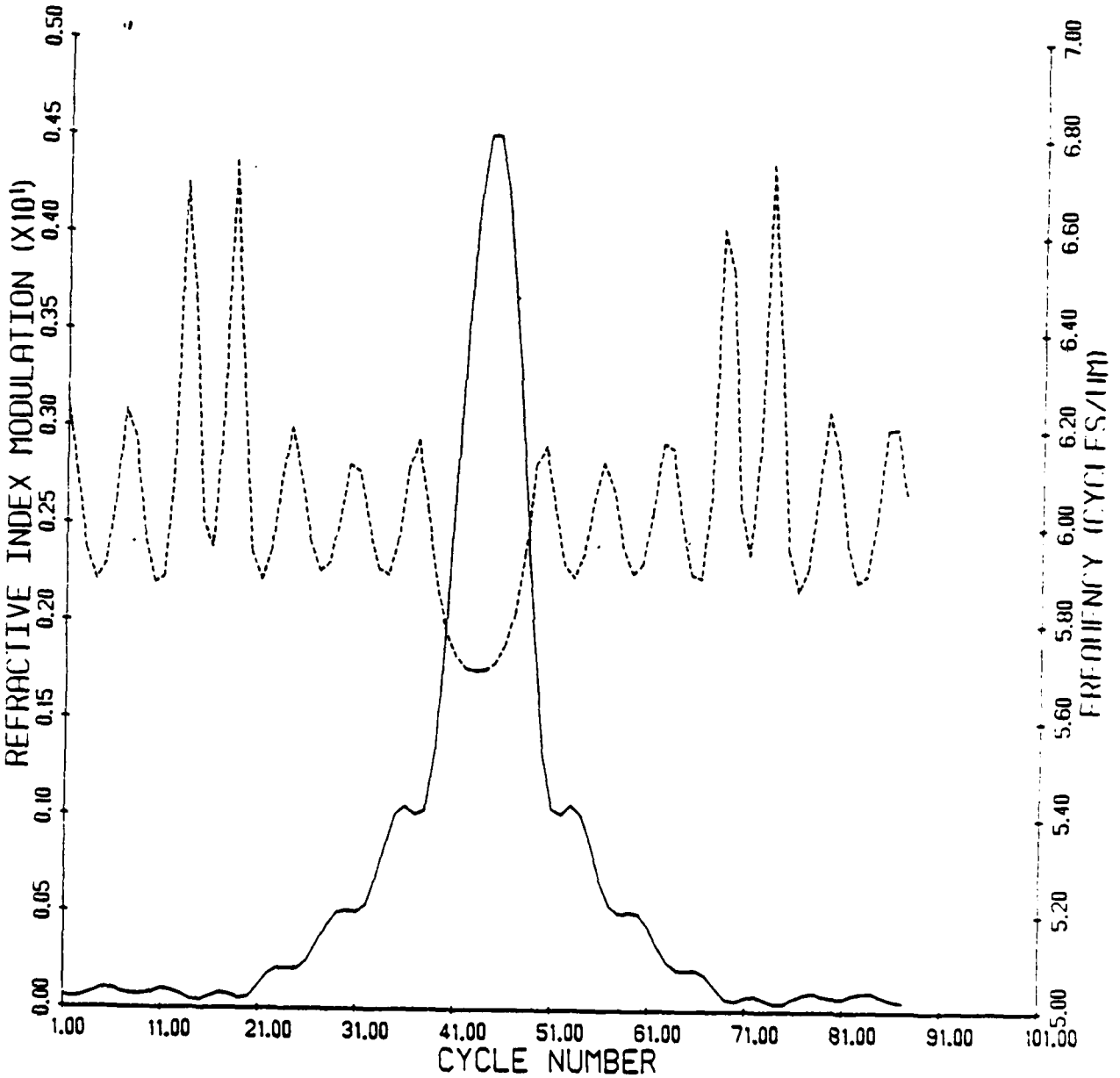

Figure 5-11. Refractive Index Modulation and Frequency vs. Cycle Number (Example 3)

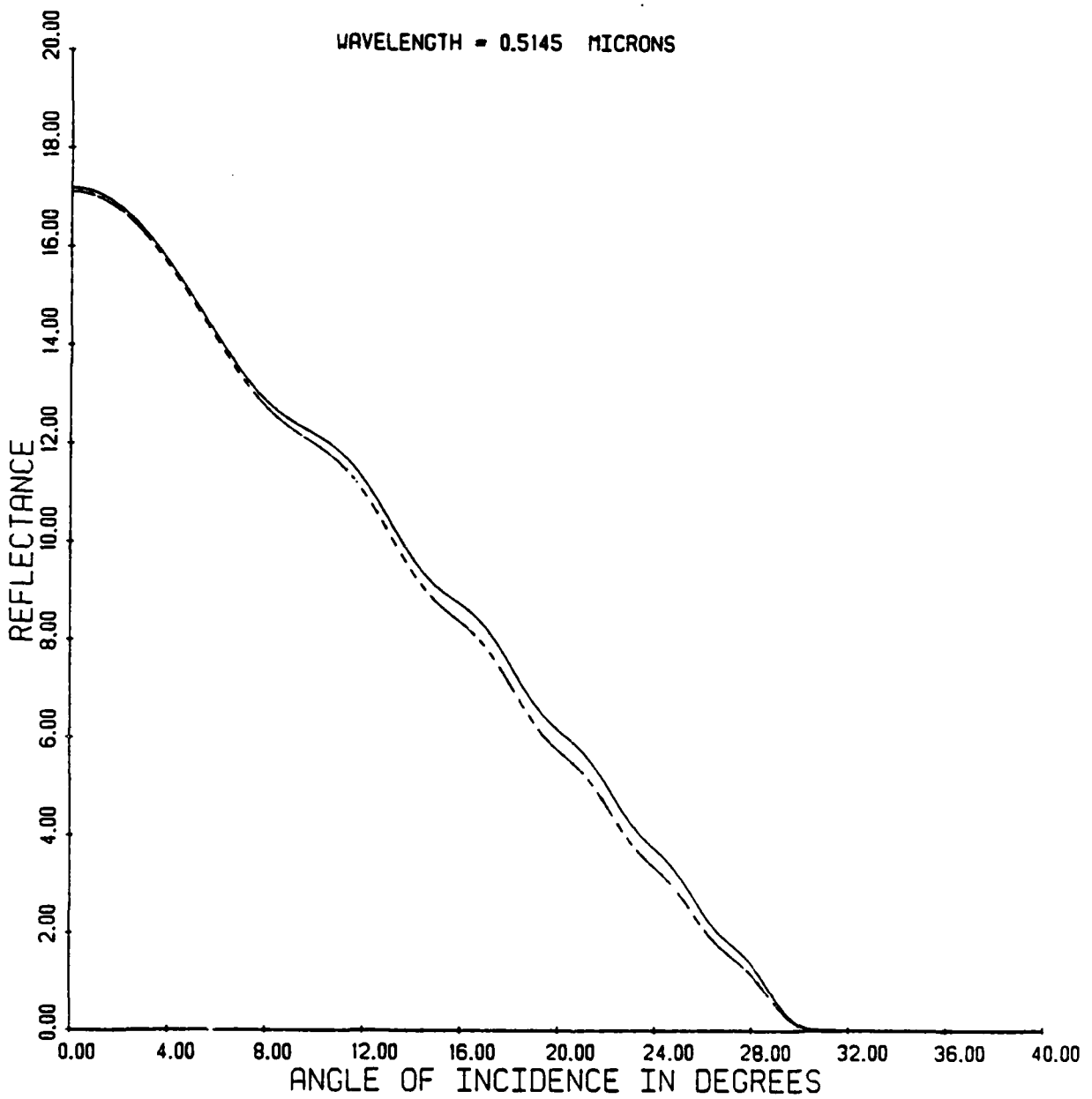

Figure 5-12. Comparison of Reflectance vs. Angle of Incidence Characteristics Computed by the TSD Method and the Multilayer Dielectric Stack Method (Example 3)

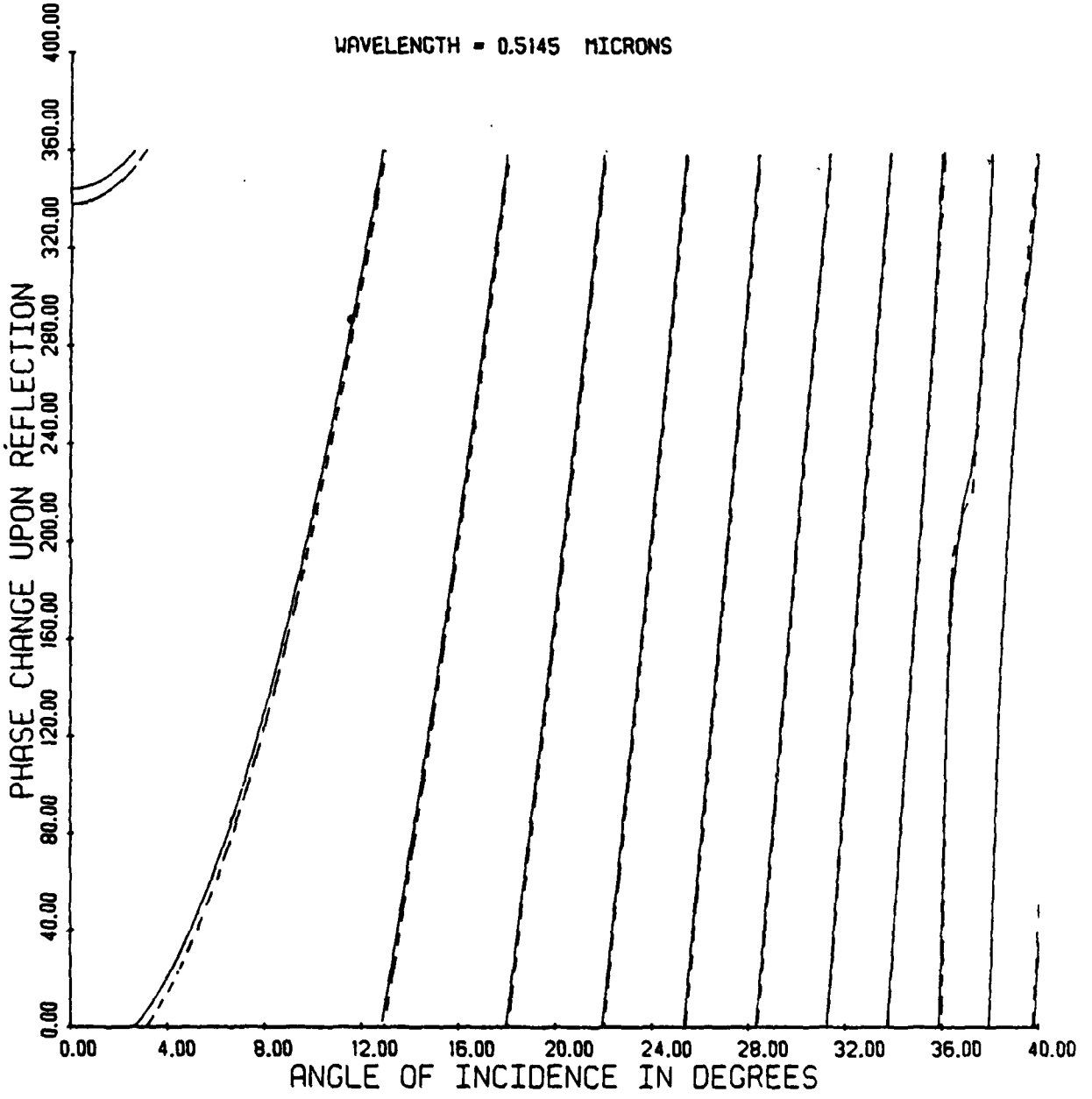

Figure 5-13. Comparison of the Phase Change Upon Reflection vs. Angle of Incidence Characteristics Computed by the TSD Method and the Multilayer Dielectric Stack Method (Example 3)

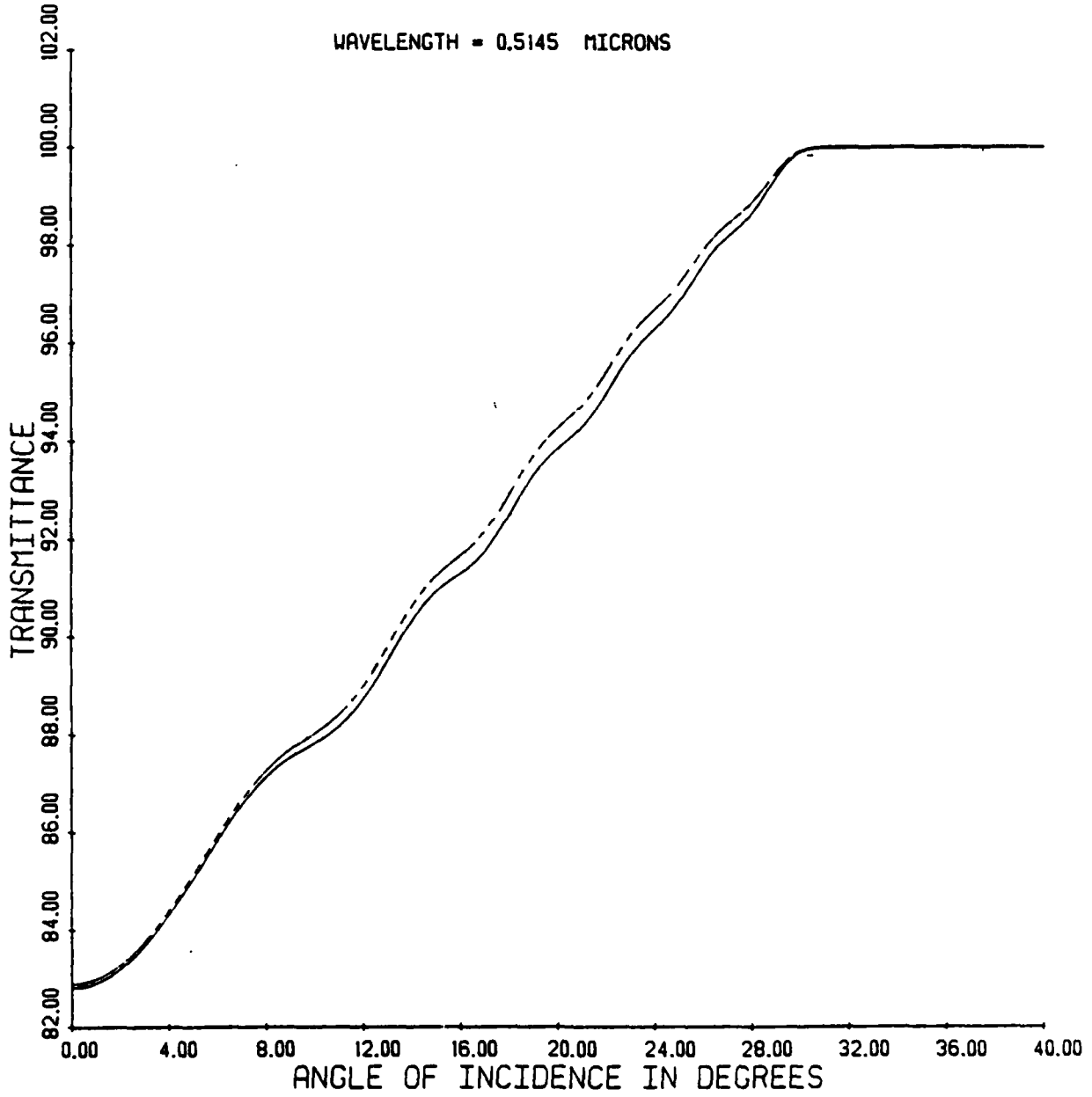

Figure 5-14. Comparison of the Transmittance vs. Angle of Incidence Characteristics Computed by the TSD Method and the Multilayer Dielectric Stack Method (Example 3)

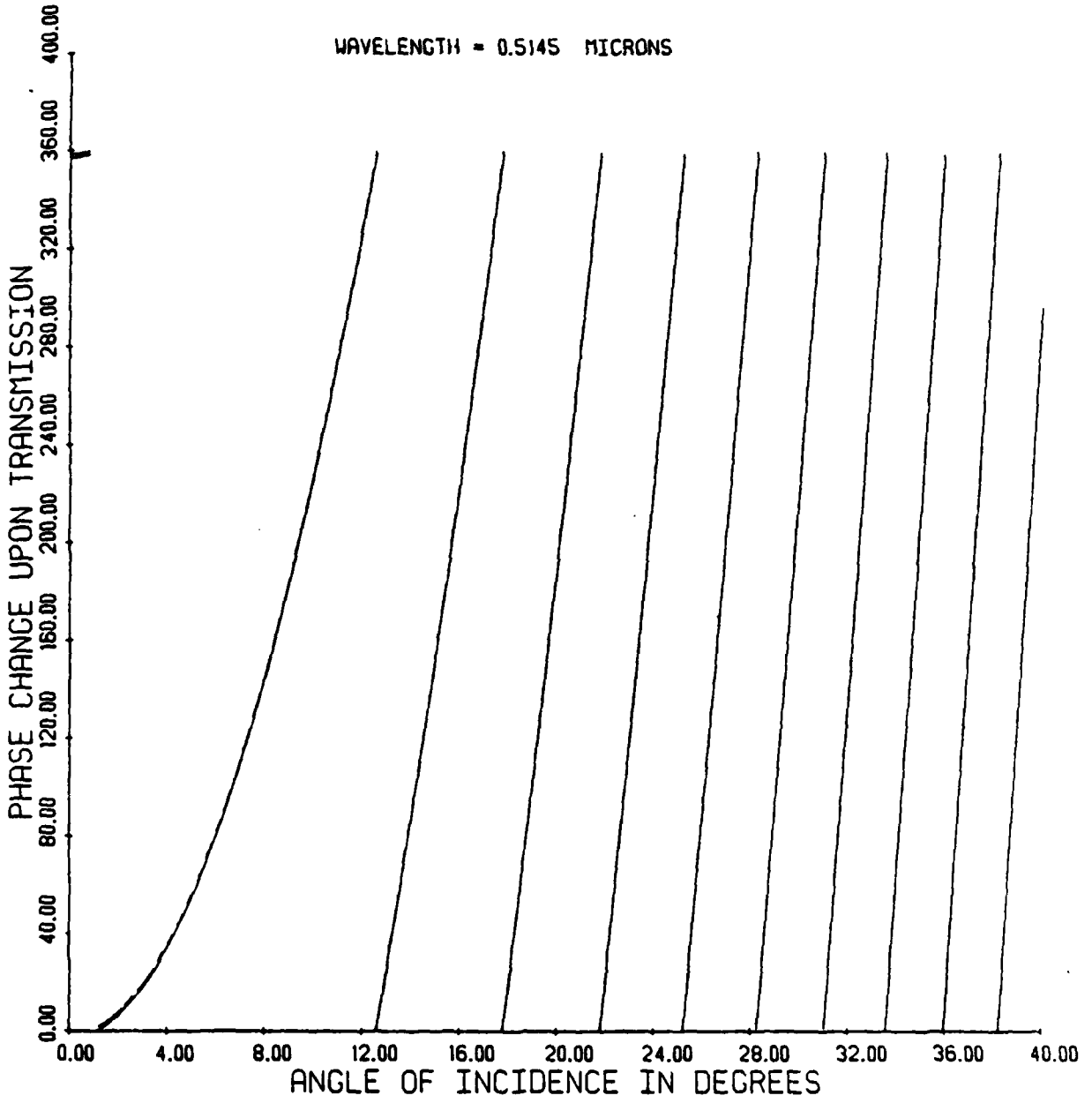

Figure 5-15. Comparison of the Phase Change Upon Transmission vs. Angle of Incidence Characteristics Computed by the TSD Method and the Multilayer Dielectric Stack Method (Example 3)

where z is measured in microns and the element thickness is 14.58 μm. The solid lines in Figures 5-2 through 5-5 correspond to results obtained by the thick layer decomposition technique, while the dashed lines correspond to results obtained by the multilayer dielectric stack technique. The thickness of each layer in the multilayer dielectric stack technique. was taken to be 0.0039 μm. It is noted that the two techniques yield results which agree quite closely. The set of very short dashed lines, which appear as dots in Figure 5-3, indicate a phase change upon reflection of approximately 356° (or equivalently -4°). The discontinuities, in the phase change upon reflection shown in Figure 5-3, are physically acceptable since they occur only at angles where the reflectance is zero. By examining the numerical values of the points plotted in Figure 5-3, one would find that the multilayer dielectric stack theory predicts that the discontinuities occur at phase changes of approximately -4° and 176°. The thick layer decomposition theory predicts that the discontinuities occur at phase changes of approximately 0° and 180°.

Figures 5-7 through 5-10 are plots of the reflectance, phase change upon reflection, transmittance, and phase change upon transmission vs. angle of incidence for the element whose refractive index profile is given in Figure 5-6. The refractive index profile of this element can be analytically described by Eq. (5-26) below

$$n(z) = 1.5 + 0.01 \left(1 + \frac{z}{6.99}\right) \sin (2\pi \cdot f.14237 \cdot z) \qquad (5\text{-}26)$$

where z is in microns and the element thickness is 6.99 μm. The solid lines in Figures 5-7 through 5-10 correspond to results obtained by the thick layer decompositon technique, while the dashed lines correspond to results obtained by the multilayer dielectric stack technique. The thickness of each layer in the multilayer dielectric stack technique was taken to be 0.005 μm. Once again, the two techniques yield results which agree quite closely.

Finally, Figures 5-12 through 5-15 are plots of the reflectance, phase change upon reflection, transmittance, and phase change upon transmission vs. angle of incidence for the element whose refractive index profile is given in Figure 5-11. The refractive index profile of this element does not have a simple analytic description. The solid lines in Figures 5-12 through 5-15 correspond to results obtained by the thick layer decomposition, while the dashed lines correspond to results obtained by the multilayer dielectric stack method. The thickness of each layer in the multilayer dielectric stack technique was taken to be 0.005 μm. Both techniques yield results which are in good agreement. Recall that a number of restrictions were placed on the refractive index profile in order to justify the approximations used in the development of the thick layer decomposition theory. One of these assumptions placed a limit of 0.03 on the maximum refractive index modulation. This limit is exceeded for the grating having the refractive index profile shown in Figure 5-11. Despite this fact, plots in Figures 5-12 through 5-15 indicate that the theory still yields fairly accurate results in this particular case.

In this section, we will derive analytic expressions for $H_R(\lambda, \theta_0)$ and $H_T(\lambda, \theta_0)$ of a flat, holographic, reflection grating having a refractive index profile, n(z), given by

$$n(z) = n_0 + A \sin (2\pi fz) \tag{5-27}$$

For convenience, the grating is assumed to be surrounded by a dielectric of refractive index n_0 and the thickness, D, of the grating is taken to be an integer multiple of 1/f (i.e., D = N/f where N is some integer).

We start by stating the following theorem from linear algebra [2]

Theorem

Let B

$$B = \begin{bmatrix} b_{11} & b_{12} \\ b_{21} & b_{22} \end{bmatrix} \tag{5-28}$$

be a two by two unimodular matrix (i.e., $b_{11}b_{22} - b_{12}b_{21} = 1$). Then the N^{th} power of B for an arbitrary integer N is given by

$$B^N = \begin{pmatrix} b_{11}F_{n-1} - F_{n-2} & b_{12}F_{N-1} \\ b_{21}F_{N-1} & b_{22}F_{N-1} - F_{N-2} \end{pmatrix} \tag{5-29}$$

where

$$\gamma = \begin{cases} \cos^{-1}\left(\frac{1}{2}(b_{11} + b_{22})\right), & \frac{1}{2}(b_{11} + b_{22}) \leq 1 \\ \cosh^{-1}\left(\frac{1}{2}(b_{11} + b_{22})\right) & \frac{1}{2}(b_{11} + b_{22}) \geq 1 \end{cases} \tag{5-30}$$

$$F_N = \begin{cases} (\sin (N + 1)\gamma)/\sin \gamma, & \frac{1}{2}(b_{11} + b_{22}) \leq 1 \\ (\sinh (N + 1))\gamma/\sinh \gamma, & \frac{1}{2}(b_{11} + b_{22}) \geq 1 \end{cases} \tag{5-31}$$

Equation (5-27) indicates that the f_j's and A_j's of Eqs. (5-22), (5-23), and (5-24) are independent of j. Therefore, the Q.'s of Eq. (5-22) are also independent of j. Consequently, Eqs. (5-22), (5-23), and (5-24) can be rewritten as

$$Q_j = Q_1 = \frac{\exp(i\phi_1)}{\sqrt{1 - a_1^2}} \begin{bmatrix} 1 & a_1 \exp(-i\phi_1) \\ a_1 \exp(-i\phi_1) & \exp(-2i\phi_1) \end{bmatrix} \tag{5-32}$$

where

$$\phi_j = \phi_1 = (kn_0 \cos\theta_0)/f \tag{5-33}$$

$$a_j = a_1 = -A\alpha\Big(\text{sinc}\,[(\pi f - kn_0 \cos\theta_0)/f] + \text{sinc}\,[(\pi f + kn \cos\theta_0)/f]\Big) \tag{5-34}$$

We note that Q_j is unimodular. It follows from the theorem above that

$$Q_j^N = \begin{bmatrix} \frac{\exp(i\phi_1)}{\sqrt{1 - a_1^2}} F_{N-1} - F_{N-2} & \frac{a_1}{\sqrt{1 - a_1^2}} F_{N-1} \\ \frac{a_1}{\sqrt{1 - a_1^2}} F_{N-1} & \frac{\exp(-i\phi_1)}{\sqrt{1 - a_1^2}} F_{N-1} - F_{N-2} \end{bmatrix} \tag{5-35}$$

where

$$F_N = \begin{cases} \sin\left[(N+1)\cos^{-1}\left(\frac{\cos\phi_1}{\sqrt{1 - a_1^2}}\right)\right] \Big/ \sin\left[\cos^{-1}\left(\frac{\cos\phi_1}{\sqrt{1 - a_1^2}}\right)\right] & \text{for } \left|\frac{\cos\phi_1}{\sqrt{1 - a_1^2}}\right| < 1 \\ \sinh\left[(N+1)\cosh^{-1}\left(\frac{\cos\phi_1}{\sqrt{1 - a_1^2}}\right)\right] \Big/ \sinh\left[\cosh^{-1}\left(\frac{\cos\phi_1}{\sqrt{1 - a_1^2}}\right)\right] & \text{for } \left|\frac{\cos\phi_1}{\sqrt{1 - a_1^2}}\right| > 1 \end{cases}$$

Now by Eqs. (5-16), (5-17) and (5-18)

$$Q = Q_j^N \tag{5-36}$$

$$H_R(\lambda, \theta_0) = \frac{\dfrac{a_1}{\sqrt{1 - a_1^2}} F_{N-1}}{\exp(i\phi_1)\left[\dfrac{1}{\sqrt{1 - a_1^2}} F_{N-1} - F_{N-2}\right]} \tag{5-37}$$

$$H_T(\lambda, \theta_0) = \frac{1}{\exp(i\phi_1)\left[\dfrac{1}{\sqrt{1 - a_1^2}} F_{N-1} - F_{N-2}\right]} \tag{5-38}$$

Equations (5-37) and (5-38) above are completely general expressions for $H_R(\lambda, \theta_0)$ and $H_T(\lambda, \theta_0)$. On the other hand, analytic expression for $H_R(\lambda, \theta_0)$ and $H_T(\lambda, \theta_0)$ derived from a coupled wave theory approach require θ_0 to either approximately or exactly satisfy the Bragg condition and also require that the transmitted wave be strongly depleted.

Notes to Chapter 5

[1] See Chapter 8 for a discussion of this assumption.

[2] P. Yeh, A. Yariv, C. Hong, "Electromagnetic Propagation in Periodic Stratified Media. I. General Theory, Journal of the Optical Society of America, Vol. 67, No. 4, April 1977.

6
GENERAL PROPERTIES OF HOLOGRAPHIC REFLECTION GRATINGS

In the previous chapters we developed techniques for determining the diffracted field from a flat, holographic, phase, reflection grating which has a refractive index variation only in the z direction. The refractive index was assumed to be a continuous function of z. In this chapter we will simplify the form of the transfer matrix, prove a theorem concerning the mutual interaction between two gratings when placed in contact, discuss the effects of polarization, indicate the interrelationship between wavelength and incident angle, and determine a formula for the transfer matrix which does not involve matrix multiplications.

6.1 SIMPLIFICATION OF THE TRANSFER MATRIX

We start by considering a flat, holographic, phase reflection grating which has a refractive index variation only in the z direction. This refractive index variation is arbitrary and not necessarily continuous. The grating is assumed to be of infinite extent in its x and y dimensions. The front and rear surfaces are adjacent to dielectrics having refractive indices n_f and n_b respectively (see Figure 6-1). In all future dicussions, the word grating will refer to a structure having the above characteristics.

Many of the results derived in Chapter 4 do not explicitly depend upon the form of the refractive index variation. In particular, the grating or any slab thereof can be characterized by a two by two transfer matrix Q.

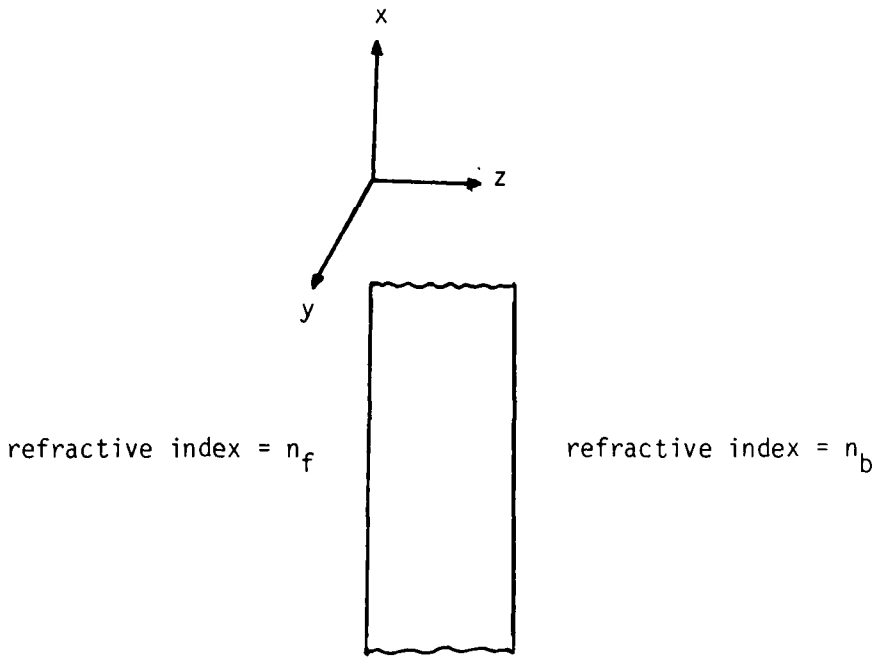

Figure 6-1. Holographic Reflection Grating

$$Q = \frac{1}{t_R}\begin{bmatrix} 1 & -r_L \\ r_R & t_L t_R - r_R r_L \end{bmatrix} \tag{6-1}$$

where r_R, r_L, t_R, and t_L are the right going reflection coefficient, left going reflection coefficient, right going transmission coefficient, and the left going transmission coefficient, respectively. Recall that r_R and t_R are functions of the free space wavelength, λ, and the incident angle, θ_0, at the front surface of the grating. r_L and t_L are functions of the free space wavelength and the incident angle at the back surface of the grating. We wish to simplify the form of the transfer matrix Q. The incident angles at the front and back surfaces are assumed to be related by Snell's Law.

The reversibility theorem of stratified media is given, without proof, by Eqs. (6-2) and (6-3) below. [1]

$$r_R t_R^* + t_R r_L^* = 0 \tag{6-2}$$

$$r_L t_L^* + t_L r_R^* = 0 \tag{6-3}$$

r_R, r_L, t_R and t_L can be written in polar form. We do so in Eqs. (6-4) through (6-7) below.

$$r_R = |r_R| \exp(i\gamma_R) \tag{6-4}$$

$$r_L = |r_L| \exp(i\gamma_L) \tag{6-5}$$

$$t_R = |t_R| \exp(i\Gamma_R) \tag{6-6}$$

$$t_L = |t_L| \exp(i\Gamma_L) \tag{6-7}$$

It is worthwhile at this point to make explicit and to justify the underlying assumption that has been made throughout this report. Suppose that the front surface of the optical element in Figure 6-1 is illuminated by a plane wave at an incident angle θ_0. Then the assumption is that the field at any plane $z = z_0$ within the element can be written as the field due to the coherent superposition of two plane waves. Both plane waves lie in the plane of incidence of the grating, but one travels in the +z direction while the other in the -z direction. The plane waves make angles of $\theta(z_0)$ and 180 - $\theta(z_0)$ degrees with the z-axis, where $\theta(z_0)$ is given by Snell's Law

$$\theta(z_0) = \sin^{-1}\left(\frac{n_f \sin\theta_0}{n(z_0)}\right) \tag{6-8}$$

This assumption can be rigorously justified by viewing the grating as a dielectric multilayer stack composed of an infinity of infinitesimally thin layers. The theory developed in Chapter 3 can then be applied to the grating. The validity of the above assumption follows from that theory. Equations (6-2) and (6-3) become with the aid of Eqs. (6-4) through (6-7).

$$r_L = |r_L| \exp(i\gamma_L) = -|r_R| \exp[i(2\Gamma_R - \gamma_R)] \tag{6-9}$$

$$r_L = |r_L| \exp(i\gamma_L) = -|r_R| \exp[i(2\Gamma_L - \gamma_R)] \tag{6-10}$$

It immediately follows that

$$|r_L| = |r_R| \tag{6-11}$$

$$\gamma_L = 2\Gamma_R - \gamma_R + \pi \tag{6-12}$$

$$\Gamma_R = \Gamma_L \tag{6-13}$$

Furthermore, Eqs. (6-4) and (6-9) yield

$$r_L = -r_R^* \exp(i2\Gamma_R) \tag{6-14}$$

Energy conservation dictates that

$$|r_R|^2 + |t_R|^2 g = 1 \tag{6-15}$$

$$|r_L|^2 + |t_L|^2/g = 1 \tag{6-16}$$

where

$$g = \frac{n_b \cos\theta_0'}{n_f \cos\theta_0}, \text{ for s or p polarization} \tag{6-17}$$

Combining Eqs. (6-6) and (6-15) yields

$$t_R = \frac{(1 - |r_R|^2)^{1/2}}{g^{1/2}} \exp(i\Gamma_R) \tag{6-18}$$

Combining Eqs. (6-7), (6-11) and (6-16 yields

$$t_L = (1 - |r_R|^2)^{1/2} g^{1/2} \exp(i\Gamma_L) \tag{6-19}$$

Therefore,

$$t_R t_L = (1 - |r_R|^2) \exp [i(\Gamma_L + \Gamma_R)] \tag{6-20}$$

which with the aid of Eq. (6-13) becomes

$$t_R t_L = (1 - |r_R|^2) \exp (i2\Gamma_R) \tag{6-21}$$

Now by Eq. (6-14)

$$r_L r_R = -|r_R|^2 \exp (i2\Gamma_R) \tag{6-22}$$

Combining Eqs. (6-21) and (6-22) one has

$$t_L t_R - r_L r_R = \exp (i2\Gamma_R) \tag{6-23}$$

With Eqs. (6-14) and (6-23), the transfer matrix, Q, given by Eq. (6-1) finally becomes

$$Q = \frac{1}{t_R} \begin{bmatrix} 1 & r_R^* \exp (i2\Gamma_R) \\ r_R & \exp (i2\Gamma_R) \end{bmatrix} \tag{6-24}$$

6.2 THE ELEMENT ADDITION THEOREM

We are now in a position to prove a useful theorem.

Theorem 6-1:

Let two gratings, called one and two, be placed in contact surface to surface. Grating one has transfer matrix Q_1 and corresponding r_{R_1} and t_{R_1}. Grating two has transfer matrix Q_2

and corresponding r_{R_1} and t_{R_2}. There is no discontinuity in refractive index at the grating to grating interface. Let the combined element have transfer matrix $Q_{1 \text{ and } 2}$ and corresponding $r_{R_1 \text{ and } 2}$ and $t_{R_1 \text{ and } 2}$. Then

$$Q_{1 \text{ and } 2} = Q_1 \cdot Q_2 \tag{6-25}$$

$$r_{R_1 \text{ and } 2} = \frac{r_{R_1} + r_{R_2} \exp(i2\Gamma_{R_1})}{1 + r^*_{R_1} r_{R_2} \exp(i2\Gamma_{R_1})} \tag{6-26}$$

$$t_{R_1 \text{ and } 2} = \frac{t_{R_1} t_{R_2}}{1 + r^*_{R_1} r_{R_2} \exp(i2\Gamma_{R_1})} \tag{6-27}$$

Proof:

Equation (6-25) was developed earlier as Eq. (4-78) of Chapter 4. Equations (6-26) and (6-27) follow immediately from Eqs. (6-24) and (6-25). In the remainder of this report we will assume, for simplicity, that the refractive indices of the holographic element at its front and rear surfaces match those of the surrounding medium.

6.3 POLARIZATION EFFECTS

The transfer matrix, Q, and consequently the right going reflection and transmission coefficients of a grating, are functions of three parameters -- polarization, wavelength, and angle. It was shown in Chapter 4 that the transfer matrix, Q, can be decomposed into a product of transfer matrices, Q_j, as given below.

$$Q = \prod_{j=1}^{N} Q_j \tag{6-28}$$

The Q_j's are given by Eqs. (5-5a), (5-5b), (5-19), and (5-20) of Chapter 5. These equations are repeated below for convenience.

$$Q_j = \frac{\exp\left[(ikn_0 \cos\theta_0)\Delta_j\right)}{\sqrt{1 - a_j^2}} \begin{bmatrix} 1 & a_j \exp\left[(-ikn_0 \cos\theta_0)\Delta_j\right] \\ a_j \exp\left[(-ikn_0 \cos\theta_0)\Delta_j\right] & \exp\left[(-2ikn_0 \cos\theta_0)\Delta_j\right] \end{bmatrix} \tag{6-29}$$

$$a_j = \pm \pi f_j A_j \alpha \Delta_j \left(\text{sinc}\left[(\pi f_j - kn_0 \cos\theta_0)\Delta_j\right] + \text{sinc}\left[(\pi f_j + kn_0 \cos\theta_0)\Delta_j\right]\right) \tag{6-30}$$

$$\alpha = \begin{cases} \dfrac{1}{n_0 \cos^2\theta_0}, & \text{for s polarization} \\ \dfrac{1 - \tan^2\theta_0}{n_0}, & \text{for p polarization} \end{cases} \tag{6-31}$$

A number of conclusions can be drawn from the equations above. The first of these is stated as a theorem.

Theorem 2:

Consider two gratings, called one and two. Grating one is illuminated at an angle of incidence θ_0 with s polarized light and grating two is illuminated at the same angle of incidence with p polarized light. Grating one has a refractive index profile, n(z), given by

$$n(z) = n_0 + \Delta n(z)$$

and grating two has a refractive index profile, n(z), given by

$$n(z) = n_0 + e \cdot \Delta n(z)$$

The constant e is defined below

$$e = \frac{1}{\cos^2\theta_0(1 - \tan^2\theta_0)}$$

Then the transfer matrix, Q, of grating one as a function of λ_0 is identically equal to the transfer matrix, Q, of grating two as a function of λ_0.

Proof:

Equations (6-28), (6-29), and (6-30) indicate that the transfer matrix Q is independent of polarization for a fixed θ_0 provided

$$A_j\alpha \text{ for s polarization} = A_j\alpha \text{ for p polarization} \qquad (6\text{-}32)$$

Equation (6-32) can be combined with Eq. (6-31) to yield

$$A_j \frac{1}{n_0 \cos^2\theta_0} \text{ for s polarization} = A_j \frac{1 - \tan^2\theta_0}{n_0} \text{ for p polarization} \qquad (6\text{-}33)$$

It then follows immediately that Eq. (6-32) is equivalent to

$$A_j \text{ for p polarization} = A_j \frac{1}{\cos^2\theta_0(1 - \tan^2\theta_0)} \text{ for s polarization}$$

or

$$\Delta n(z) \text{ for p polarization} = e \cdot \Delta n(z) \text{ for p polarization}$$

Theorem 6-2 states that for a fixed angle of incidence changing the polarization is completely equivalent to multiplying the refractive index modulation by a constant. Although the theorem is strictly

valid only for θ_0 fixed, it gives reasonably accurate results over any range of incident angles for which e does not change appreciably.

6.4 THE INTERRELATIONSHIP BETWEEN WAVELENGTH AND INCIDENT ANGLE

To emphasize that Q_j, and consequently Q, is a function of three parameters -- polarization, wavelength, and angle of incidence -- let us write

$$Q_j = Q_j \text{ (polarization, } \lambda, \theta_0) \tag{6-34}$$

and

$$Q = Q \text{ (polarization, } \lambda, \theta_0) \tag{6-35}$$

We now make the following assertion.

Assertion 1:

Suppose

$$\frac{\cos \tilde{\theta}_0}{\tilde{\lambda}} = \frac{\cos \theta_0}{\lambda} \tag{6-36}$$

and

$$\alpha(\text{at } \tilde{\theta}_0) \tilde{=} \alpha(\text{at } \theta_0) \tag{6-37}$$

Then

$$Q_j \text{ (polarization, } \tilde{\lambda}, \tilde{\theta}_0) \tilde{=} Q_j \text{ (polarization, } \lambda, \theta_0) \tag{6-38}$$

and

$$Q \text{ (polarization, } \tilde{\lambda}, \tilde{\theta}_0) \tilde{=} Q \text{ (polarization, } \lambda, \theta_0) \tag{6-39}$$

Plausibility Argument

It can be seen from Eqs. (6-29), (6-30), and (6-31) that the exception of the single factor, α, θ_0 and λ appear in the matrix Q_j (and consequently Q) only in the combination $\cos \theta_0/\lambda$. On the other hand, we see by Eq. (6-31) that α is a function of θ_0 but not λ. Experience indicates that small changes in α result in small changes in Q. (I am unable, however, to prove this analytically.) Thus, the above assertion follows immediately.

Now let

$$\chi \triangleq \frac{\cos \theta_0}{\lambda} \tag{6-40}$$

Then

$$d\chi = \frac{-\lambda(\sin \theta_0)\, d\theta_0 + (\cos \theta_0)\, d\lambda}{\lambda^2} \tag{6-41}$$

and so

$$d\lambda = \lambda \tan \theta_0\, d\theta_0 \tag{6-42}$$

Therefore, by Assertion 1

$$Q\,(\text{polarization}, \lambda + (\lambda \tan \theta_0)\, d\theta_0, \theta_0) \simeq Q\,(\text{polarization}, \lambda, \theta_0 + d\theta_0) \tag{6-43}$$

Equation (6-43) shows the connection between angular selectivity and wavelength selectivity in a holographic grating. In particular, it indicates that changing the wavelength by $\lambda(\tan \theta_0)\, d\theta_0$ is roughly equivalent to changing the angle by $d\theta_0$.

In the remainder of this chapter we prove four theorems which will be used in the following chapter to obtain an approximate solution to the inverse scattering problem. The first two of these theorems have strikingly similar counterparts in the theory of multilayer dielectric stacks.

6.5 DESCRIPTION OF THE TRANSFER MATRIX, Q, VIA THE PARAMETERS f_j AND a_j

Equations (6-28) through (6-31) express the transfer matrix, Q, as a product of transfer matrices Q_j. Each matrix Q_j in turn is determined by the refractive index profile. Without loss of generality, one may assume that $\Delta_j = 1/f_j$. We wish to derive an expression for Q which involves only a_j's and f_j's and no matrix multiplications. First define Φ_j by

$$\Phi_j = \frac{kn_0}{f_j}\cos\theta_0 \qquad (6\text{-}44)$$

$$(\Phi_0 \equiv 0)$$

Then Eq. (6-29) becomes

$$Q_j = \frac{\exp(i\Phi_j)}{\sqrt{1-a_j^2}}\begin{bmatrix} 1 & a_j\exp(-i\Phi_j) \\ a_j\exp(-i\Phi_j) & \exp(-i2\Phi_j) \end{bmatrix} \qquad (6\text{-}45)$$

We make the definitions given below

$$W_j = \begin{bmatrix} 1 & a_j \exp(-i\phi_j) \\ a_j \exp(-i\phi_j) & \exp(-i2\phi_j) \end{bmatrix} \qquad (6\text{-}46)$$

The class of even products of order m, designated Ep(m), are expressions of the form

$$a_{\alpha_1} a_{\alpha_2} \cdots a_{\alpha_m} \exp\left[-i(\phi_{\alpha_1} + \phi_{\alpha_2} \cdots + \phi_{\alpha_m}) + i \sum_{j=0}^{m-1} \sum_{n=\alpha_j+1}^{\alpha_{j+1}-1} ((-1)^j - 1)\phi_n\right]$$

$$\alpha_0 \triangleq 0$$

$$\sum_{n=\alpha_j+1}^{\alpha_{j+1}-1} ((-1)^j - 1)\phi_n \triangleq 0 \quad \text{for} \quad \alpha_j + 1 < \alpha_{j+1} - 1 \qquad (6\text{-}47)$$

where m is a positive even integer and $\alpha_1, \alpha_2, \ldots, \alpha_m$ is a monotonically increasing sequence of positive integers. An element of this class will be denoted by ep(m). The class of odd products of order m, designated op(m), are expressions of the form

$$a_{\alpha_1} a_{\alpha_2} \cdots a_{\alpha_m} \exp\left[-i(\phi_{\alpha_1} + \phi_{\alpha_2} + \cdots + \phi_{\alpha_m}) + i \sum_{j=0}^{m-1} \sum_{n=\alpha_j+1}^{\alpha_{j+1}-1} ((-1)^{j+1} - 1)\phi_n\right]$$

$$\alpha_0 \triangleq 0$$

$$\sum_{n=\alpha_j+1}^{\alpha_{j+1}-1} ((-1)^{j+1} - 1)\phi_n \triangleq 0 \quad \text{for} \quad \alpha_j + 1 < \alpha_{j+1} - 1$$

where m is a positive odd integer and $\ell_1, \ell_2, \ldots, \ell_m$ is a monotonically increasing sequence of positive integers. An element of this class will be denoted by op(m).

Using the definitions above, we state the following theorem.

Theorem 6-3:

$$\prod_{j=1}^{N} W_j = \begin{bmatrix} X_{11}^{(N)} & X_{12}^{(N)} \\ X_{21}^{(N)} & X_{22}^{(N)} \end{bmatrix} \tag{6-50}$$

where

$$X_{11}^{(N)} = 1 + (\text{sum of all ep(m)}, \ell_m \leq N) \tag{6-51}$$

$$X_{21}^{(N)} = (\text{sum of all op(m)}, \ell_m \leq N) \tag{6-52}$$

$$X_{12}^{(N)} = X_{21}^{(N)*} \exp\left[-i2\left(\sum_{j=1}^{N} \phi_j\right)\right] \tag{6-53}$$

$$X_{22}^{(N)} = X_{11}^{(N)*} \exp\left[-i2\left(\sum_{j=1}^{N} \phi_j\right)\right] \tag{6-54}$$

Proof:

Theorem 6-3 will be proved by mathematical induction. It is trivial to show that Theorem 6-3 is true for N = 1. Now suppose the theorem is true for $N = N_0$, then it is sufficient to show that it is also true for $N = N_0 + 1$. We write

$$\begin{bmatrix} e & b \\ c & d \end{bmatrix} \triangleq \prod_{j=1}^{N_0+1} W_j = \left(\prod_{j=1}^{N_0} W_j\right) W_{N_0+1}$$

$$= \begin{bmatrix} x_{11}^{(N_0)} & x_{12}^{(N_0)} \\ x_{21}^{(N_0)} & x_{22}^{(N_0)} \end{bmatrix} \begin{bmatrix} 1 & a_{N_0+1} \exp(-i\phi_{N_0+1}) \\ a_{N_0+1} \exp(-i\phi_{N_0+1}) & \exp(-i2\phi_{N_0+1}) \end{bmatrix} \tag{6-55}$$

Therefore,

$$e = x_{11}^{(N_0)} + x_{12}^{(N_0)} a_{N_0+1} \exp(-i\phi_{N_0+1}) \tag{6-56}$$

$$b = x_{11}^{(N_0)} a_{N_0+1} \exp(-i\phi_{N_0+1}) + x_{12}^{(N_0)} \exp(-i2\phi_{N_0+1}) \tag{6-57}$$

$$c = x_{21}^{(N_0)} + x_{22}^{(N_0)} a_{N_0+1} \exp(-i\phi_{N_0+1}) \tag{6-58}$$

$$d = x_{21}^{(N_0)} a_{N_0+1} \exp(-i\phi_{N_0+1}) + x_{22}^{(N_0)} \exp(-2i\phi_{N_0+1}) \tag{6-59}$$

It remains to show that

$$e = x_{11}^{(N_o+1)} \tag{6-60}$$

$$c = x_{21}^{(N_o+1)} \tag{6-61}$$

$$b = c^* \exp\left[-i2\left(\sum_{j=1}^{N_o+1} \phi_j\right)\right] \tag{6-62}$$

$$d = e^* \exp\left[-i2\left(\sum_{j=1}^{N_o+1} \phi_j\right)\right] \tag{6-63}$$

We prove Eq. (6-60) first. Equation (6-56) can be rewritten, by using Eqs. (6-51) and (6-53)

$$e = x_{11}^{(N_o)} + x_{21}^{(N_o)*} \cdot \exp\left[-i2\left(\sum_{j=1}^{N_o} \phi_j\right) a_{N_o+1} \exp\left(-i\phi_{N_o+1}\right)\right.$$

$$= 1 + (\text{sum of all ep}(m),\ \ell_m \leq N_o) + (\text{sum of all op}(m),\ \ell_n \leq N_o)^*$$

$$\cdot \exp\left[-i2\left(\sum_{j=1}^{N_o} \phi_j\right)\right] a_{N_o+1} \exp\left(-i\phi_{N_o+1}\right) \tag{6-64}$$

Consider now the arbitrary odd product of order m given below ($m \leq N_o$)

$$op(m) = a_{\ell_1} a_{\ell_2} \cdots a_{\ell_m} \exp\left[-i(\phi_{\ell_1} + \phi_{\ell_2} + \cdots + \phi_{\ell_m}) + i \sum_{j=0}^{m-1} \sum_{n=\ell_j+1}^{\ell_{j+1}-1} ((-1)^{j+1} - 1)\phi_n\right] \tag{6-65}$$

Then

$$op(m)^* \exp\left[-i2\left(\sum_{j=1}^{N_o} \phi_j\right)\right] a_{N_o+1} \exp(-i\phi_{N_o+1}) =$$

$$a_{\ell_1} a_{\ell_2} \cdots a_{\ell_m} a_{m+1} \exp\left[-i(\phi_{\ell_1} + \phi_{\ell_2} + \cdots + \phi_{\ell_m} + \phi_{\ell_{m+1}}) + i \sum_{j=0}^{m} \sum_{n=\ell_j+1}^{\ell_{j+1}-1} ((-1)^j - 1)\phi_n\right] \quad \text{where} \quad \ell_{m+1} = N_o + 1 \tag{6-66}$$

Note that the right hand side of Eq. (6-66) is just an element of EP(m), $\ell_m \leq N_o + 1$. Furthermore, it is easy to see that all elements of EP(m), $\ell_m \leq N_o + 1$ and only those elements can be generated by multiplying some $op(m)^*$, $\ell_m \leq N_o$ by

$$\exp\left[-i2\left(\sum_{j=1}^{N_o} \phi_j\right)\right] a_{N_o+1} \exp(-i\phi_{N_o+1})$$

Therefore

$$e = 1 + \text{sum of all } ep(m), \ell_m \leq N_o + 1$$

$$= X_{11}^{(N_0+1)}$$

Next we will prove Eq. (6-61). Equation (6-58) can be rewritten using Eqs. (6-51), (6-52) and (6-54) as

$$c = x_{21}^{(N_o)} + x_{11}^{(N_o)*} \exp\left[-i2\left(\sum_{j=1}^{N_o}\phi_j\right)\right] a_{N_o+1} \exp\left(-i\phi_{N_o+1}\right)$$

$$= \left(\text{sum of all op(m), } \ell_m \leq N_o\right)$$

$$+ \left(1 + \text{the sum of all ep(m), } \ell_m \leq N_o\right)^* \cdot \exp\left[-i2\left(\sum_{j=1}^{N_o}\phi_j\right)\right]$$

$$\cdot a_{N_o+1} \exp\left(-i\phi_{N_o+1}\right) \qquad (6\text{-}67)$$

Consider now the arbitrary even product of order m given below ($\ell_m \leq N_o$)

$$ep(m) = a_{\ell_1} a_{\ell_2} \ldots a_{\ell_m} \exp\left[-i\left(\phi_{\ell_1} + \phi_{\ell_2} + \ldots + \phi_{\ell_m}\right)\right.$$

$$\left. + i\sum_{j=0}^{m-1}\sum_{n=\ell_j+1}^{\ell_{j+1}-1}\left((-1)^j - 1\right)\phi_n\right] \qquad (6\text{-}68)$$

Then

$$ep(m)^* \exp\left[-i2\left(\sum_{j=1}^{N_o}\phi_j\right)\right] a_{N_o+1} \exp\left(-i\phi_{N_o+1}\right) =$$

(Equation continued on next page.)

$$a_{\ell_1} a_{\ell_2} \ldots a_{\ell_m} a_{\ell_{m+1}} \exp\left[-i(\phi_{\ell_1} + \phi_{\ell_2} + \ldots + \phi_{\ell_m} + \phi_{\ell_{m+1}}\right.$$

$$\left. + i \sum_{j=0}^{m} \sum_{n=\ell_j+1}^{\ell_{j+1}-1} ((-1)^{j+1} - 1)\phi_n\right] \quad \text{where} \quad \ell_{m+1} = N_o + 1 \tag{6-69}$$

Note that the right hand side of Eq. (6-69) is just an element of OP(m), $\ell_m \leq N_o + 1$. Furthermore, it is easy to see all elements of OP(m), $\ell_m \leq N_o + 1$, and only those elements can be generated by multiplying 1 or some op(m), $\ell_m \leq N_o$ by

$$\exp\left[-i2\left(\sum_{j=1}^{N_o} \phi_j\right)\right] a_{N_o+1} \exp\left(-i\phi_{N_o+1}\right)$$

Therefore

$$c = \text{sum of all op(m)}, \ \ell_m \leq N_o + 1$$

$$= x_{21}^{(N_o+1)}$$

Next we will prove Eq. (6-62). Equation (6-57) can be rewritten using Eqs. (6-53) and (6-54) as

$$b = x_{22}^{(N_o)*} \exp\left[-i2\left(\sum_{j=1}^{N_o} \phi_j\right)\right] a_{N_o+1} \exp\left(-i\phi_{N_o+1}\right)$$

(Equation continued on next page.)

$$+ x_{21}^{(N_o)*} \exp\left[-i2\left(\sum_{j=1}^{N_o} \phi_j\right)\right] \exp\left(-i2\phi_{N_o+1}\right)$$

$$= a_{N_o+1} \exp\left(i\phi_{N_o+1}\right) x_{22}^{(N_o)*} \exp\left[-i2\left(\sum_{j=1}^{N_o+1} \phi_j\right)\right]$$

$$+ x_{21}^{(N_o)*} \exp\left[-i2\left(\sum_{j=1}^{N_o+1} \phi_j\right)\right] \qquad (6\text{-}70)$$

Now from Eqs. (6-58) and (6-70),

$$b = c^* \exp\left[-i2\left(\sum_{j=1}^{N_o+1} \phi_j\right)\right]$$

Finally, Eq. (6-63) will be proven. Equation (6-59) can be rewritten, using Eqs. (6-53) and (6-54) as

$$d = x_{12}^{(N_o)*} \exp\left[-i2\left(\sum_{j=1}^{N_o} \phi_j\right)\right] a_{N_o+1} \exp\left(-i\phi_{N_o+1}\right)$$

$$+ x_{11}^{(N_o)*} \exp\left[-i2\left(\sum_{j=1}^{N_o} \phi_j\right)\right] \exp\left(-i2\phi_{N_o+1}\right)$$

(Equation continued on next page.)

$$= \overset{(N_o)^*}{x_{11}} \exp\left[-i2\left(\sum_{j=1}^{N_o+1} \phi_j\right)\right]$$

$$+ \overset{(N_o)^*}{x_{12}} a_{N_o+1} \exp\left(i\phi_{N_o+1}\right) \exp\left[-2\left(\sum_{j=1}^{N_o+1} \psi_j\right)\right] \qquad (6\text{-}71)$$

Now from Eqs. (6-56) and (6-71),

$$d = e^* \exp\left[-i2\left(\sum_{j=1}^{N_o+1} \phi_j\right)\right]$$

The proof is complete.

Theorem 6-3 is a significant result. Below, we will explore some of its implications. Using the theorem it immediately follows that the transfer matrix Q can be written as

$$Q = \frac{\exp\left(i \sum_{j=1}^{N} \psi_j\right)}{\prod_{j=1}^{N} \sqrt{1 - a_j^2}} \begin{bmatrix} (1 + \text{sum of all ep}(m),\ \ell_m \leq N) & (\text{sum of all op}(m),\ \ell_m \leq N)^* \exp\left(-i2 \sum_{j=1}^{N} \psi_j\right) \\ (\text{sum of all op}(m),\ \ell_m \leq N) & (1 + \text{sum of all ep}(m),\ \ell_m \leq N)^* \exp\left(-i2 \sum_{j=1}^{N} \psi_j\right) \end{bmatrix}$$

(6-72)

here N is the number of slabs into which the grating has been divided. Then by Eqs. (6-1) and (6-72)

$$t_R = \frac{\prod_{j=1}^{N} \sqrt{1 - a_j^2}}{1 + \text{sum of all } ep(m),\ \ell_m \leq N} \exp\left(-i \sum_{j=1}^{N} \phi_j\right) \qquad (6\text{-}73)$$

$$r_R = \frac{\text{sum of all } op(m),\ \ell_m \leq N}{1 + \text{sum of all } ep(m), \ell_m \leq N} \qquad (6\text{-}74)$$

Eqs. (6-73) and (6-74) can be easily expanded when N is small. As an example, for N = 2, we have

$$t_R = \frac{\sqrt{1 - a_1^2} \cdot \sqrt{1 - a_2^2}}{1 + a_1 a_2 \exp\left(-i(\phi_1 + \phi_2)\right)} \exp\left(-i(\phi_1 + \phi_2)\right)$$

$$r_R = \frac{a_1 \exp\left(-i\phi_1\right) + a_2 \exp\left(-i(2\phi_1 + \phi_2)\right)}{1 + a_1 a_2 \exp\left(-i(\phi_1 + \phi_2)\right)}$$

and for N = 3 we have

$$t_R = \frac{\sqrt{1 - a_1^2}\sqrt{1 - a_2^2}\sqrt{1 - a_3^2} \exp\left(-i(\phi_1 + \phi_2 + \phi_3)\right)}{1 + a_1 a_2 \exp\left(-i(\phi_1 + \phi_2)\right) + a_2 a_3 \exp\left(-i(\phi_2 + \phi_3)\right) + a_1 a_3 \exp\left(-i(\phi_1 + 2\phi_2 + \phi_3)\right)}$$

$$r_R = \frac{a_1 \exp\left(-i\phi_1\right) + a_2 \exp\left(-i(2\phi_1 + \phi_2)\right) + a_3 \exp\left(-i(2\phi_1 + 2\phi_2 + \phi_3)\right) + a_1 a_2 a_3 \left(-i(\phi_1 + \phi_2 + \phi_3)\right)}{1 + a_1 a_2 \exp\left(-i(\phi_1 + \phi_2)\right) + a_2 a_3 \exp\left(-i(\phi_2 + \phi_3)\right) + a_1 a_3 \exp\left(-i(\phi_1 + 2\phi_2 + \phi_3)\right)}$$

It should be pointed out that Eqs. (6-73) and (6-74) are analogous to the complete Airy summation formulas for multilayer dielectric stacks [1].

Note that Eqs. (6-73) and (6-74) can be combined to yield the following result

$$\frac{r_R}{t_R} \cdot \left(\prod_{j=1}^{N} \sqrt{1 - a_j^2}\right) \cdot \exp\left(-i \sum_{j=1}^{N} \phi_j\right) = \text{sum of all op(m)}, \ell_m \leq N \tag{6-75}$$

But ρ_R, the right going reflectance, equals $|r_R|^2$, and the right going transmittance, T_R, must equal $1 - \rho_R$ because of energy conservation. Thus, Eq. (6-75) becomes

$$\left(\frac{\rho_R}{1 - \rho_R}\right)^{1/2} \left(\prod_{j=1}^{N} \sqrt{1 - a_j^2}\right) = |\text{sum of all op(m)}, \ell_m \leq N| \tag{6-76}$$

We will return to Eqs. (6-73), (6-74) and (6-75) when we investigate the theory of holographic grating filter design in the following chapter.

We note from Eq. (6-24) that, in general,

$$Q_j = \frac{1}{t_{R_j}} \begin{bmatrix} 1 & r_{R_j}^* \exp(i2\Gamma_{R_j}) \\ r_{R_j} & \exp(i2\Gamma_{R_j}) \end{bmatrix} \tag{6-77}$$

and

$$Q = \prod_{j=1}^{N} Q_j \tag{6-78}$$

Theorem 6-3 is generalized below. We start by making the following definitions.

$$Z_j \triangleq \begin{bmatrix} 1 & r^*_{R_j} \exp(i2\Gamma_{R_j}) \\ r_{R_j} & \exp(i2\Gamma_{R_j}) \end{bmatrix} \tag{6-79}$$

The class of generalized even products of order m, designated GEP(m) are expressions of the form

$$b_{\ell_1} b_{\ell_2} \cdots b_{\ell_m} \exp\left[i \sum_{j=0}^{m-1} \sum_{n=\ell_j}^{\ell_{j+1}-1} (1 - (-1)^j)\Gamma_{R_j}\right]$$

$$b_{\ell_j} \triangleq \begin{cases} r^*_{R_j} & \text{for } j \text{ an odd integer} \\ r_{R_j} & \text{for } j \text{ an even integer} \end{cases}$$

$$\ell_o \triangleq 0$$

$$\Gamma_{R_o} \triangleq 0 \tag{6-80}$$

where m is a positive even integer and $\ell_1, \ell_2, \ldots, \ell_m$ is a monotonically increasing sequence of positive integers. An element of this class will be denoted gep(m). The class of generalized odd products of order m, designated GOP(m), are expressions of the form

$$b_{\ell_1} b_{\ell_2} \cdots b_{\ell_m} \exp\left[\sum_{j=0}^{m-1} \sum_{n=\ell_j}^{\ell_{j+1}-1} (1 - (-1)^{j+1}) \Gamma_{R_j}\right]$$

$$b_{\ell_j} \triangleq \begin{cases} r_{R_j} & \text{for } j \text{ an odd integer} \\ r^*_{R_j} & \text{for } j \text{ an even integer} \end{cases}$$

$$\ell_o \triangleq 0$$

$$\Gamma_{R_o} \triangleq 0 \qquad (6\text{-}81)$$

where m is a positive odd integer and $\ell_1, \ell_2, \ldots, \ell_m$ is a monotonically increasing sequence of positive integers. An element of this class will be denoted by gop(m).

Using the definitions above, we state the following theorem which is a generalization of Theorem 6-3.

Theorem 6-4:

$$\prod_{j=1}^{N} Z_j = \begin{bmatrix} V_{11}^{(N)} & V_{12}^{(N)} \\ V_{21}^{(N)} & V_{22}^{(N)} \end{bmatrix} \qquad (6\text{-}82)$$

where

$$V_{11}^{(N)} = 1 + \text{sum of all gep}(m),\ \ell_m \leq N \qquad (6\text{-}83)$$

$$V_{21}^{(N)} = \text{sum of all gop}(m),\ \ell_m \leq N \qquad (6\text{-}84)$$

$$V_{12}^{(N)} = V_{21}^{(N)*} \exp\left[i2\left(\sum_{j=1}^{N} \Gamma_{R_j}\right)\right] \tag{6-85}$$

$$V_{22}^{(N)} = V_{11}^{(N)*} \exp\left[i2\left(\sum_{j=1}^{N} \Gamma_{R_j}\right)\right] \tag{6-86}$$

Proof:

Theorem 6-4 will be proved by mathematical induction. It is trivial to show that Theorem 6-4 is true for N = 1. Now suppose the theorem is true for $N = N_o$, then it is sufficient to show that it is also true for $N = N_o + 1$. We write

$$\begin{bmatrix} e & b \\ c & d \end{bmatrix} \triangleq \prod_{j=1}^{N_o+1} Z_j = \left(\prod_{j=1}^{N_o} Z_j\right) Z_{N_o+1}$$

$$= \begin{bmatrix} V_{11}^{(N_o)} & V_{12}^{(N_o)} \\ V_{21}^{(N_o)} & V_{22}^{(N_o)} \end{bmatrix} \begin{bmatrix} 1 & r_{R_{N_o+1}}^{*} \exp\left(i2\Gamma_{R_{N_o+1}}\right) \\ r_{R_{N_o+1}} & \exp\left(i2\Gamma_{R_{N_o+1}}\right) \end{bmatrix}$$

Therefore,

$$e = V_{11}^{(N_o)} + V_{12}^{(N_o)} r_{R_{N_o+1}} \tag{6-88}$$

$$b = V_{11}^{(N_o)} r^*_{R_{N_o+1}} \exp(i2\pi R_{N_o+1}) + V_{12}^{(N_o)} \exp(i2\pi R_{N_o+1}) \quad (6\text{-}89)$$

$$c = V_{21}^{(N_o)} + V_{22}^{(N_o)} r_{R_{N_o+1}} \quad (6\text{-}90)$$

$$d = V_{21}^{(N_o)} r^*_{R_{N_o+1}} \exp(i2\pi R_{N_o+1}) + V_{22}^{(N_o)} \exp(i2\pi R_{N_o+1}) \quad (6\text{-}91)$$

It remains to show that

$$e = V_{11}^{(N_o+1)} \quad (6\text{-}92)$$

$$c = V_{21}^{(N_o+1)} \quad (6\text{-}93)$$

$$b = c^* \exp\left[i2\left(\sum_{j=1}^{N_o+1} r_{R_j}\right)\right] \quad (6\text{-}94)$$

$$d = e^* \exp\left[i2\left(\sum_{j=1}^{N_o+1} r_{R_j}\right)\right] \quad (6\text{-}95)$$

We prove Eq. (6-92) first. Equation (6-88) can be rewritten by using Eqs. (6-83), (6-84), and (6-85) as

$$e = V_{11}^{(N_o)} + V_{21}^{(N_o)*} \exp\left[i2 \sum_{j=1}^{N_o} r_j\right] r_{R_{N_o+1}}$$

$$= (1 + \text{sum of all } gep(m),\ \ell_m \leq N)$$

$$+ (\text{sum of all } gop(m),\ \ell_m \leq N)^*$$

$$\cdot \exp\left[i2 \sum_{j=1}^{N_o} r_{R_j}\right] r_{R_{N_o+1}} \tag{6-96}$$

Consider now the arbitrary generalized odd product of order m given below ($\ell_m \leq N_o$)

$$gop(m) = b_{\ell_1} b_{\ell_2} \ldots b_{\ell_m} \exp\left[i \sum_{j=0}^{m-1} \sum_{n=\ell_j}^{\ell_{j+1}-1} (1 - (-1)^{j+1}) r_{R_n}\right] \tag{6-97}$$

Then

$$gop(m)^* \exp\left[i2\left(\sum_{j=1}^{N_o} r_j\right)\right] r_{R_{N_o+1}} =$$

$$b^*_{\ell_1} b^*_{\ell_2} \ldots b^*_{\ell_m} b_{\ell_{m+1}} \left[\sum_{j=0}^{m} \sum_{n=\ell_j}^{\ell_{j+1}-1} (1 - (-1)^j) r_{R_n}\right] \tag{6-98}$$

where

$$\ell_{m+1} = N_o + 1 \quad \text{and} \quad b_{\ell_{m+1}} = r_{R_{N_o+1}}$$

Note that the right hand side of Eq. (6-98) is just an element of GEP(m), $\ell_m = N_o + 1$. Furthermore, it is easy to see that all elements of GEP(m), $\ell_m = N_o + 1$ and only those elements can be generated by multiplying some gop(m)*, $\ell_m \leq N_o$ by

$$\exp\left[i2\left(\sum_{j=1}^{N_o} \Gamma_{R_j}\right)\right] r_{R_{N_o+1}}$$

Therefore,

$$e = 1 + \text{sum of all gep(m)}, \ \ell_m \leq N_o + 1$$

$$= V_{11}^{(N_o+1)}$$

Next we will prove Eq. (6-93). Equation (6-90) can be rewritten using Eqs. (6-83), (6-84), and (6-86) as

$$c = V_{21}^{(N_o)} + V_{11}^{(N_o)*} \exp\left[i2\left(\sum_{j=1}^{N_o} \Gamma_{R_j}\right)\right] r_{R_{N_o+1}}$$

$$= (\text{sum of all gop(m)}, \ \ell_m \leq N_o)$$

(Equation continued on next page.)

$$+ (1 + \text{sum of all gep}(m),\ \ell_m \leq N_o)^*$$

$$\cdot \exp\left[i2\left(\sum_{j=1}^{N_o} \Gamma_{R_j}\right)\right] r_{R_{N_o+1}} \tag{6-99}$$

Consider now the arbitrary even product of order m given below ($\ell_m \leq N_o$).

$$\text{gep}(m) = b_{\ell_1} b_{\ell_2} \cdots b_{\ell_m} \exp\left[\sum_{j=0}^{m-1} \sum_{n=\ell_j}^{\ell_{j+1}-1} (1 - (-1)^j)\Gamma_{R_n}\right] \tag{6-100}$$

Then

$$\text{gep}(m)^* \exp\left[i2\left(\sum_{j=1}^{N_o} \Gamma_{R_j}\right)\right] r_{R_{N_o+1}} =$$

$$b^*_{\ell_1} b^*_{\ell_2} \cdots b^*_{\ell_m} b_{\ell_{m+1}} \exp\left[i \sum_{j=0}^{m} \sum_{n=\ell_j}^{\ell_{j+1}-1} (1 - (-1)^{j+1})\Gamma_{R_n}\right] \tag{6-101}$$

where

$$\ell_{m+1} = N_o + 1 \quad \text{and} \quad b_{\ell_{m+1}} = r_{R_{N_o+1}}$$

Note that the right hand side of Eq. (6-101) is just an element of GOP(m), $\ell_m = N_o + 1$. Furthermore, it is easy to see that all elements of gop(m), $\ell_m = N_o + 1$ and only those elements can be generated by multiplying 1 or some gop(m), $\ell_m \leq N_o$ by

$$\exp\left[i2\left(\sum_{j=1}^{N_o} \Gamma_{R_j}\right)\right] r_{R_{N_o+1}}$$

Therefore,

$$c = \text{sum of allgop}(m),\ \ell_m \leq N_o + 1$$

$$= V_{21}^{(N_o+1)}$$

Next we will prove Eq. (6-94). Equation (6-89) can be rewritten by using Eqs. (6-85) and (6-86) as

$$b = V_{22}^{(N_o)*} \exp\left[i2\left(\sum_{j=1}^{N_o} \Gamma_{R_j}\right)\right] r^*_{R_{N_o+1}} \exp\left(i2\Gamma_{R_{N_o+1}}\right)$$

$$+ V_{21}^{(N_o)*} \exp\left[i2\left(\sum_{j=1}^{N_o} \Gamma_{R_j}\right)\right] \exp\left(i2\Gamma_{R_{N_o+1}}\right)$$

$$= \left(V_{22}^{(N_o)*} r^*_{R_{N_o+1}} + V_{21}^{(N_o)*}\right) \exp\left[i2\left(\sum_{j=1}^{N_o+1} \Gamma_{R_j}\right)\right] \qquad (6\text{-}102)$$

Now from Eqs. (6-90) and (6-102)

$$b = c^* \exp\left[i2\left(\sum_{j=1}^{N_o+1} \Gamma_{R_j}\right)\right]$$

Finally, Eq. (6-95) will be proven. Eq. (6-91) can be rewritten using Eqs. (6-85) and (6-86) as

$$d = V_{12}^{(N_o)*} \exp\left[i2\left(\sum_{j=1}^{N_o} \Gamma_{R_j}\right)\right] r^*_{R_{N_o+1}} \exp\left(i2\Gamma_{R_{N_o+1}}\right)$$

$$+ V_{11}^{(N_o)*} \exp\left[i2\left(\sum_{j=1}^{N_o} \Gamma_{R_j}\right)\right] \exp\left(i2\Gamma_{R_{N_o+1}}\right)$$

$$= \left(V_{12}^{(N_o)*} r^*_{R_{N_o+1}} + V_{11}^{(N_o)*}\right) \exp\left[i2\left(\sum_{j=1}^{N_o+1} \Gamma_{R_j}\right)\right] \qquad (6\text{-}103)$$

Now from Eqs. (6-88) and (6-103)

$$d = e^* \exp\left[i2\left(\sum_{j=1}^{N_o+1} \Gamma_{R_j}\right)\right]$$

The proof is complete.

Using the above theorem it immediately follows that

$$Q = \left(\prod_{j=1}^{N} t_{R_j}^{-1}\right) \begin{bmatrix} 1 + \text{sum of all gep(m)}, \ell_m \leq N & (\text{sum of all gop(m)}, \ell_m \leq N)^* \exp\left(i2 \sum_{j=1}^{N} \Gamma_{R_j}\right) \\ \text{sum of all gop(m)}, \ell_m \leq N & (1 + \text{sum of all gep(m)}, \ell_m \leq N) \exp\left(i2 \sum_{j=1}^{N} \Gamma_{R_j}\right) \end{bmatrix} \qquad (6\text{-}104)$$

and so, by Eqs. (6-1) and (6-104)

$$t_R = \frac{\prod_{j=1}^{N} t_{R_j}}{1 + \text{sum of all } gep(m),\ \ell_m \leq N} \tag{6-105}$$

$$r_R = \frac{\text{sum of all } gop(m),\ \ell_m \leq N}{1 + \text{sum of all } gep(m),\ \ell_m \leq N} \tag{6-106}$$

Combining Eqs. (6-105) and (6-106) yields

$$\frac{r_R}{t_R}\left(\prod_{j=1}^{N} t_{R_j}\right) = \text{sum of all } gop(m),\ \ell_m \leq N \tag{6-107}$$

But $|t_{R_j}|^2 = 1 - |r_{R_j}|^2$ because of energy conservation. Furthermore, ρ_R, the right going reflectance equals $|r_R|^2$ and the right going transmittance, T_R, must equal $1 - \rho_R$ because of energy conservation. Thus, Eq. (6-107) becomes

$$\left(\frac{\rho_R}{1 - \rho_R}\right)^{1/2} \prod_{j=1}^{N} \sqrt{1 - |r_{R_j}|^2} = |\text{sum of all } gop(m),\ \ell_m \leq N| \tag{6-108}$$

At this point we wish to prove two additional theorems which will be used in the following chapter.

Theorem 6-5:

$$\text{sum of all op(1)} = \alpha(\theta_o) \int_0^D n'(z) \exp\left(-i\left(\frac{4\pi}{\lambda} n_o \cos\theta_o\right)z\right) dz$$

$$= \alpha(\theta_o)\, \mathcal{F}\{n'(z)\ \text{rect}\left(\frac{z}{D}\right)\}_{f_z = \frac{2 n_o \cos\theta_o}{\lambda}} \tag{6-109}$$

where $\mathcal{F}\{\cdot\}_{f_z}$ denotes Fourier transform evaluated at f_z

D = the grating thickness = $\sum_{j=1}^{N} \frac{1}{f_j}$

$$\text{rect}\left(\frac{z}{D}\right) \triangleq \begin{cases} 1, & 0 \leq z \leq D \\ 0, & \text{otherwise} \end{cases}$$

$'$ denotes differentiation.

Proof:

$$\int_0^D n'(z) \exp\left(-i\left(\frac{4\pi}{\lambda} n_o \cos\theta_o\right)z\right) dz =$$

$$\int_0^{1/f_1} n'(z) \exp\left(-i\left(\frac{4\pi}{\lambda} n_o \cos\theta_o\right)z\right) dz +$$

$$\sum_{m=1}^{N-1} \int_{\sum_{j=1}^{m} 1/f_j}^{\sum_{j=1}^{m+1} 1/f_j} n'(z) \exp\left(-i\left(\frac{4\pi}{\lambda} n_o \cos\theta_o\right)z\right) dz$$

But

$$\int_{\sum_{j=1}^{m} 1/f_j}^{\sum_{j=1}^{m+1} 1/f_j} n'(z)\, \exp(-i(\frac{4\pi}{\lambda}\, n_o \cos\theta_o)z)\, dz$$

becomes with a change of variable

$$\exp\left[-i(\frac{4\pi}{\lambda}\, n_o \cos\theta_o)\,(\sum_{j=1}^{m}\frac{1}{f_j})\right]\int_0^{1/f_{m+1}} n'(z+\sum_{j=1}^{m}\frac{1}{f_j})$$

$$\cdot\, \exp\,(-i(\frac{4\pi}{\lambda}\, n_o \cos\theta_o)z)\, dz$$

Furthermore,

$$n(z+\sum_{j=1}^{m}\frac{1}{f_j}) = n_{m+1}(z) = A_{m+1}\sin(2\pi f_{m+1}z)$$

Integrals of the form

$$\int_0^{1/f_{m+1}} n'_{m+1}(z)\exp\,(-i(\frac{4\pi}{\lambda}\, n_o \cos\theta_o)z)\, dz$$

have already been evaluated in Chapter 5 (Eqs. (5-4)-(5-7)). It was shown in Chapter 5 that

$$\int_0^{1/f_{m+1}} n'_{m+1}(z) \exp\left(-i\left(\frac{4\pi}{\lambda} n_o \cos\theta_o\right)z\right) dz = \frac{a_{m+1}}{\alpha(\theta_o)} \exp\left(-i\phi_{m+1}\right)$$

Also note that

$$\exp\left(-i\left(\frac{4\pi}{\lambda} n_o \cos\theta_o\right)\left(\sum_{j=1}^{m} \frac{1}{f_j}\right)\right) = \exp\left(-i2\left(\sum_{j=1}^{m} \phi_j\right)\right)$$

Therefore

$$\alpha(\theta_o) \int_0^D n'(z) \exp\left(-i\left(\frac{4\pi}{\lambda} n_o \cos\theta_o\right)z\right) dz =$$

$$a_1 \exp\left(-i\phi_1\right) + \sum_{m=2}^{N} a_m \exp\left(-i\left(2\left(\sum_{j=1}^{m-1} \phi_j\right) + \phi_m\right)\right)$$

By Equation (6-49), op(1) is an expression of the form

$$a_{\ell_1} \exp\left(-i\left(2\left(\phi_1 + \phi_2 + \ldots + \phi_{\ell_1-1}\right) + \phi_{\ell_1}\right)\right)$$

And so

$$\text{sum of all op(1)} = a_1 \exp(-i\phi_1) + \sum_{m=2}^{N} a_m \exp\left(-i\left(2\left(\sum_{j=1}^{m-1} \phi_j\right) + \phi_m\right)\right)$$

$$= \alpha(\theta_o) \int_0^D n'(z) \exp\left(-i\left(\frac{4\pi}{\lambda} n_o \cos\theta_o\right)z\right) dz$$

$$= \alpha(\theta_o) \int_{-\infty}^{\infty} n'(z)\, \text{rect}\left(\frac{z}{D}\right) \exp\left(-i\left(\frac{4\pi}{\lambda} n_o \cos\theta_o\right)z\right) dz$$

$$= \alpha(\theta_o)\, \mathcal{F}\{n'(z)\, \text{rect}\left(\frac{z}{D}\right)\}_{f_z = \frac{2n_o}{\lambda}\cos\theta_o}$$

The proof is complete.

Theorem 6-6:

$$\text{gop(1)} \tilde{-} \alpha(\theta_o) \int_0^D n'(z) \exp\left(-i\left(\frac{4\pi}{\lambda} n_o \cos\theta_o\right)z\right) dz \qquad (6\text{-}110)$$

for small $|r_{R_j}|$, j=1, ..., N

where Δ_j = the thickness of the jth slab

D = the grating thickness = $\sum_{j=1}^{N} \Delta_j$

' denotes differentation.

Proof:

We showed in Chapter 5 (Eqs. (5-3) and (5-4) with $\Gamma_j = 0$) that

$$r_{R_j} \simeq -\alpha(\theta_o) \int_0^{\Delta_j} n'(z + \sum_{m=1}^{j-1} \Delta_m) \exp\left(-i\left(\frac{4\pi}{\lambda} n_o \cos\theta_o\right)z\right) dz \qquad (6\text{-}111)$$

for small $|r_{R_j}|$. Similarly, for the left going reflection coefficient of the jth slab, r_{L_j}

$$r_{L_j} = \alpha(\theta_o) \int_0^{\Delta_j} n'\left(\left(\sum_{m=1}^{j} \Delta_m\right) - z\right) \exp\left(-i\left(\frac{4\pi}{\lambda} n_o \cos\theta_o\right)z\right) dz$$

for small $|r_{L_j}|$. Now with the substitution $t = \Delta_j - z$, the above equation becomes

$$r_{L_j} \simeq \left[-\alpha(\theta_o) \int_0^{\Delta_j} n'(t + \sum_{m=1}^{j-1} \Delta_m) \exp\left(i\left(\frac{4\pi}{\lambda} n_o \cos\theta_o\right)t\right) dt \right] \cdot$$

$$\exp\left(-i\left(\frac{4\pi}{\lambda} n_o \cos\theta_o\right)\Delta_j\right) \qquad (6\text{-}113)$$

for small $|r_{L_j}|$. Therefore, by Eqs. (6-111) and (6-113)

$$r_{L_j} = -r_{R_j}^* \exp\left(-i\left(\frac{4\pi}{\lambda} n_o \cos\theta_o\right)\Delta_j\right)$$

for small $|r_{L_j}|$ and $|r_{R_j}|$. But by Eq. (6-14)

$$r_{L_j} = -r^*_{R_j} \exp\,(i2\Gamma_{R_j})$$

and so

$$2\Gamma_{R_j} = -\frac{4\pi}{\lambda}\, n_o (\cos\,\theta_o)\Delta_j \qquad (6\text{-}114)$$

for small $|r_{R_j}|$ and $|r_{L_j}|$. Note that

$$\alpha(\theta_o) \int_0^D n'(z) \exp\,(-i(\tfrac{4\pi}{\lambda}\, n_o \cos\,\theta_o)z)\, dz$$

$$= \alpha(\theta) \int_0^{\Delta_1} n'(z) \exp\,(-i(\tfrac{4\pi}{\lambda}\, n_o \cos\,\theta_o)z)\, dz$$

$$+ \alpha(\theta) \sum_{j=2}^{N} \int_{\sum_{m=1}^{j-1}\Delta_j}^{\sum_{m=1}^{j}\Delta_j} n'(z) \exp\,(-i(\tfrac{4\pi}{\lambda}\, n_o \cos\,\theta_o)z)\, dz$$

$$= \alpha(\theta) \int_0^{\Delta_1} n'(z) \exp\,(-i(\tfrac{4\pi}{\lambda}\, n_o \cos\,\theta_o)z)\, dz$$

(Equation continued on next page.)

$$+ \alpha(\theta) \sum_{j=1}^{N} \left[\exp\left(-i\left(\frac{4\pi}{\lambda} n_o \cos\theta_o\right) \sum_{m=1}^{j-1} \Delta_j\right) \int_0^{\Delta_j} n'\left(t + \sum_{m=1}^{j-1} \Delta_j\right) \right.$$

$$\left. \cdot \exp\left(-i\left(\frac{4\pi}{\lambda} n_o \cos\theta_o\right)t\right) dt \right] \qquad (6\text{-}115)$$

(We made the substitution $t = z - \sum_{m=1}^{j-1} \Delta_j$).

Now for $|r_{R_j}|$ small $j = 1, \ldots, N$, Eq. (6-115) becomes

$$\alpha(\theta_o) \int_0^D n'(z) \exp\left(-i\left(\frac{4\pi}{\lambda} n_o \cos\theta_o\right)z\right) dz +$$

$$r_{R_1} + \sum_{j=2}^{N} r_{R_j} \exp\left(-i\left(\frac{4\pi}{\lambda} n_o \cos\theta_o\right)\sum_{m=1}^{j-1} \Delta_j\right) \qquad (6\text{-}116)$$

But we have already shown that

$$2\Gamma_{R_j} = \frac{-4\pi}{\lambda} n_o(\cos\theta_o)\Delta_j \qquad (6\text{-}114)$$

for $|r_{R_j}|$ and $|r_{L_j}|$ small, and so

$$\alpha(\theta_o) \int_0^D n'(z) \exp\left(-i\left(\frac{4\pi}{\lambda} n_o \cos\theta_o\right)z\right) dz$$

$$\simeq r_{R_1} + \sum_{j=2}^{N} r_{R_j} \exp\left(i2 \sum_{m=0}^{j-1} \Gamma_{R_m}\right) \qquad (6\text{-}117)$$

for $|r_{R_j}|$ and $|r_{L_j}|$ small, $j = 1, \ldots, N$.

By Eq. (6-10), $|r_{L_j}| = |r_{R_j}|$ and so $|r_{R_j}|$ small implies that $|r_{L_j}|$ is also small. But by Eq. (6-81) gop(1) can be written as

$$\text{gop}(1) = r_{R_1} + \sum_{j=2}^{N} r_{R_j} \exp\left(i2 \sum_{m=1}^{j-1} \Gamma_{R_m}\right)$$

and so the proof is complete. We make three remarks. First,

$$\lim_{\Delta_j \to 0} r_{R_j} = 0.$$

Secondly, gop(1) asymptotically approaches

$$\alpha(\theta_o) \int_0^D n'(z) \exp\left(-i\left(\frac{4\pi}{\lambda} n_o \cos\theta_o\right)z\right) dz$$

as the Δ_j's approach zero. Finally,

$$\alpha(\theta_o) \int_0^D n'(z) \exp\left(-i\left(\frac{4\pi}{\lambda} n_o \cos \theta_o\right)z\right) dz =$$

$$\alpha(\theta_o)\, \mathcal{F}\{n'(z)\ \text{rect}\ (\tfrac{z}{D})\}_{f_z = \frac{2n_o \cos \theta_o}{\lambda}}$$

and so

$$gop(1) \simeq \alpha(\theta_o)\, \mathcal{F}\{n'(z)\ \text{rect}\ (\tfrac{z}{D})\}_{f_z = \frac{2n_o \cos \theta_o}{\lambda}}$$

Notes to Chapter 6

[1] Z. Knittl, Optics of Thin Films, John Wiley & Sons, New York, 1976

[2] * denotes conjugation.

[3] See Equation (5-3) with r_j set to zero.

7
THEORY OF HOLOGRAPHIC GRATING DESIGN

The ultimate goal of any applied science is the successful application of fundamental principles to the design of useful devices. In almost all cases, the development of techniques for analyzing observed phenomena predates the development of techniques for designing devices based on those phenomena. Furthermore, design capability is generally far more difficult to attain than analysis capability. Design is an engineering problem, and as such, is often as much an art as a science. The design of holographic gratings is in many respects similar to the design of multilayer dielectric devices. A multilayer dielectric device is a stack of thin homogeneous dielectric layers (see Figure 3-1). The study of such structures is often referred to as the optics of thin films. We digress briefly to discuss the history of the optics of thin films.

The interference colors produced by soap bubbles and by oils on water were described as early as the 17th century. Isaac Newton was unable to explain this phenomena with his corpuscular theory of light. It was not until the development of physical optics by Young and Fresnel that the colors of thin films was discovered to be caused by the interference of light. The Fabry-Perot interferometer was the first practical device based on the principle of interference.

In 1917, the spectral colors of the covers of some beetles observed in reflection was explained by Lord Rayleigh [1]. The covers of the beetles was essentially a laminar structure analogous to the "high-low, high-low" stacks of multilayer dielectric interference filters. At that time, however, no techniques for fabricating multilayer dielectric structures were available and Lord Rayleigh's paper received little attention. The first real appearance of thin film optics can be traced to 1904 when a patent was granted for an antireflection technique [2].

Practical developments of thin film optics didn't occur until the 1930's when they sprouted from advances in vacuum technology. It became possible then to vacuum deposit thin transparent materials of specified thicknesses onto substrates. Thus was the atmosphere in the period of 1937 to 1947 during which the first theories for antireflecting coatings and monochromatic interference filters were developed. It was not until 1950 however, that a general treatment of electromagnetic wave propagation through stratified media was published [3]. This treatment was later simplified by the introduction of matrix techniques (see Chapter 3).

In this early period the primary focus of research was mainly in the area of analysis, closed form expressions for reflectivities of multilayer dielectric stacks were conceptually simple but had large numbers of parameters (the refractive index of each layer, the thickness of each layer, and the number of layers). Determining these parameters to yield desired reflectivity characteristics is an extremely difficult design problem. Great progress has been made in this area [4, 5, 6]. Initially, design theory was limited to very special problems such as antireflection coatings. Later, however, theoretical work was undertaken to develop systematic design procedures applicable to wider classes of problems. Although a tremendous amount of effort has been expended in an effort to develop these procedures and significant progress has been made, the goal has not been completely reached. The design of multilayer dielectric stacks is to an extent still an art as is the design of optical lens systems. Approximate techniques are often used to obtain a first cut solution to design a problem. The design is then analyzed using simple, exact techniques, and refinements are made as needed to the original design. The use of a digital computer greatly facilitates this iterative procedure.

The theoretical problem of design consists of specifying the parameters in the expressions for reflectivity so as to yield desired device

characteristics. In order to physically realize the device however, these parameters must satisfy certain technological constraints. For multilayer dielectric stacks, these constrains limit the maximum number of layers in the stack, and also the materials which can be used to form dielectric layers.

We have developed a theory for analyzing holographic grating filters. An alternate, currently available analysis technique based on multilayer dielectric structures was already known, though not used, prior to our work (see Chapter 4). The original motivation for our research was to develop an analysis technique which would be computationally more efficient. We were successful in this endeavor. Furthermore, we will show that our analysis technique can be used to gain considerable insight into the design problem. Equations (6-74), and (6-107) of Chapter 6 are key results which we'll exploit in order to develop design techniques.

The design parameters in holographic grating filters are the A_j's and f_j's. As in the design of multilayer dielectric stacks, these parameters must satisfy certain technological constraints. For the holographic case, these constraints place restrictions on the types of refractive index profiles which can be holographically recorded in available materials. It has already been mentioned in earlier chapters that these refractive index profiles are quasi-sinusoidal (i.e., $4\ \mu m^{-1} \leq f_j \leq 6\ \mu m^{-1}$) of small index modulation (i.e., $|A_j| \leq 0.03$). Furthermore, the element thickness (i.e., $\sum_{j=1}^{N} \frac{1}{f_j}$) is limited to a thickness of less than approximately 30 μm. Refractive index profiles which do not lie in this class are not valid solutions to the design problem. Discussions of actual procedures for fabricating a holographic filter will be deferred to Chapter 8. The design problem can now be succinctly stated as follows:

> Given t_R and r_R as a function of θ_o, λ, and polarization, determine the A_j's and f_j's which yield those characteristics. These A_j's and f_j's must also satisfy the constraints

$$|A_j| \leq 0.03$$

$$4\ \mu m^{-1} \leq f_j \leq 6\ \mu m^{-1}$$

$$\text{emulsion thickness} = \sum_{j=1}^{N} \frac{1}{f_j} \leq 30\ \mu m$$

A solution for a design problem may not always exist.

Equations (6-73), (6-74), (6-105) and (6-106) of Chapter 6 are analogous to the Airy summation formulas for multilayer dielectric stacks [4]. There is good reason to believe that a number of techniques used in the design of multilayer dielectric stacks may, with modification, be applicable to the holographic grating design problem. This area has not been explored as of yet, but it appears promising. Our discussion will be limited to a simple, approximate holographic design technique.

Before we begin, let us discuss the motivation behind this work. There is a market for multilayer dielectric devices as attested to by the wide spread use as antireflection coatings, dielectric mirrors, polarizing beam splitters, and interference filters. All of these devices are currently fabricated using evaporated thin film technology. The possibility exists for fabricating holographically, devices similar to these. Also, one would hope to produce, holographically, devices which cannot be realized using multilayer dielectric structures. An example of such a device is a head-up display unit for aircraft [7]. The fabrication of a holographic element is conceptionally simpler than the fabrication of multilayer dielectric structures since it is basically a photographic process. At this point, it is only fair to say that the practical realization of sophisticated holograhic grating devices is uncertain. Only time will tell.

In almost instances where a holographic optical element is used, the element is embedded in a medium having a nominal refractive index of one. Such a medium is of course air. We will, however, restrict our discussion

to the case where the element is imbedded in an index matching medium assumed to have a nominal refractive index of 1.5. The reason behind this decision is mainly pedagogical, though it does simplify the development of design techniques. In any case, the analysis techniques developed so far place no restrictions on the imbedding medium. As a last point, we note that Eqs. (6-73), (6-74), (6-105) and (6-106) of Chapter 6 are strictly applicable when the imbedding medium is of refractive index 1.5. They can, however, be extended to the more general case.

Equations (6-74), (6-107) and (6-108) of Chapter 6 are repeated below for reference.

$$r_R = \frac{\text{sum of all op(m), } \ell_m \leq N}{1 + \text{sum of all ep(m), } \ell_m \leq N} \tag{7-1}$$

$$\frac{r_R}{t_R}\left(\prod_{j=1}^{N} t_{R_j}\right) = \text{sum of all gop(m), } \ell_m \leq N \tag{7-2}$$

$$\left(\frac{\rho_R}{1-\rho_R}\right)^{1/2}\left(\prod_{j=1}^{N}\sqrt{1-\left|r_{R_j}\right|^2}\right) = \left|\text{sum of all gop(m), } \ell_m \leq N\right| \tag{7-3}$$

t_R is the right going transmission coefficient of the grating, r_R is the right going reflection coefficient of the grating, and ρ_R is the right goint reflectance of the grating. r_{R_j} and t_{R_j} ar the right going reflection and transmission coefficients repectively of the j^{th} slab of the grating. We note that in Eqs. (7-2) and (7-3) the thickenss of this j^{th} slab is arbitrary and therefore not necessarily an integral number of periods of the refractive index profile. In Eq. (7-1), however, the j^{th} slab has a thickness equal to the period of the j^{th} cycle of the refractive index profile.

Let us examine Eq. (7-1) first. We note from Eqs. (6-47) and (6-49) of Chapter 6 that both op(m) and ep(m), $m \geq 2$ are sums of terms which are of order greater than or equal to two in the a_j's (i.e., each term contains a product of at least two a_j's). As can be seen from Eq. (5-24) of Chapter 5, the a_j's are rather small quantities. Thus, as a first approximation all ep(m) and op(m), $m \geq 2$ will be neglected in Eq. (7-1). Then this equation becomes to a first order approximation

$$r_R \simeq \text{sum of all op(1)} \tag{7-4}$$

(note ep(1) $\equiv$ 0)

From Theorem 6-5, Eq. (7-4) is rewritten as

$$r_R \simeq \alpha(\theta_0)\mathcal{F}\left\{n'(z)\ \text{rect}\left(\frac{z}{D}\right)\right\}_{f_z = \frac{2n_0}{\lambda}\cos\theta_0} \tag{7-5}$$

Equation (7-5) is a well known result. Recall that it was rigorously derived from Maxwell's equations in Chapter 4 for the case of low reflectivity (i.e., $|r_R|^2$ small). A much better approximation (i.e., one which is less restrictive on the magnitude of r_R) can be obtained from Eqs. (7-2) and (7-3) by neglecting all terms which involve products of three or more r_{R_i}'s when the r_{R_i}'s are small. We note from Eqs. (6-80) and (6-81 of Chapter 6 that gep(m), $m \geq 3$ and gop(m), $m \geq 3$ are sums of terms which each term contains a product of at least three r_{R_j}'s. Thus, as a second order approximation all gop(m), $m \geq 3$ and gep(m), $m \geq 3$ will be neglected in Eqs. (7-2) and (7-3). Then these equations become to a second order approximation.

$$\frac{r_R}{t_R}\left(\prod_{j=1}^{N}\sqrt{1 - |r_{R_j}|^2}\right)\exp\left(-i\left(\frac{2\pi}{\lambda}n_0\cos\theta_0\right)D\right) \simeq \text{gop(1)} \tag{7-6}$$

(see comments following Eq. (7-7)).

$$\left(\frac{\rho_R}{1-\rho_R}\right)^{1/2}\left(\prod_{j=1}^{N}\sqrt{1-\left|r_{R_j}\right|^2}\right) \approx \left|gop(1)\right| \qquad (7\text{-}7)$$

Note that $gop(2) \equiv 0$ and also that

$$\prod_{j=1}^{N} t_{R_j} = \prod_{j=1}^{N} \left|t_{R_j}\right| \exp\left(i\Gamma_{R_j}\right)$$

$$= \left(\prod_{j=1}^{N}\sqrt{1-\left|r_{R_j}\right|^2}\right) \exp\left(i\prod_{j=1}^{N}\Gamma_{R_j}\right)$$

But from the Eq. (6-114) of Chapter 6, we have

$$\Gamma_{R_j} \approx \left(-\frac{2\pi}{\lambda_0} n_0 \cos\theta_0\right)\Delta_j \quad \text{for } r_{R_j} \text{ small}$$

Therefore

$$\prod_{j=1}^{N} t_{R_j} \approx \left(\prod_{j=1}^{N}\sqrt{1-\left|r_{R_j}\right|^2}\right) \exp\left(-i\left(\frac{2\pi}{\lambda} n_0 \cos\theta_0\right)\sum_{j=1}^{N}\Delta_j\right)$$

$$= \left(\prod_{j=1}^{N}\sqrt{1-\left|r_{R_j}\right|^2}\right) \exp\left(-i\left(\frac{2\pi}{\lambda} n_0 \cos\theta_0\right) D\right)$$

From Theorem 6-6, Eqs. (7-6) and (7-7) can be rewritten as

$$\frac{r_R}{t_R}\left(\prod_{j=1}^{N}\sqrt{1-\left|r_{R_j}\right|^2}\right)\exp\left(-i\left(\frac{2\pi}{\lambda_0}n_0\cos\theta_0\right)D\right) \simeq \alpha(\theta_0)\mathcal{F}\left\{n'(z)\ \mathrm{rect}\left(\frac{z}{D}\right)\right\}_{f_z=\frac{2n_0}{\lambda}\cos\theta_0} \tag{7-8}$$

$$\left(\frac{\rho_R}{1-\rho_R}\right)^{1/2}\left(\prod_{j=1}^{N}\sqrt{1-\left|r_{R_j}\right|^2}\right) \simeq \left|\alpha(\theta_0)\mathcal{F}\left\{n'(z)\ \mathrm{rect}\left(\frac{z}{D}\right)\right\}_{f_z=\frac{2n_0}{\lambda}\cos\theta_0}\right| \tag{7-9}$$

Equations (7-4)-(7-9) above are analogous to results derived in multilayer dielectric stack theory [4]. In that theory, these results play an important role in the area of design. Equations (7-5), (7-6) and (7-7) will serve as the basis of our design procedure. The design strategy using a first order approximation is as follows:

We are given r_R vs. θ_0 for fixed λ and polarization or r_R vs. λ for fixed θ_0 and polarization. Write $r_R/\alpha(\theta_0)$ as a function of $f_z = \frac{2n_0}{\lambda}\cos\theta_0$. Then take the inverse Fourier transform of $\frac{r_R}{\alpha(\theta_0)}$ to obtain $n'(z)\ \mathrm{rect}\left(\frac{z}{D}\right)$ and consequently $n'(z)$, $0 \le z \le D$. Finally, $n(z)$, $0 \le z \le D$ can be obtained from $n'(z)$ by integration. For a design using a second order approximation, the above procedure is modified.

We are given r_R and t_R vs. θ_0 for fixed λ and polarization or r_R and t_R vs. λ for fixed θ_0 and polarization. Make an initial estimate of $n(z)$ (and consequently the A_j's and f_j's). Use our analysis technique to compute the r_{R_j}'s as a function of $f_z = \frac{2n_0}{\lambda}\cos\theta_0$. Write

$$\frac{r_R}{t_R^{\alpha(\theta_0)}}\left(\prod_{j=1}^{N}\sqrt{1-\left|r_{R_j}\right|^2}\right)\exp\left(-i\left(\frac{2\pi}{\lambda}n_0\cos\theta_0\right)D\right)$$

as a function of $f_z = \frac{2n_0}{\lambda}\cos\theta$. Then take the inverse Fourier transform of

$$\frac{r_R}{t_R^{\alpha(\theta_0)}}\left(\prod_{j=1}^{N}\sqrt{1-\left|r_{R_j}\right|^2}\right)\exp\left(-i\left(\frac{2\pi}{\lambda}n_0\cos\theta_0\right)D\right)$$

to obtain a new estimate of $n'(z)\ \mathrm{rect}\left(\frac{z}{D}\right)$. $n(z)$, $0 \leq z \leq D$ and consequently the A_j's and f_j's can then be obtained by integration. Repeat the above process until $n(z)$ does not change significantly from one iteration to the next. There are a number of important points which were not explicitly mentioned in the above discussion. Let us first reconsider the design technique which was based on the first order approximation. Note that

(1) It is valid only in situations where the maximum value of $|r_R|^2$ is small.

(2) Energy conservation requires that $|r_R|^2 + |t_R|^2 = 1$. Thus $|r_R|^2$ and $|t_R|^2$ cannot be specified independently.

(3) Inversion of the Fourier transform requires knowledge of $\frac{r_R}{\alpha(\theta_0)}$, expressed as a function of $f_z = \frac{2n_0}{\lambda}\cos\theta_0$, for <u>all</u> f_z, $-\infty \leq f_z \leq \infty$. λ and θ_0, however, lie in the intervals $4\ \mu m \leq \lambda \leq 7\ \mu m$ and $0° \leq \theta_0 \leq 42°$ (42° is approximately the critical angle of gelatin when imbedded in air). Thus, $\frac{r_R}{\alpha(\theta_0)}$ is <u>at most</u> known for f_z in the interval $\frac{2(1.5)}{.7\ \mu m}\cos 42° = 3.2\ \mu m^{-1}$ to $\frac{2(1.5)}{.4\ \mu m}\cos 0 = 7.5\ \mu m^{-1}$. Values must be assigned to $\frac{r_R}{\alpha(\theta_0)}$ for all f_z outside of the known interval. Although this

assignment will not effect the r_R vs. θ_0 (or λ) characteristic over that interval, it will affect the n(z) obtained from the design procedure. Note that $\frac{r_R}{\alpha(\theta_0)}$ at f_z must equal $\left(\frac{r_R}{\alpha(\theta_0)}\right)^*$ at $-f_z$ if n'(z) is to be real valued.

(4) It is likely that the inverse Fourier transform of $\frac{r_R}{\alpha(\theta_0)}$ will not vanish outside of some finite interval on the positive z axis. Our theory, however, requires it to be of the form n'(z) rect $(\frac{z}{D})$. Therefore, it will be necessary to truncate this inverse transform to a finite size and to shift it along the z axis so that it will vanish outside of some interval [0, D], $D \geq 0$. This operation will yield a r_R vs. θ_0 (or λ) characteristic which differs from the specified one. The effect of the shifting operation is to alter the r_R vs. θ_0 (or λ) characteristic by a multiplicative phase factor $\exp\left[-i\left(\frac{2n_0}{\lambda}\cos\theta_0\right)s_0\right]$, where s_0 is the distance along the z axis by which the transform was shifted (this result follows immediately from the theory of Fourier transforms). Thus, the phase characteristic of r_R vs. θ_0 (or λ) can be designed only up to this multiplicative phase factor. The effect of truncating the inverse transform to a finite extent D (note D is the element thickness) is to alter the specified $\frac{r_R}{\alpha(\theta_0)}$ vs. f_z characteristic by convolving it with the function sinc (Df_z). This conclusion also follows from Fourier transform theory. The larger the value of D, the less effect this truncation will have. D, however, is the element thickness. We have already noted that this is limited to about 30 mm by current fabrication technology.

(5) There is no guarantee that the solution obtained will be in the class of achievable refractive index profiles. If it does not lie in this class, then it isn't a valid solution. $\frac{r_R}{\alpha(\theta_0)}$ and n'(z) rect $(\frac{z}{D})$ are approximate Fourier transform pairs. Therefore $\frac{r_R}{\alpha(\theta_0)}$, expressed as a function of f_z, should be a narrowband signal with center frequency between 4 μm^{-1} and 6 μm^{-1}. This follows from the fact that n'(z) is a quasi-sinusoidal function of nominal frequency 4 μm^{-1} to 6 μm^{-1}.

(6) In many cases only the reflectance, i.e., $|r_R|^2$, is specified. Therefore only the modulas of the Fourier transform of n'(z) rect $(\frac{z}{D})$ is known. Phase information must be assigned to r_R in order to obtain n(z). This information should be chosen so as to maximize the probability of achieving a realizable refractive index profile.

For the design technique which was based on the second order approximation we note that

(1) It is valid in situations where the maximum value of $|r_R|^2$ is fairly large.

(2) Energy conservation requires that $|r_R|^2 + |t_R|^2 = 1$. Thus $|r_R|^2$ and $|t_R|^2$ cannot be specified independently.

(3) It is a design procedure for r_R/t_R rather than for r_R or t_R alone.

(4) Inversion of the Fourier transform requires knowledge of

$$\frac{r_R}{t_R \alpha(\theta_0)} \prod_{j=1}^{N} \sqrt{1 - |r_{R_j}|^2} \exp\left(-i\left(\frac{2\pi n_0}{\lambda} \cos \theta_0\right) D\right)$$ expressed as function

of $f_z = \frac{2n_0}{\lambda_0} \cos \theta_0$, for <u>all</u> f_z, $-\infty < f_z < \infty$. As before, this information will only be known over some finite interval and must be assigned values elsewhere. Note that

$$\frac{r_R}{t_R^{\alpha(\theta_0)}} \prod_{j=1}^{N} \sqrt{1 - \left|r_{R_j}\right|^2} \exp\left(-i\left(\frac{2\pi n_0}{\lambda} \cos \theta_0\right)D\right) \quad \text{at } f_z$$

must equal

$$\left(\frac{r_R}{t_R^{\alpha(\theta_0)}} \prod_{j=1}^{N} \sqrt{1 - \left|r_{R_j}\right|^2} \exp\left(-i\left(\frac{2\pi n_0}{\lambda} \cos \theta_0\right) D\right)\right)^*$$

at $-f_z$ if $n'(z)$ is to be real valued.

(5) It is likely that the inverse Fourier transform of

$$\frac{r_R}{t_R^{\alpha(\theta_0)}} \prod_{j=1}^{N} \sqrt{1 - \left|r_{R_j}\right|^2} \exp\left(-i\left(\frac{2\pi n_0}{\lambda_0} \cos \theta_0\right)D\right)$$

will not vanish outside of some finite interval on the positive z azis. Our theory, however, requires it to be of the form $n'(z)$ rect $(\frac{z}{D})$. Therefore, it will be necessary to truncate this inverse transform to a finite size and to shift it along the z axis so that it will vanish outside of some interval $[0, D]$, $D \geq 0$. This operation will yield a r_R/t_R vs. θ_0 (or λ) characteristic which differs from the one specified. The effect of the shifting operation is to alter the r_R/t_R characteristic by a multiplicative phase factor

$\exp\left[-i\left(\frac{2n_0}{\lambda}\cos\theta_0\right)s_0\right]$, where s_0 is the distance along the z axis by which the transform was shifted (this result follows immediately from the theory of Fourier transforms). Thus, the phase characteristic of r_R/t_R vs. θ_0 (or λ) can be designed only up to this multiplicative phase factor. The effect of truncating the inverse transform to a finite extend D (note D is the element thickness) does not have a simple analytic description. The larger the value of D of course, the less effect this truncation will have.

(6) There is no guarantee that the solution obtained will be in the class of achievable refractive index profiles. If it does not lie in the class then it isn't a valid solution.

(7) In many cases only the reflectance, i.e., $|r_R|^2$, is specified. Therefore only the modulus of the Fourier transform of $n'(z)$ rect $(\frac{z}{D})$ is known. Phase information must be assigned to r_R/t_R in order to obtain $n(z)$. This information should be chosen so as to maximize the probability of achieving realizable refractive index profiles.

(8) The thickness of the layers (i.e., the Δ_j's) must be chosen. Experience indicates that the quality of the approximation

$$\text{sum of all gop}(m),\ \ell_m \leq N \approx \text{gop}(1)$$

increases as the maximum values of $r_{R_j}{}^2$ $j = 1, \ldots, N$ increase. On the other hand, the quality of the approximation

$$\text{gop}(1) \propto \alpha(\theta_0)\mathcal{F}\left\{n'(z)\ \text{rect}\ (\tfrac{z}{D})\right\}_{f_z = \frac{2n_0}{\lambda}\cos\theta_0}$$

decreases as the maximum values $|r_{R_j}|^2$ $j = 1, \ldots N$ increase. Furthermore, the maximum values of $|r_{R_j}|^2$ $j = 1, \ldots, N$ are directly proportional to the Δ_j's, thus some compromise must be made in choosing these Δ_j's.

We have already pointed out that Eqs. (7-1), (7-2) and (7-3) are analogous to key formulas in the theory of multilayer dielectric stacks. In that theory the a_j's are roughly equivalent to the reflectivities at the boundaries between pairs of homogeneous dielectric layers, and the ϕ_j's are essentially equivalent to the optical thicknesses of the homogeneous dielectric layers. These equivalent a_j's are functions of the refractive indicies of the layers, the incident angle and the polarization, but not the wavelength. The equivalent ϕ_j's are functions of the incident angle, the wavelength, the thicknesses of the layers, and the refractive indicies of the layers. In most multilayer dielectric design techniques the reflectivity or the transmittance is specified as a function of wavelength for some fixed angle of incidence. Note that phase information is usually not specified, and consequently one does not exercise any control over the resulting phase characteristics. Furthermore since the angle of incidence is fixed, the a_j's will be unknown constants. The multilayer dielectric stack is generally assumed to be tuned, i.e., the ϕ_j's are all integer multiples of one another. The expression for $|r_R|^2$ can then be written as a rational function of z by making the substitution $z = \exp(-i\phi)$. The desired characteristic for $r_R{}^2$ is also written as a rational function of z. The two functions are equated which yields algebraic equations for unknown a_j's. These equations are then solved. From the a_j's, the refractive indices of each of the layers can be determined. Finally, the thicknesses of the layers are chosen so that the system is tuned.

AD-A097 201 ENVIRONMENTAL RESEARCH INST OF MICHIGAN ANN ARBOR RA--ETC F/G 14/5
THICK PHASE HOLOGRAMS.(U)
JAN 81 K A WINICK F49620-78-C-0061
UNCLASSIFIED ERIM-134200-10-F AFOSR-TR-81-0196 NL

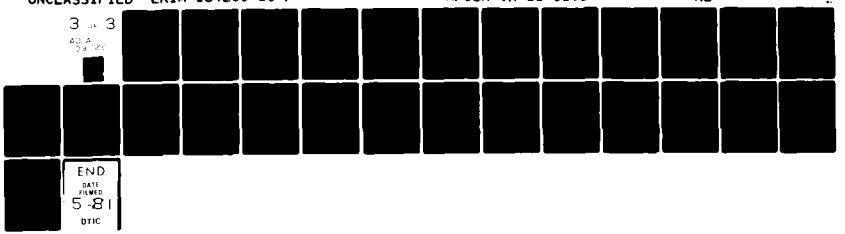

END
DATE FILMED
5-81
DTIC

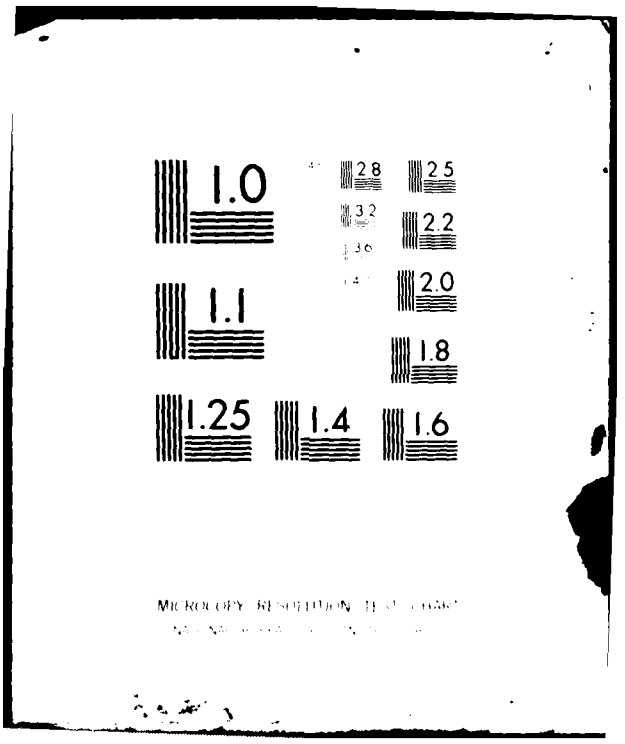
1.0
1.1
1.25
1.4
1.6
2.0
1.8
2.2
2.5
2.8
3.2
3.6
MICROCOPY RESOLUTION TEST CHART

Below we list some of the major differences between our holographic design technique and the general multilayer dielectric design technique.

(1) In the holographic case the a_j's are a function of polarization, incident angle and wavelength. Therefore for a fixed polarization and incident angle, the a_j's cannot be considered as unknown constants.

(2) The holographic design approach allows for the systematic design of detuned systems, i.e., systems where the ϕ_j's are not integer multiples of one another.

(3) The holographic design approach is based on approximate methods which require a limit to be placed on the maximum value of $|r_R|^2$.

(4) The holographic design approach is based on performing Fourier transforms, whereas the multilayer dielectric design method is based on solving algebraic equations.

(5) Even if the difference listed in (1) and (2) above did not exist, the number of a_j's in the holographic design problem generally is much larger than the number in the multilayer design problem. This factor would greatly increase the complexity of solving the required algebraic equations for the a_j's.

We used the first order design technique to determine a quasi-sinusoidal refractive index profile which corresponds to a linear reflectance vs. angle of incidence characteristic (i.e., $|r_R|^2 = 20 - \frac{2}{3}\theta_0$). Figure 5-11 shows the computed refractive index profile truncated to nominally a 15 μm extent and Figure 5-12 shows the corresponding plot of reflectance vs. angle of incidence. It can be seen from Figure 5-12 that the reflectance curve departs from the specified linear characteristic most noticeably in the region around $\theta_0 = 0$. This could have been anticipated from Eq. (7-5). Note that $f_z = 2n_0 \cos\theta_0/\lambda$ varies

very slowly as a function of θ_0 in the region around $\theta_0 = 0$. Therefore, r_R/α will vary quite rapidly as a function of f_z in this same region. This implies that the function $r_R(f_z)/\alpha(f_z)$ has a significant amount of high frequency content. It then follows from Eq. (7-5) that n'(z) will have a considerable amount of "energy" which lies outside of some small region around z = 0. Restricting the grating thickness to nominally 15 μm, as was done in our design calculations, resulted in a distorted linear characteristic. This distortion would not have been present if this thickness restriction had not imposed.

The second order design technique was used to achieve sidelobe suppression in a wavelength selective filter. Figure 7-1 is a plot of reflectance vs. wavelength for a grating which has a sinusoidal refractive index variation ($a_j = 0.02$, $f_j = 5.28$, $j = 1, \ldots, 80$). Notice the large sidelobe levels. We sought a design which would have a reflectance (vs. wavelength) identical to the central lobe of the curve in Figure 7-1 and which would be zero elsewhere. Using the 2nd order design technique (with the grating thickness restricted to nominally 15 μm), we arrived at the refractive index profile shown in Figure 7-3 after four iterations. The corresponding reflectance vs. wavelength characteristic is shown in Figure 7-2. For the initial starting point of this second order design we chose the a_j's and f_j's to be the same as those of the sinusoidal grating ($a_j = 0.02$, $f_j = 5.28$, $j = 1, \ldots, 80$). The thickness of the layers (i.e., the Δ_k's $k = 1, \ldots, M$) were chosen so that maximum value of $|r_{R_K}(f_z)|^2 \simeq 7\%$ $K = 1, \ldots, M$. Notice that the sidelobe level has been reduced considerably. The width of the reflection, however, band has increased. We attribute this reflection band broadening to the thickness restriction which was imposed on the grating design.

We wish to make some qualitative comments regarding the class of achievable spectral and angular grating characteristics. A strong re-

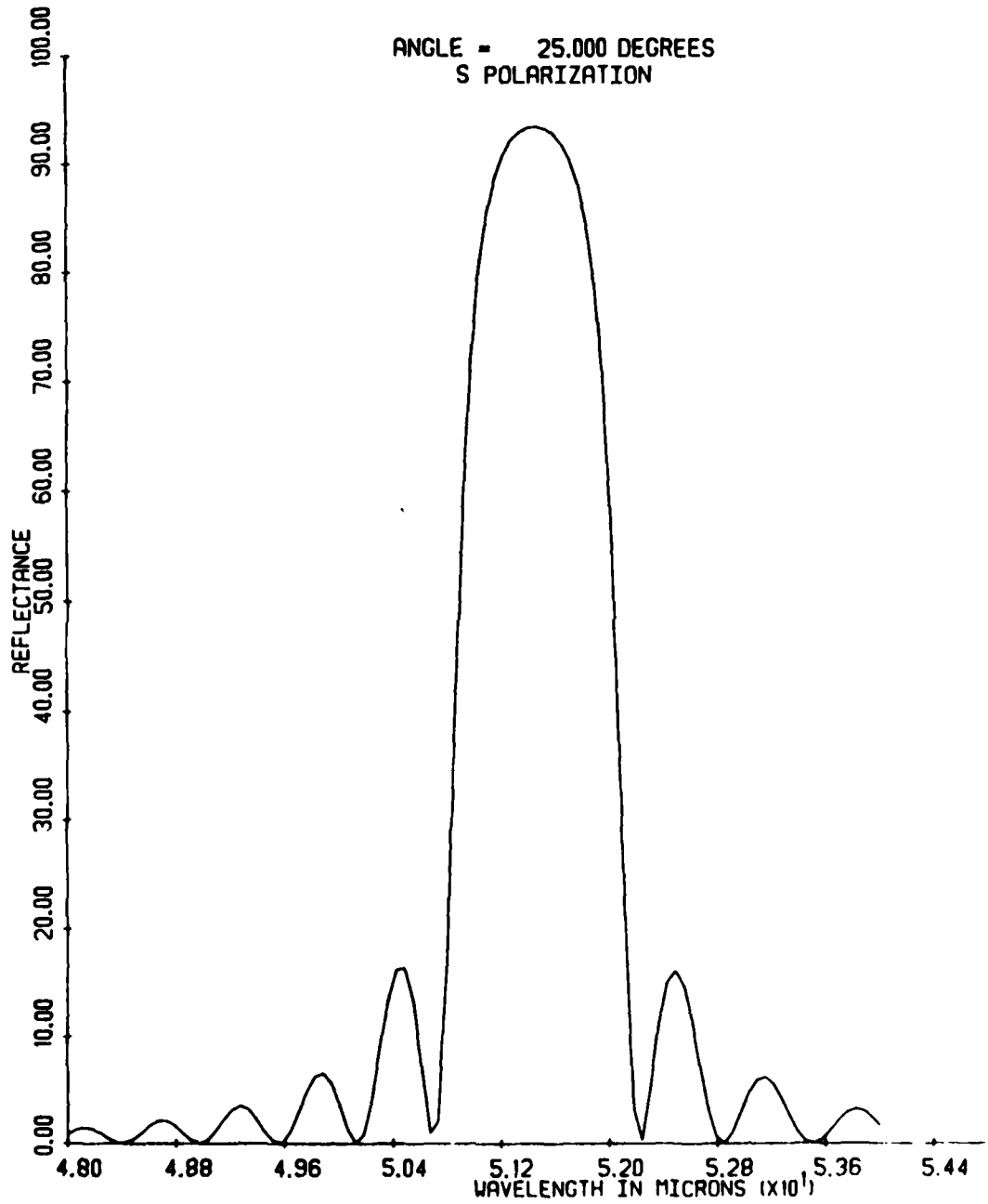

Figure 7-1. Typical Sinusoidal Reflection Grating Characteristic Exhibiting High Side Lobe Levels

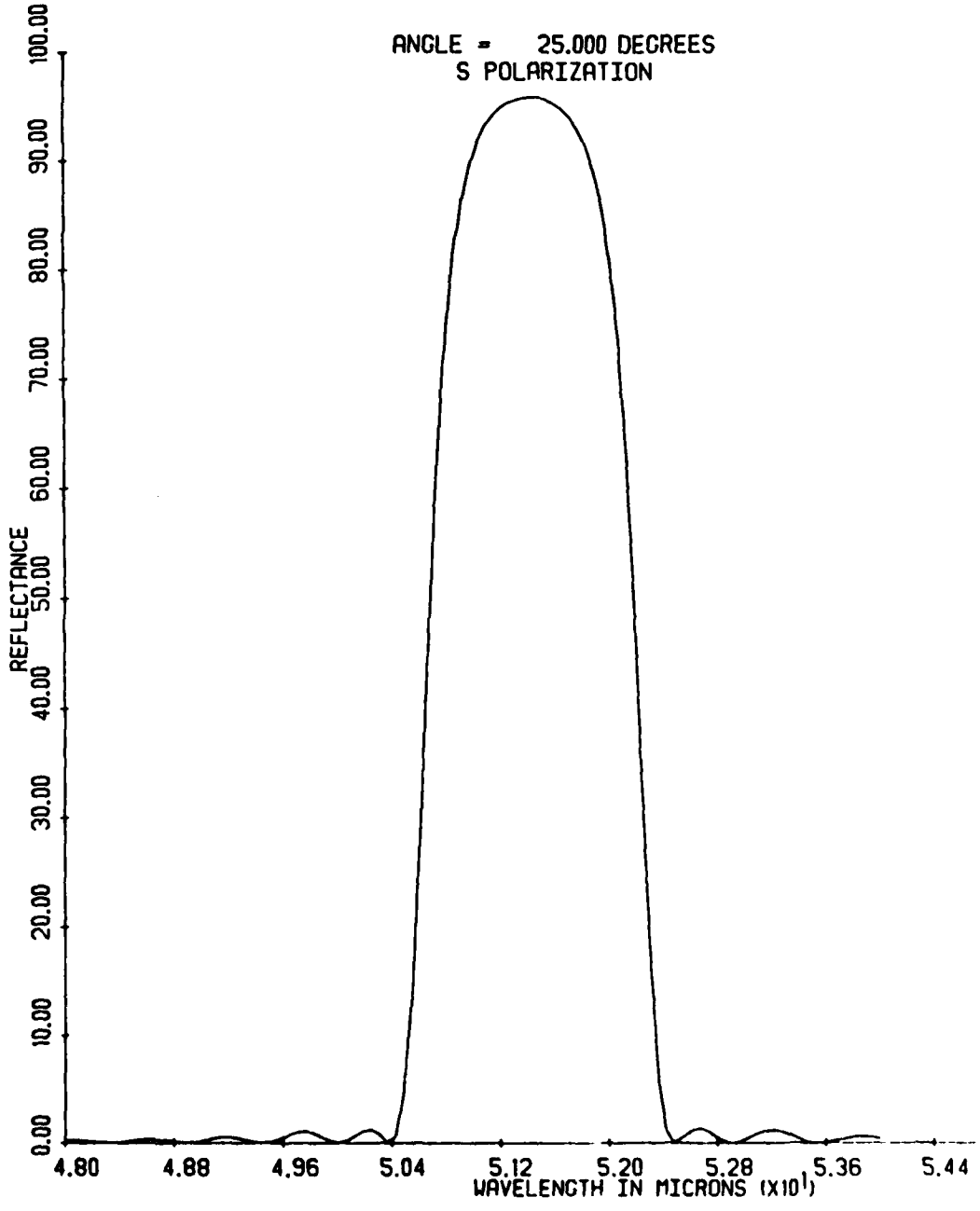

Figure 7-2. Quasi-Sinusoidal Reflection Grating Characteristic Exhibiting Reduced Side Lobe Levels

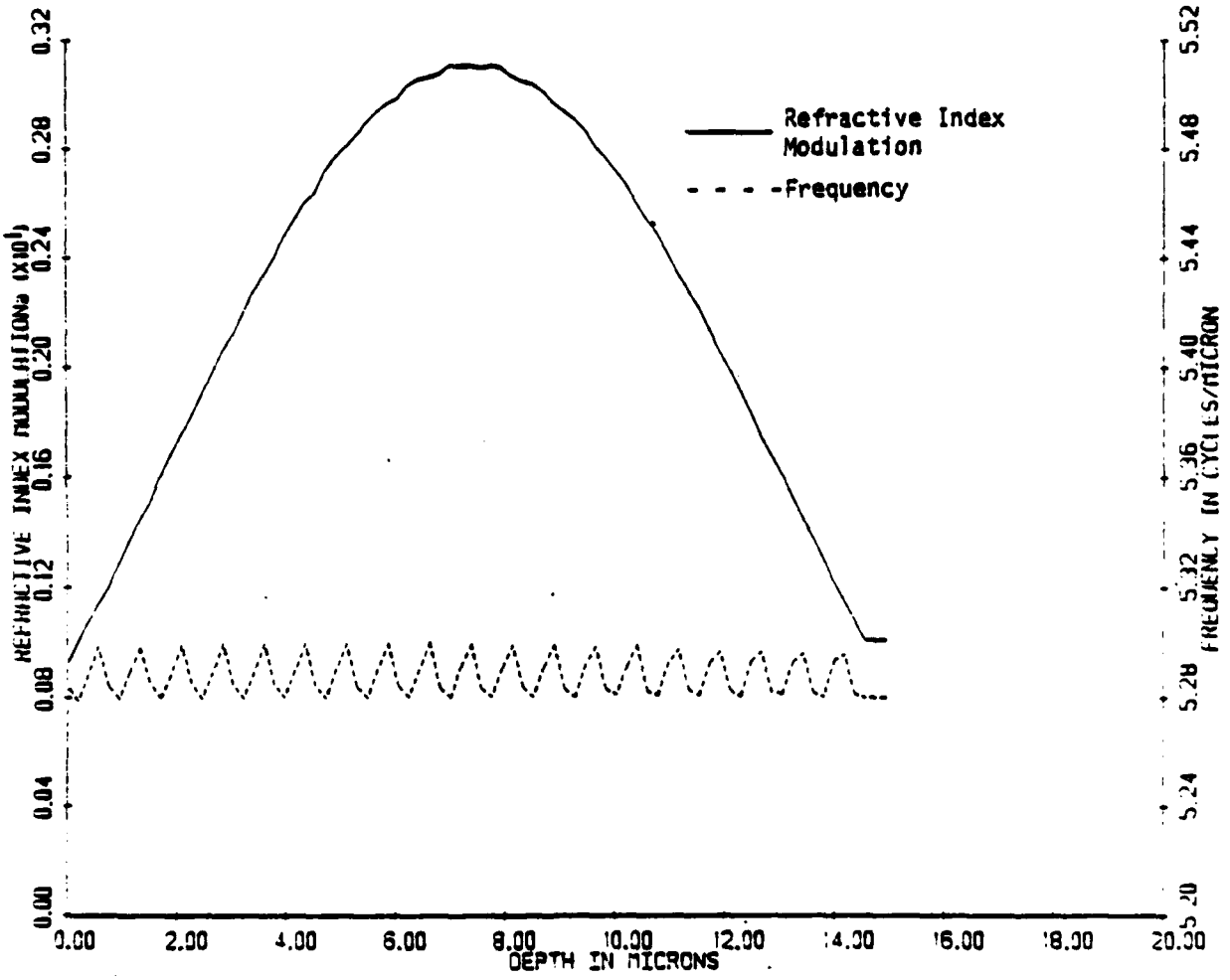

Figure 7-3. Quasi-Sinusoidal Refractive Index Profile of a Reflection Grating Which Exhibits Reduced Side Lobe Levels

lationship has been shown to exist between the Fourier transform and the design problem. This relationship leads us to make the following conjectures:

1. The rate at which r_R changes as a function of $f_z = \frac{2n_0 \cos \theta_0}{\lambda}$ will determine the nominal thickness of the grating required to yield this $r_R(f_z)$.
2. If r_R changes too rapidly as a function of f_z a very thick grating will be required.
3. If r_R changes too slowly as a function of f_z, a thin grating will be required. If this thin grating is to exhibit significant diffraction efficiency (i.e., $|r_R(f_z)|^2$ is to be large for some set of f_z's), then its peak index modulation must be high. It may be sufficiently high that our analysis techniques are no longer applicable or that the grating cannot be produced in currently available materials.

Notes to Chapter 7

[1] Lord Rayleigh, Proceedings of the Royal Society of London, A93, 565 (1917).

[2] British Patent No. 29561 (1904).

[3] F. Abeles, Ann. d. Phys., 5, 596 (1950).

[4] Z. Knittl, Optics of Thin Films, John Wiley & Sons, New York, 1976.

[5] E. Wolf, Progress in Optics, Vol. VII, Chapter 2, North-Holland Publishing Co., Amsterdam, 1969.

[6] J.A. Dobrowolski, "Optical Interference Filters for Adjustment of Spectral Response," Applied Optics, Vol. 9, No. 6, June 1970.

[7] Holographic Combiners for Head-Up Displays, Final Technical Report No. AFAL-TR-77-110, Radar and Optics Division, Environmental Research Institute of Michigan, Ann Arbor, Michigan, 1977.

8
FABRICATION

In the previous chapters we developed both analysis and design techniques for holographic gratings. Recall that the class of gratings considered were flat dielectrics having refractive index variations only along the z direction (see Figure 2-1). These refractive index variations were quasi-sinusoidal. This chapter explores techniques for holographically producing these refractive index variations in a recording material. We assume an ideal recording material which is nonabsorbing and which has a linear response. The nonabsorbing nature of the material implies that the optical field incident on the material during recording is not attenuated as propagates through it. Furthermore, if I(z) designates the intensity of the optical field within the material during recording, then from our assumption of linearity, the resulting refractive index profile, n(z), will be given by

$$n(z) = c_0 + c_1 I(z) \tag{3-1}$$

where c_0 and c_1 are constants. It is usually true that $c_1 I(z) << c_0$, and we will assume this to be the case. The practical effects of departures from an ideal recording material will be discussed later.

Now let us write I(z) as some bias, I_0, plus a spatially varying term $\Delta I(z)$.

$$I(z) = I_0 + \Delta I(z) \tag{8-2}$$

Then Eq. (8-1) becomes

$$n(z) = (c_0 + c_1 I_0) + c_1 \Delta I(z) \tag{8-3}$$

Similarly we can write n(z) as some bias, n_0, plus a spatially varying term n(z).

$$n(z) = n_0 + \Delta n(z) \tag{8-4}$$

Comparing Eqs. (8-3) and (8-4) yields

$$n_0 = c_0 + c_1 I_0 \simeq c_0 \tag{8-5a}$$

$$\Delta I(z) = \frac{\Delta n(z)}{c_1} \tag{8-5b}$$

But as discussed earlier, n(z) is quasi-sinusoidal. Therefore $\Delta n(z)$ can be written as

$$\Delta n(z) = A(z) \cos [2\pi f(z) z] \tag{8-6}$$

where

$$4\ \mu m^{-1} \leq f(z) \leq 6\ \mu m^{-1}$$

and where A(z) and f(z) are slowly varying functions of z (i.e., A(z) and f(z) can be assumed constant over intervals of length $1/4\ \mu m^{-1}$). Combining Eqs. (8-5b) and (8-6) now yields

$$\Delta I(z) = \frac{A(z)}{c_1} \cos [2\pi f(z) z] \tag{8-7}$$

Our goal then is to holographically produce an optical field having a spatially varying portion, $\Delta I(z)$, given by Eq. (8-7) above. Note that the $\Delta I(z)$ of Eq. (8-7) is only defined inside the recording material

which is assumed to be of thickness D. We define the extension, $\overline{\Delta I}(z)$, of $\Delta I(z)$ by

$$\overline{\Delta I}(z) = \begin{cases} \Delta I(z), & 0 \leq z \leq D \\ g(z), & \text{otherwise} \end{cases} \tag{8-8}$$

where $g(z)$ is some real valued function which is arbitrary and which will be chosen later.

Let $F\overline{\Delta I}(B)$ denote the Fourier transform of $\overline{\Delta I}(z)$, that is

$$F\overline{\Delta I}(B) = \int_{-\infty}^{\infty} \overline{\Delta I(z)} \exp(-i2\pi Bz)\, dz \tag{8-9}$$

Then

$$\overline{\Delta I}(z) = \int_{-\infty}^{\infty} F\overline{\Delta I}(B) \exp(i2\pi Bz)\, dz \tag{8-10}$$

Now $F\overline{\Delta I}(B) = F\overline{\Delta I}(-B)^*$ since $\overline{\Delta I}(z)$ is real valued. Therefore

$$\overline{\Delta I}(z) = \int_{0}^{\infty} 2 \cdot \text{Real Part of } [F\overline{\Delta I}(B) \exp(i2\pi Bz)]\, dz \tag{8-11}$$

If we write $F\overline{\Delta I}(B)$ as

$$F\overline{\Delta I}(B) = |F\overline{\Delta I}(B)| \exp[i\sigma(B)] \tag{8-12}$$

then Eq. (8-10) becomes

$$\overline{\Delta I}(z) = \int_0^\infty 2|F\overline{\Delta I}(B)| \cos\left(2\pi Bz + \sigma(B)\right) dB \tag{8-13}$$

Let $[B_{min}, B_{max}]$ designate the frequency content range of $\overline{\Delta I}(z)$, i.e., $|F\overline{\Delta I}(B)|$ will be nominally zero for $|B| > B_{max}$ or $|B| < B_{min}$. Then Eq. (8-13) can be written as

$$\overline{\Delta I}(z) \simeq \int_{B_{min}}^{B_{max}} 2|F\overline{\Delta I}(B)| \cos\left(2\pi Bz + \sigma(B)\right) dB \tag{8-14}$$

We choose the function g(z) so as to minimize $B_{max} - B_{min}$.

The integral in Eq. (8-14) can be approximated by the discrete sum given below

$$\sum_{j=0}^{N-1} 2\delta \left|F\overline{\Delta I}\left(B_{min} + j\delta\right)\right| \cos\left(2\pi(B_{min} + j\delta)z + \sigma\left(B_{min} + j\delta\right)\right) \tag{8-15}$$

where δ and N are constants such that $B_{min} + (N - 1)\delta = B_{max}$. Therefore

$$\overline{\Delta I}(z) \simeq \sum_{j=0}^{N-1} 2\delta |F\overline{\Delta I}(B_{min} + j\delta)| \cos\left(2\pi(B_{min} + j\delta)z + \sigma(B_{min} + j\delta)\right) \tag{8-16}$$

The "goodness" of the approximation increases as δ decreases. Consider now the setup shown in Figure 8-1. A reflection hologram is recorded in a holographic material using two plane waves. Both beams make an

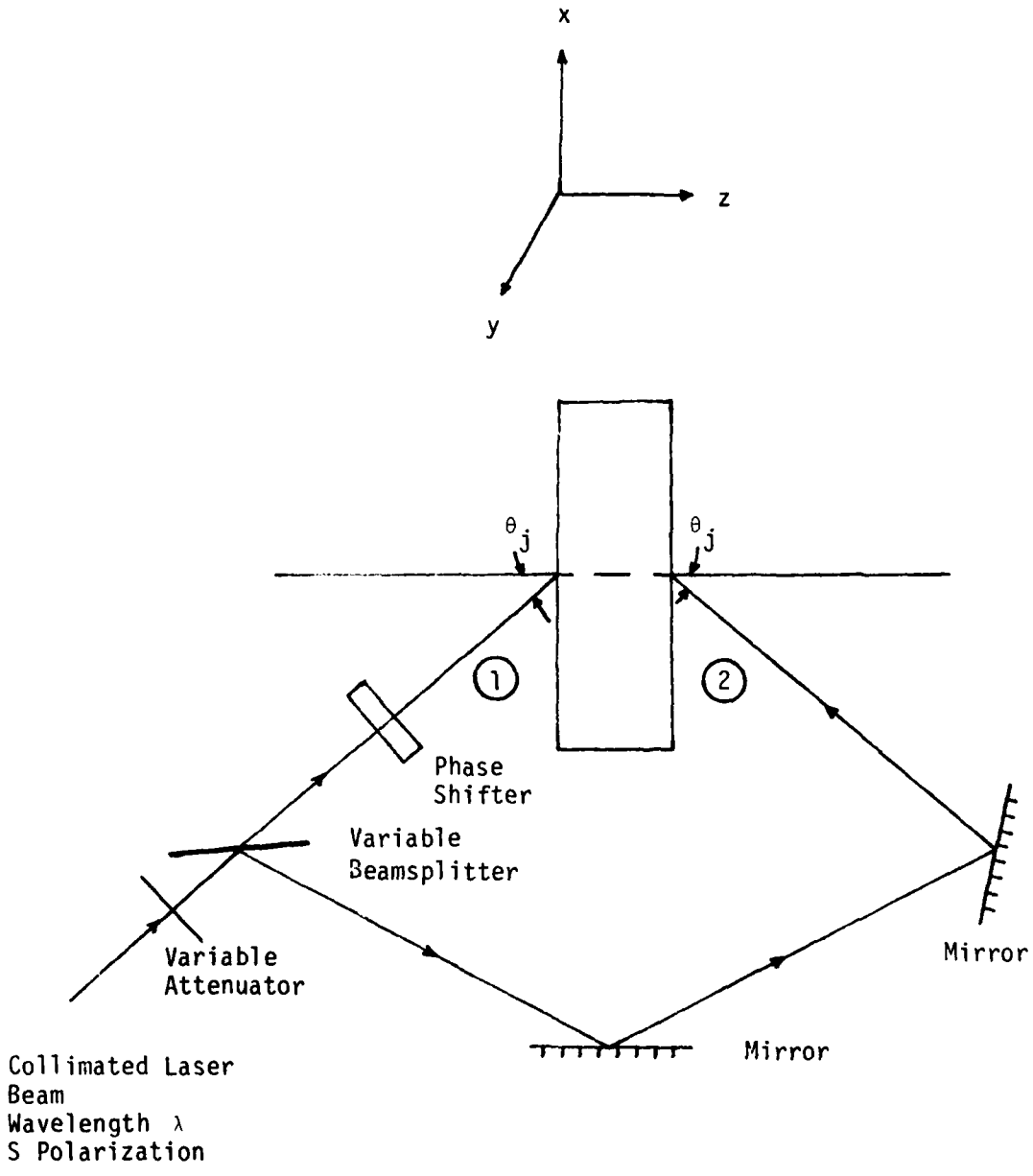

Figure 8-1. Two Beam Interferometric, Multiple Exposure Technique for Fabricating Quasi-Sinusoidal, Holographic, Reflection Gratings

angle of θ_j to the normal of the recording material where

$$\theta_j = \cos^{-1}\left[\frac{\lambda(B_{min} + j\delta)}{2n_0}\right] \tag{8-17}$$

The beamsplitter is adjusted so that the beam intensities, I_{1j} and I_{2j}, are equal, and the attenuator is adjusted so that

$$I_{1j} = I_{2j} = \delta|F\overline{\Delta I}(B_{min} + j\delta)| \tag{8-18}$$

The phase shifter is set so that the phase of beam one, Φ_j relative to beam two at $z = 0$ is given by

$$\Phi_j = \sigma(B_{min} + j\delta) \tag{8-19}$$

Then the resulting intensity pattern, $I_j(z)$, due to the interference between the two beams will be given by

$$I_j(z) = I_{1j} + I_{2j} + 2\sqrt{I_{1j}I_{2j}}\cos\left(2\pi\left(\frac{2n_0\cos\theta_j}{\lambda_0}\right)z + \Phi_j\right)$$

$$= 2\delta|F\Delta I(B_{min} + j\delta)| + 2\delta|F\Delta I(B_{min} + j\delta|$$

$$\cos\left(2\pi(B_{min} + j\delta)z + \sigma(B_{min} + j\delta)\right) \tag{8-20}$$

Now by making a series of N different exposures, as described above the resulting exposure will be equivalent to a single exposure having an intensity pattern given by

$$\sum_{j=0}^{N-1} I_j(z) = \sum_{j=0}^{N-1} 2\delta \left| F\overline{\Delta I}(B_{min} + j\delta) \right| +$$

$$\sum_{j=0}^{N-1} 2\delta \left| F\overline{\Delta I}(B_{min} + j\delta) \right| \cos \left(2\pi(B_{min} + j\delta)\, z + \sigma(B_{min} + j\delta)\right) \tag{8-21}$$

Note that the term $\sum_{j=0}^{N-1} 2\delta \left| F\overline{\Delta I}(B_{min} + j\delta) \right|$ in Eq. (8-21) is just a bias,

Therefore,

$$\sum_{j=0}^{N-1} I_j(z) \simeq \text{bias} + \overline{\Delta I}(z) \tag{8-22}$$

Thus, we have been successful in producing holographically the desired spatially varying intensity pattern.

We note that a refractive index mismatch exists between the recording material and air. This mismatch will result in multiple reflections at the air/recording material interfaces during fabrication. These multiple reflections will result in a distorted intensity pattern which can be significantly different from the one desired. As a consequence, these multiple reflections must be elminated. This is accomplished by immersing the recording material in a refractive index matching medium.

The above scheme for producing holographically the desired spatially varying intensity pattern has a number of serious limitations. First, it is extremely difficult to determine whether the phase shifter is set appropriately (i.e., whether $\Phi_j = \sigma(B_{min} + j\delta)$). Techniques for determining this would most likely utilize reflections which occur at the air/recording material interfaces. As we have just seen these reflections will be non-existant, since the recording material must be immersed in a refractive index matching medium. Secondly, the above scheme is quite tedious. It requires one to make a large number of sequential exposures, with a critical alignment being performed before each new exposure.

An alternate approach for producing holographically $\overline{\Delta I}(z)$ is to use the setup shown in Figure 8-1 with θ_j fixed $j = 1, \ldots, N$, but vary λ from exposure to exposure. Thus with

$$\theta_j = \theta_{fixed} \quad j = 1, \ldots, N$$

λ_j should be given by

$$\lambda_j = \frac{2n_0 \cos \theta_{fixed}}{B_{min} + j\delta} \tag{8-23}$$

This is not a suitable solution since the required λ_j's as given by Eq. (8-23) will generally include some wavelengths for which the recording material is insensitive (currently available phase holographic recording materials are not panchromatic). Furthermore, a dye laser plus a variety of dyes would be necessary to generate all the λ_j's.

Consider now Figure 8-2. It provides still a third method for producing holographically $\overline{\Delta I}(z)$. The set-up is equivalent to the one shown in Figure 8-1 except beam number two is produced from the reflection off of a mirror placed directly in back of the recording material.

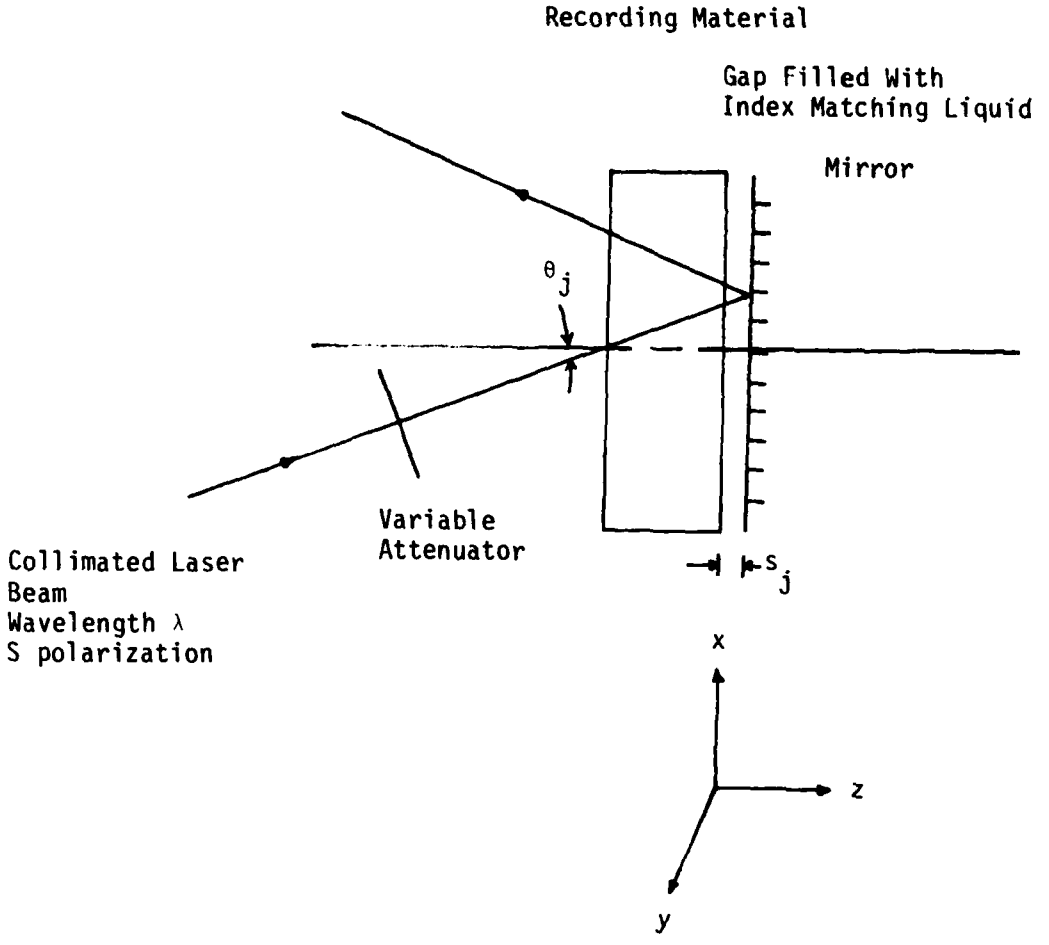

Figure 8-2. Single Beam, Multiple Exposure Interferometric Technique for Fabricating Quasi-Sinusoidal Holographic, Reflection Gratings

The phase of beam one relative to that of beam two is determined by the spacing, s_j, between the recording material and the mirror. This spacing will be different for each exposure. This method suffers from the same problems as before, namely the inability to determine the phase difference between the two beams and the necessity of making many exposures.

Below we describe an approach which eliminates these two problems in a large number of situations. First, choose g(z) in Eq. (8-8) so that $\overline{\Delta I}(z)$ is an even function of z, i.e.,

$$\overline{\Delta I}(z) = \overline{\Delta I}(-z) \tag{8-24}$$

Then by Eq. (8-9)

$$F\overline{\Delta I}(B)^* = \int_{-\infty}^{\infty} \overline{\Delta I}(z)^* \exp(i2\pi Bz)\, dz$$

$$= \int_{\infty}^{-\infty} \overline{\Delta I}(-\xi)^* \exp(i2\pi B(-\xi))\, d(-\xi)$$

(we made the substitution $z = -\xi$)

$$= \int_{-\infty}^{\infty} \overline{\Delta I}(\xi) \exp(-i2\pi B\xi)\, d\xi$$

(from Eq. (8-24) and the fact that $\overline{\Delta I}(z)$ is a real function)

$$= F\overline{\Delta I}(B) \tag{8-25}$$

Equation (8-25) indicates that $F\overline{\Delta I}(B)$ is a real function. Consequently $\sigma(B_{min} + j\delta)$ in Eq. (8-20) will be either 0 or π. Equation (8-21) can now be rewritten as

$$\sum_{j=0}^{N-1} I_j(z) = \sum_{j=0}^{N-1} 2\delta \left| F\overline{\Delta I}(B_{min} + j\delta) \right| + \sum_{j=0}^{N-1} 2u_j\delta \left| F\overline{\Delta I}(B_{min} + j\delta) \right| \cos\left(2\pi(B_{min} + j\delta)z\right) \qquad (8\text{-}26)$$

where

$$u_j \triangleq \begin{cases} 1 & \text{for } F\overline{\Delta I}(B_{min} + j\delta) \geq 0 \\ -1 & \text{otherwise} \end{cases}$$

Thus, if we use the scheme illustrated in Figure 8-2, then the required relative phase shift between the two beams will always be either 0 or π. A relative phase shift of π corresponds to s_j equals zero, whereas a relative phase shift of zero corresponds to [1].

$$\frac{4\pi}{\lambda_0} n_0(\cos\theta_j)s_j = \pi$$

Now θ_j is the angle the incoming beam makes with the normal to the recording material. This angle is measured internal to the recording material and hence cannot exceed the critical angle, θ_c. The most likely candidate for a recording material is dichromated gelatin, which has a nominal refractive index of 1.5.

Therefore

$$\theta_c \simeq \sin \frac{1}{1.5} \simeq 42°$$

and so

$$\theta_j \leq 42°$$

Suppose s_j $j = 1, \ldots, N$ is chosen such that

$$\frac{4\pi}{\lambda_0} n_0(\cos 30°) s_j = \pi$$

then

$$\frac{4\pi}{\lambda_0} n_0(\cos 0°) s_j \simeq 1.15\ \pi$$

and

$$\frac{4\pi}{\lambda_0} n_0(\cos 42°) s_j \simeq 0.86\ \pi$$

Therefore if s_j $j = 1, \ldots, N$ is a constant having a value

$$s_j = 1/4(\lambda_0/n_0)/(\cos 30°)\ \lambda_0/(n_0 \cos \theta_0)$$

then for <u>any</u> angle, θ_j, between zero degrees and the critical angle, the relative phase between beam one and beam two will lie within the interval $[0.86\ \pi, 1.15\ \pi]$. Thus the relative phase difference won't differ appreciably from π. It should also be noted that the worst case situation has analyzed. In most fabrication problems the range of θ_j will be smaller, and consequently, the above interval will also be smaller.

We have shown that a good approximation to the required intensity pattern can be generated using the setup shown in Figure 8-2. Two sets of exposures are made. The first set corresponds to a π phase difference between the two beams (at $z = 0$) and is accomplished by placing the mir-

ror approximately a quarter wavelength away from the recording material. It is impossible to place a conventional mirror in direct contact with the recording material since neither the mirror nor recording material can be made perfectly flat. We circumvent this problem by using liquid mercury as the mirror. We propose that the quarter wave separation between the recording material and the mercury is realized by coating the recording material with a thin layer of plastic. This is to be done by dip coating. The recording material is dipped into a solvent containing the plastic, and then is slowly withdrawn at a constant speed [2]. As it is withdrawn, it pulls along some of the solvent which rapidly evaporates leaving behind a thin film of plastic. The thickness of this film will be a function of, among other things, the plastic concentration in the solvent, the ambient humidity and temperature, and the speed at which the recording material is withdrawn. The thin film of plastic can be removed by redipping the recording material in the solvent alone.

We have suggested a technique for avoiding the difficult problem of setting the phase difference between the two beams. We now wish to present a method which will eliminate the need to make many exposures. With this method two exposures will be sufficient. Consider the set up shown in Figure 8-3. The input transparency has an amplitude transmittance variation only along the x direction. The combination of spherical lens #1 and cylindrical lens #1 image this transparency, in the form of a slit along the x direction, onto a rotating diffuser. The rotating diffuser makes each point on this slit spatially incoherent with any other. Therefore, each of these points will act as independent point source radiators. Spherical lens #2 collimates each of these point sources. The collimated beams cannot interfere with one another since they are derived from independent point sources.

A point on the slit, having x coordinated x_p, will result in a collimated beam making an angle of

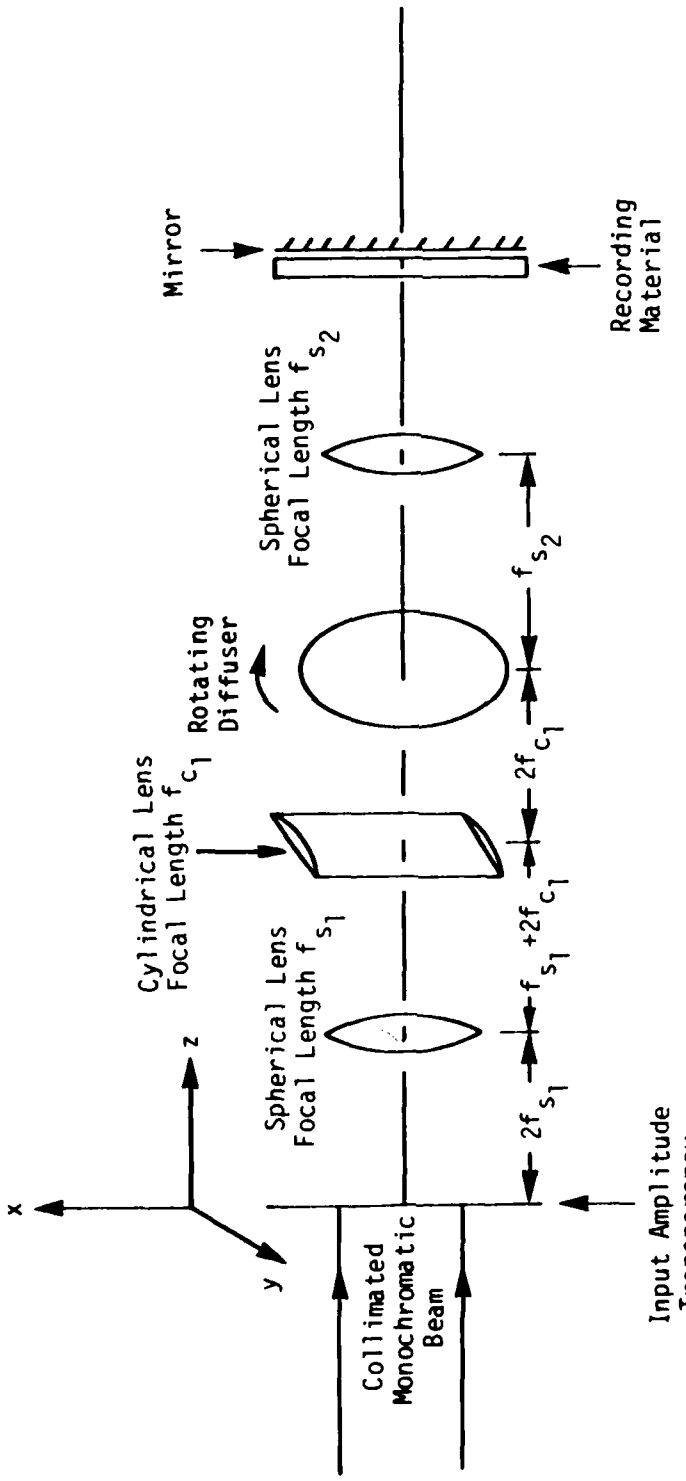

Figure 8-3. One Beam, Double Exposure, Interferometric Technique for Fabricating Quasi-Sinusoidal, Holographic, Reflection Gratings

$$\tan^{-1} \frac{x_p}{f_{s_2}} \tag{8-37}$$

measured from the normal to the recording material. Furthermore, this point source will have an intensity proportional to the square of the amplitude transmittance of the input transparency at $x = x_p$. Thus by choosing two appropriate input transparencies and making two exposures, one with the first transparency in the system and a plastic film coating on the recording material and the other with the second transparency in the system and no coating on the recording material, the intensity profile described by Eq. (8-26) can be generated. The first transparency corresponds to the terms with $u_j = 1$ in that equation, while the second transparency corresponds to terms with $u_j = -1$.

Recall that we originally approximated the integral of Eq. (8-14) by the discrete sum of Eq. (8-15). The discrete sum, of course, becomes the integral as $\delta \to 0$ and $N \to \infty$. The number N equaled the number of exposures one had to make. Consequently, practical considerations put an upper bound on N. In the new technique described above, however, there is no practical limitation on N, since each point on the input transparency represents one exposure. Thus, the integral form of Eq. (8-14) can be realized.

Till now, we have not discussed the limitations of currently available holographic recording materials. This topic has been extensively studied elsewhere, and it is not our aim to explore this area here. We will, however, mention some of the salient points which are directly applicable to the problem addressed by this report.

The holographic gratings studied in this report are all volume phase holograms. The important characteristics of any volume phase recording material are its resolving power, its spectal sensitivity, its maximum index modulation; its linearity, its dynamic range, its absorbtion, its maximum thickness, its stability and its signal to noise ratio. A

volume phase recording material suitable for reflection holograms must be capable of resolving over 5000 line pairs/mm. There are only three materials which have this resolving power. They are dichromated gelatin (DG), bleached high resolution silver halide photographic plates (BHRP), and some photorefractive crystals such as lithium niobate. Photorefractive crystals, however, are not stable, and recorded holograms degrade with time. Photorefractive materials also have maximum refractive index modulations four orders of magnitude less than either dichromated gelatin ($\sim$ .05) or bleached photographic plates and are a factor of six orders of magnitude slower than bleached photographic plates (three orders of magnitude slower than dichromated gelatin). They can, however, be orders of magnitude thicker than the other two phase materials. Dichromated gelatin has very high signal to noise ratio and is far superior in this characteristic to bleached photographic plates. It's less sensitive by some three orders of magnitude than BHRP and is totally insensitive to wavelengths longer than about 5500 Å. BHRP, on the otherhand, can have a panchromatic response. The thickness of DG and BHRP are approximately the same (nominally 15 μm). Both materials exhibit considerable absorbtion. Therefore, the incident beams attenuate as they propagate into the materials, making fabrication of specified refractive index profiles a difficult problem. The attenuation appears to be greater in BHRP than in DG. As far as stability is concerned dichromated gelatin is quite stable, but BHRP tends to degrade with exposure to light (especially UV). No information seems to be available on the linearity or dynamic range of either dichromated gelatin or bleached high resolution plates. These two characteristics will significantly affect the ability to fabricate specified quasi-sinusoidal refractive index profiles in any phase recording material. We point out that excellent sinusoidal reflection gratings, having almost 100% diffraction efficiency, have been fabricated in dichromated gelatin [3]. Thus, there is reason to believe that it may be possible to fabriate specified quasi-sinusoidal reflection gratings in DG.

Notes to Chapter 8

[1] A perfect mirror changes the phase of the electric field (s polarization) upon reflection by π.

[2] We have had some success with Foral 105 (Organics Department, Hercules Incorporated, Wilmington, Delaware, U.S.A.).

[3] Holographic Combiners for Head-Up Displays, Final Technical Report No. AFAL-TR-77-110, Radar and Optics Division, Environmental Research Institute of Michigan, Ann Arbor, Michigan, 1977.

9
CONCLUSIONS AND AREAS FOR FUTURE RESEARCH

This report has been a study of holographically produced phase reflection gratings. The objectives have been to obtain a fundamental understanding at optical propagation through such gratings, to develop techniques for designing gratings having specified characteristics, and to indicate approaches for fabricating these gratings. The present research was motivated by the possibility of holographically producing reflection grating structures that could perform spectral and angular filtering operations which currently available devices cannot. In this chapter, the report material is briefly summarized, and areas for future research are proposed.

As a first step toward achieving the above-mentioned goals, we demonstrated the applicability of frequency domain concepts to holographic reflection gratings. The use of such gratings as position-invariant frequency domain filters was also discussed.

Next, computationally efficient techniques were developed for analyzing optical propagation through holographic reflection gratings. Previous theories were too restrictive. They generally required periodic refractive index variations and strong depletion of the undiffracted field. Furthermore, they were not computationally efficient. We used our theory to determine some of the basic properties of holographic reflection gratings such as the effects of polarization and the interrelationship between the angle of incidence and wavelength. Simple analytic expressions for the reflection and transmission coefficients of sinusoidal reflection gratings were also derived.

In chapter 7 the design problem (or inverse scattering problem) was explored. We devised approximate techniques for determining the grating refractive index profile required to yield specified spectral and angular characteristics. The relationship between these techniques and design

techniques developed for multilayer dielectric interference filters was discussed.

The following chapter presented a nonconventional interferometric approach for fabricating holographic reflection gratings having quasi-sinusoidal refractive index profiles. Recording material considerations were also mentioned.

There are a number of topics which this report did not address which warrant further investigation. First, it would be instructive to compare, in detail, Kogelnik's coupled wave theory predictions and our analytic results for reflection gratings having sinusoidal refractive index profiles. Secondly, our design technique should be thoroughly investigated in order to determine its ultimate limitations. The technique should then be used to specify the types of angular and spectral characteristics which are achievable by holographic gratings. Special purpose holographic gratings haveing quasi-sinusoidal refractive index profiles should also be fabricated and their performances evaluated. Finally, the connection between corrugated, thin film waveguide gratings and holographic reflection gratings might be explored. Such waveguide gratings already have a number of significant applications. The theory developed in this report may be useful in analyzing and designing these waveguide gratings.

APPENDIX

Papers and technical presentations prepared during the second year effort of this contract.

A paper by K.A. Winick entitled "Holographic Interference Filters" was presented at the Annual Optical Society of America Meeting, October 13-17, 1980, in Chicago. This paper will be submitted for publication in 1981.

This final technical report will constitute the bulk of K.A. Winick's doctoral dissertation at the University of Michigan.

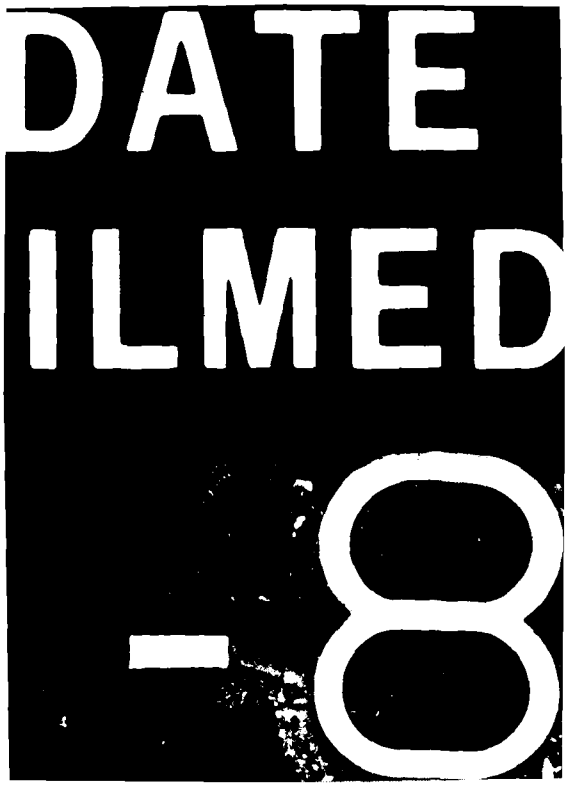
DATE
ILMED
-8